May 2019

Relevant Operators of Particle Physics and Cosmology

Cem Eroncel
Syracuse University

Abstract

Although the Standard Model of Particle Physics can reproduce the results of all the experiments performed to this date, it can only be an effective theory of fundamental physics. However, treating the Standard Model this way brings its own set of challenges; namely, the coefficients of relevant operators become extremely sensitive to UV physics. The relevant operator of the Standard Model is the Higgs mass which causes the "hierarchy problem", while the cosmological constant term of cosmology results in the "cosmological constant problem". In this thesis defense, I will discuss about how these issues can guide us in the pursuit of searching for new physics, both from a model building perspective and from a phenomenological perspective.

Relevant Operators of Particle Physics and Cosmology

by

Cem Eröncel

B.Sc. (Electrical Engineering) Istanbul Technical University, Istanbul, 2010

M.Sc. (Physics) Boğaziçi University, Istanbul, 2013

DISSERTATION

Submitted in partial fulfillment of the requirements for the degree of

Doctor of Philosophy in Physics

Syracuse University

May 2019

Acknowledgements

First of all, I want to start by expressing my deepest appreciation to my supervisor Jay Hubisz for his endless support and patience which made this dissertation possible. His approach to theoretical physics was and will be invaluable for my career as a physicist.

I also would like to offer my special thanks to other members of my dissertation committee Simon Catterall, Scott Watson, Jack Laiho, and Duncan Brown for their comments on this dissertation and insightful questions during my thesis defense. I am also extremely grateful to William Wylie who kindly agreed to be the chair of my thesis defense committee.

I am deeply indebted to my colleague Gabriele Rigo since none of the work in this thesis would have been possible without him. I also would like to extend my deepest gratitude to Csaba Csáki and John Terning who created the foundation for the work which eventually became part of this dissertation. I also wish to thank Bharath Sambasivam for his encouraging questions and support during the final stages of writing this dissertation.

I want to extend my sincere thanks to Carl Rosenzweig for his constructive criticism and advice on the work I conducted during my doctoral studies. I am also grateful to Aiyalam Balachandran and Kameshwar Wali for their thought-provoking questions during the weekly group meetings.

I also had a great pleasure of discussing physics with members of the high energy group at the Cornell University, especially with Csaba Csáki, Yuval Grossman, Sungwoo Hong, Gabriel Lee, and Ofri Talem. I very much appreciate their hospitality during much of my doctoral studies. Thanks should also go to former Cornell members Brando Bellazzini, Javier Sarra, Eric Kuflik, Yonit Hochberg, Jeff Asaf Dror, and Salvator Lombardo for helpful conversations.

I am very grateful to former and current Ph.D. students of Syracuse University Physics Department Suraj Shankar, Francesco Serafin, Brandon Melcher, Raghav Govind Jha, Mahesh Chandrasekhar Gandikota, S.M. Emtiaz, Nouman Tariq Butt, Swetha Bhagwat, Scott Bassler, Ogan Özsoy, Lorena Magaña Zertuche in no particular order for their friendship and

support. I want to thank specially to Gizem Sengör for her never-ending love and support during the most challenging times of my Ph.D.

I also would like to thank the people I met outside the Physics Department Sonya Xinyue Xiao, Mandy-Ruiwen Zheng and Irene Domenico with whom I share many beautiful memories. Especially I want to thank Duygu Yeni and Ergin Çenebaşı for their invaluable friendship and support.

Of course, the completion of my dissertation would not have been possible without my parents, who stood behind every decision I made and never stopped supporting me during all stages of my life.

List of Publications

Chapters 3 and 4 of this dissertation comprise of work carried out for the following papers respectively.

- C. Eröncel, J. Hubisz and G. Rigo, *Self-Organized Higgs Criticality*, *JHEP* **03** (2019) 046, [1804.0004]

- C. Csáki, C. Eröncel, J. Hubisz, G. Rigo and J. Terning, *Neutron Star Mergers Chirp About Vacuum Energy*, *JHEP* **09** (2018) 087, [1802.04813]

List of Conventions and Symbols

Throughout this dissertation we will use the following conventions and symbols:

- Greek letters are used for labeling the four dimensional spacetime indices, while Roman letters are used for labeling higher dimensional spacetime indices.
- Repeated indices are summed over.
- We will use the metric signature diag$(+,-,-,\ldots)$.
- All expressions are in natural units where $\hbar = 1$ and $c = 1$.
- We will employ the Feynman slash notation $\not{D} \equiv \gamma^\mu D_\mu$, where $\{\gamma^\mu\}$ are γ-matrices.
- For a given matter action S_m, the stress-energy tensor T_{mn} is defined by

$$T_{mn} = \frac{2}{\sqrt{|g|}} \frac{\delta S_m}{\delta g^{mn}}.$$

List of Abbreviations

Throughout this dissertation we will use the following abbreviations:

- SM: Standard Model
- EFT: Effective Field Theory
- VEV: Vacuum Expectation Value
- NGB: Nambu-Goldstone Boson
- pNGB: pseudo-Nambu-Goldstone Boson
- DOF: Degree of Freedom
- GSW: Glashow-Weinberg-Salam
- QED: Quantum Electrodynamics
- RG: Renormalization Group
- $\overline{\text{MS}}$: Minimal Subtraction2
- QCD: Quantum Chromodynamics
- GUT: Grand Unified Theory
- QFT: Quantum Field Theory
- SUSY: Supersymmetry
- MSSM: Minimal Supersymmetric Model
- CH: Composite Higgs
- BSM: Beyond the Standard Model
- MCHM: Minimal Composite Higgs Model

- EOM: Equation of Motion
- KK: Kaluza-Klein
- AdS: Anti-de-Sitter
- RS: Randall-Sundrum
- GW: Goldberger-Wise
- CFT: Conformal Field Theory

Contents

List of Figures

List of Tables

Chapter 1

Introduction

Without a doubt, the Standard Model of Particle Physics (SM) can be considered as one of the most significant victories of Theoretical High Energy Physics in the last century. It provides the most accurate and complete description of fundamental particles and the interactions between them. The last remaining piece of it, the Higgs boson, was finally discovered in July 2012 at CERN [1, 2], thereby it has been verified up to the energy scale and experimental accuracy that today's collider technology can reach.

Despite of its success, the SM is not the final theory of fundamental interactions. In this chapter, we will try to explain why this is the case. After a brief review of SM, we will argue why SM should be treated as an *Effective Field Theory (EFT)*. But we will see that this treatment brings deep conceptual issues which arise due to existence of *relevant operators*. Finally we will conclude this chapter with an outline of the dissertation.

1.1 Brief Review of the Standard Model

SM is a *non-abelian gauge theory*, with the *gauge group* given by $\mathsf{SU}(3)_C \otimes \mathsf{SU}(2)_L \otimes \mathsf{U}(1)_Y$. These gauge symmetries describe three of the four known fundamental forces. The $\mathsf{SU}(3)_C$ group describes the *strong force* while the product group $\mathsf{SU}(2)_L \otimes \mathsf{U}(1)_Y$ describes the weak force and electromagnetism unified at high energies. At low energies, this group is

spontaneously broken to a subgroup $\mathsf{U}(1)_{\rm EM}$ due to *Higgs mechanism*, and as a result the electromagnetism and the weak force are portrayed as separate interactions.

Being a quantum field theory, the fundamental building blocks of the SM are *quantum fields*, which are categorized in terms of their transformation properties under the SM gauge group and the Lorentz group.

First category consists of *gauge bosons*, which are the necessary ingredients of a gauge theory. These are *spin-1* fields and they transform under the *adjoint representation* of the corresponding gauge group. Physically, these fields are *force carriers* since the interactions between *matter particles* are carried using them. The gauge fields corresponding to the group $\mathsf{SU}(3)_C$ are called *gluons*, while the ones corresponding to the group $\mathsf{SU}(2)_L \otimes \mathsf{U}(1)_Y$ are called *electroweak bosons*. The number of gauge fields are determined by the dimension of the representation. Since the dimension of the adjoint representations of the $\mathsf{SU}(N)$ group is N^2-1, there are 8 gluons and 4 electroweak bosons. With all these information, we can write the *Yang-Mills* part of the SM Lagrangian in terms of the *gauge field strengths* as

$$\mathcal{L}_{\rm YM} = \underbrace{-\frac{1}{4g_3^2}\sum_{a=1}^{8} G^a_{\mu\nu}G^{\mu\nu a}}_{\mathsf{SU}(3)_C} \underbrace{-\frac{1}{4g^2}\sum_{b=1}^{3} W^b_{\mu\nu}W^{\mu\nu b}}_{\mathsf{SU}(2)_L} \underbrace{-\frac{1}{4g'^2}B_{\mu\nu}B^{\mu\nu}}_{\mathsf{U}(1)_Y}, \tag{1.1}$$

where g_3, g and g' are *gauge coupling constants* of $\mathsf{SU}(3)_C$, $\mathsf{SU}(2)_L$ and $\mathsf{U}(1)_Y$ respectively.

Second category contains the *spin 1/2* fields, known as *fermions*. These fields are not required in order to define a gauge theory, however they need to exist in the SM because phenomenologically we know these particles do exist. They can be classified into two categories depending on whether they transform under the strong group $\mathsf{SU}(3)_C$ or not. While the *quarks* transform under $\mathsf{SU}(3)_C$, the *leptons* do not. Another classification can be made according to their representations under the Lorentz group. *Left-handed* and *right-handed* fermions transform in the $\left(\frac{1}{2},0\right)$ and $\left(0,\frac{1}{2}\right)$ representation of the Lorentz group respectively. For some unknown reason, the transformation of left and right-handed fermions under the $\mathsf{SU}(2)_L$ group are not the same. While the left-handed fermions transform in the *fundamen-*

tal representation, the right-handed fermions are *singlets*, i.e. they do not transform under $\mathsf{SU}(2)_L$. On the other hand, all quarks transform under the fundamental representation of the strong group $\mathsf{SU}(3)_C$.

Since the left-handed fermions are in the fundamental representation of $\mathsf{SU}(2)_L$, both left-handed quarks and leptons need to be paired separately in *doublets*. Again for some unknown reason, there are 3 copies of quark and lepton doublets, known as *generations*. Thus, the left-handed fermion content of the SM can be described as

$$L^i = \left\{ \begin{pmatrix} \nu_{eL} \\ e_L \end{pmatrix}, \begin{pmatrix} \nu_{\mu L} \\ \mu_L \end{pmatrix}, \begin{pmatrix} \nu_{\tau L} \\ \tau_L \end{pmatrix} \right\} \quad , \quad Q^i = \left\{ \begin{pmatrix} u_L \\ d_L \end{pmatrix}, \begin{pmatrix} c_L \\ s_L \end{pmatrix}, \begin{pmatrix} t_L \\ b_L \end{pmatrix} \right\}, \tag{1.2}$$

where $i = 1, 2, 3$ is the generation index. The right-handed fermions will be the singlet versions of these states with the exception of neutrinos since no right-handed neutrino has been observed so far. Thus the right-handed fermion content is given by

$$e^i_R = \{e_R, \mu_R, \tau_R\} \quad , \quad u^i_R = \{u_R, c_R, t_R\} \quad , \quad d^i_R = \{d_R, s_R, b_R\}. \tag{1.3}$$

Then, the *fermion kinetic terms* in the SM Lagrangian are written by

$$\mathcal{L}_K = i\bar{L}^i \not{D} L^i + i\bar{Q}^i \not{D} Q^i + i\bar{e}^i_R \not{D} e^i_R + i\bar{u}^i_R \not{D} u^i_R + i\bar{d}^i_R \not{D} d^i_R, \tag{1.4}$$

where $\not{D} \equiv \gamma^\mu D_\mu$ and D_μ is the *gauge covariant derivative* corresponding to the representation of the fermion and sum over the generation index i is assumed.

All the SM particles do transform under the $\mathsf{U}(1)_Y$ group and their transformation properties under this group are determined by their *hypercharges*. Since $\mathsf{U}(1)_Y$ is an *abelian* group, in contrast to the $\mathsf{SU}(3)_C$ and $\mathsf{SU}(2)_L$ groups which are *non-abelian*, the hypercharges are in general arbitrary real numbers. However in the SM they need to be rational numbers in order that the SM is a consistent quantum field theory. More specifically, the hypercharges need to be rational numbers satisfying some relations in order that the *gauge anomalies* do

	$\mathsf{SU}(3)_C$	$\mathsf{SU}(2)_L$	$\mathsf{U}(1)_Y$
Gluons $\{G^a\}_{a=1}^8$	**Ad**	**1**	0
Electroweak bosons $\{W^a\}_{a=1}^4$	**1**	**Ad**	0
Left-handed leptons $\{L^i\}_{i=1}^3$	**1**	$\square$	$-\frac{1}{2}$
Right-handed leptons $\{e_R^i\}_{i=1}^3$	**1**	**1**	-1
Left-handed quarks $\{Q^i\}_{i=1}^3$	$\square$	$\square$	$\frac{1}{6}$
Right-handed up-type quarks $\{u_R^i\}_{i=1}^3$	$\square$	**1**	$\frac{2}{3}$
Right-handed down-type quarks $\{d_R^i\}_{i=1}^3$	$\square$	**1**	$-\frac{1}{3}$
Higgs H	**1**	$\square$	$\frac{1}{2}$

Table 1.1: Particle content of the Standard Model. **Ad** and $\square$ represent *adjoint* and *fundamental* representations respectively. **1** means that the particles are *singlets* under the gauge group.

vanish. The cancellation of gauge anomalies is a requirement for a consistent quantum field theory, since otherwise unitarity will not be preserved and the theory will contain negative norm states. The representations of the SM fields, plus the Higgs field which we will describe soon, under the SM gauge group are shown in Table 1.1.

So far we did not include any mass term, although we know that all quarks and fermions, as well as some gauge bosons, $W^\pm$ and Z, are massive. But we can't write mass terms for these particles explicitly, since these terms are not gauge invariant. This tells us that in order to generate mass terms for the fermions and gauge bosons, the gauge symmetry needs to be spontaneously broken. This phenomenon can be explained using the *Higgs Mechanism* [3–5]. In this mechanism, one adds to the SM field content a *spin-0* complex scalar field *multiplet* H, the *Higgs field*, which is a doublet under the $\mathsf{SU}(2)_L$ and singlet under the $\mathsf{SU}(3)_C$. One

also assumes a *potential* for the Higgs given by

$$V(|H|) = -m_H^2|H|^2 + \lambda_H|H|^4, \quad \lambda_H > 0. \tag{1.5}$$

If $m_H^2 < 0$, then this potential is clasically minimized at $H = 0$, hence the *vacuum expectation value (VEV)* of the Higgs becomes $\langle H \rangle = 0$. However, when $m_H^2 > 0$ the Higgs acquires a *non-zero* VEV given by $\langle |H| \rangle = \frac{m_H}{\sqrt{2\lambda_H}} \neq 0$. This non-zero VEV spontaneously breaks the $\mathsf{SU}(2)_L \otimes \mathsf{U}(1)_Y$ symmetry into $\mathsf{U}(1)_{\text{EM}}$, which is the gauge group of electromagnetism. This phenomenon is known as the *electroweak symmetry breaking*.

To see how the gauge bosons $W^\pm$ and Z get their masses, we should consider the full electroweak Lagrangian including the Higgs:

$$\mathcal{L}_{\text{EW}} = -\frac{1}{4}W^a_{\mu\nu}W^{\mu\nu a} - \frac{1}{4}B_{\mu\nu}B^{\mu\nu} + (D_\mu H)^\dagger(D^\mu H) - V(|H|), \tag{1.6}$$

where $V(|H|)$ is given by (1.5). This is the *Glashow-Weinberg-Salam* model of electroweak unification [6–8]. The coupling between the Higgs and the electroweak bosons arises due to the gauge covariant derivative term which is explicitly given by

$$D_\mu H = \partial_\mu H - igW^a_\mu \tau^a H - \frac{1}{2}g' B_\mu H. \tag{1.7}$$

In this expression $\{\tau^a\}$ are canonically normalized *Pauli matrices*, $\tau^a = \frac{1}{2}\sigma^a$, which are the generators of $\mathsf{SU}(2)$ Lie algebra. $\{W^a_\mu, B_\mu\}$ are electroweak gauge bosons, g and g' are $\mathsf{SU}(2)_L$ and $\mathsf{U}(1)_Y$ gauge couplings respectively, and $\frac{1}{2}$ factor comes from the fact that the Higgs doublet has hypercharge $Y = \frac{1}{2}$. For a vanishing Higgs VEV, (1.6) reduces to the Lagrangian of the pure $\mathsf{SU}(2)_L \otimes \mathsf{U}(1)_Y$ gauge theory with massless gauge bosons. However if the Higgs gets a VEV, then we need to expand around this new vacuum. This can be done

by expanding the Higgs field after the symmetry breaking as

$$H = \exp\left\{2i\frac{\pi^a\tau^a}{v_H}\right\}\begin{pmatrix}0\\ \frac{1}{\sqrt{2}}(v_H+h)\end{pmatrix}, \tag{1.8}$$

where $v_H = \frac{m_H}{\sqrt{\lambda_H}}$. The $\{\pi^a\}$'s are the analog of the *Nambu-Goldstone bosons (NGBs)* which arises due to spontaneous breaking of continuous *global* symmetries. The number of NGBs is equal to the number of broken generators, so the breaking $\mathsf{SU}(2)_L \otimes \mathsf{U}(1)_Y \to \mathsf{U}(1)_{\text{EM}}$ introduces $4-1=3$ NGBs. The field h is the *massive* excitation of the Higgs field H around the new vacuum and it represents the *Higgs particle*.

The particle content after the symmetry breaking can be studied by substituting the expansion (1.8) into the Lagrangian (1.6) and choosing the unitary gauge to set $\pi^a = 0$. Also some field redefinitions are needed to diagonalize the mass terms:

$$\begin{aligned} Z_\mu &\equiv \cos\theta_w W^3_\mu - \sin\theta_w B_\mu, \\ A_\mu &\equiv \sin\theta_w W^3_\mu + \cos\theta_w B_\mu, \\ W^\pm_\mu &\equiv \frac{1}{\sqrt{2}}\left(W^1_\mu \mp iW^2_\mu\right)^2, \end{aligned} \tag{1.9}$$

where $\theta_w = \frac{g'}{g}$. With these redefinitions, the kinetic and mass terms in (1.6) after the symmetry breaking becomes

$$\begin{aligned} \mathcal{L}_{\text{EW}\to\text{EM}} \supset &-\frac{1}{4}F_{\mu\nu}F^{\mu\nu} - \frac{1}{4}Z_{\mu\nu}Z^{\mu\nu} + \frac{1}{2}m_z^2 Z_\mu Z^\mu \\ &-\frac{1}{2}\left(\partial_\mu W^+_\nu - \partial_\nu W^+_\mu\right)\left(\partial^\mu W^{\nu-} - \partial^\nu W^{\mu-}\right) + m_W^2 W^+_\mu W^{\mu-} \\ &+\frac{1}{2}\partial_\mu h \partial^\mu h - \frac{1}{2}m_h^2 h^2, \end{aligned} \tag{1.10}$$

where $F_{\mu\nu} = \partial_\mu A_\nu - \partial_\nu A_\mu$, $Z_{\mu\nu} = \partial_\mu Z_\nu - \partial_\nu - Z_\mu$, and the mass terms are

$$m_z = \frac{g v_H}{2\cos\theta_w} \quad , \quad m_W = \frac{g v_H}{2} \quad , \quad m_h = \sqrt{2}m_H. \tag{1.11}$$

We see that the $W^{\pm}$ and Z bosons which were massless before the electroweak symmetry breaking now become massive, but the gauge boson A_μ, which corresponds to the *photon*, remains massless. As shown by Eugene Wigner in 1939, the number of degrees of freedom (DOF) of massive spin-s field is $2s+1$, while the number of DOF of *any* massless field is 2 [9]. Therefore, the massive gauge bosons should *get* a degree of freedom due to symmetry breaking and it should come from the Higgs field. The three degrees of freedom that $\{W^{\pm}, Z\}$ bosons need come from the NGBs $\{\pi^a\}$. Thus we say that the NGBs are *eaten* by the gauge bosons as a result of spontaneous symmetry breaking.

We will conclude this section by explaining how the fermions, more specifically charged leptons and quarks, can get their masses. The SM fermions as shown in (1.2) and (1.3) are 2-component *Weyl fermions*, so they are by definition massless. In order to write a mass term for a fermion, we need to mix left-handed and right-handed Weyl fermions. For instance, a mass term for the electron will be of the form $\bar{e}_L e_R$. The problem is that such a term does break $\mathsf{SU}(2)_L$, so it is not allowed by gauge invariance. This shows that, just as the massive gauge bosons, the fermions need to get their masses by the Higgs mechanism. In order this to happen, they need to couple to the Higgs field. This can be accomplished by adding *Yukawa* terms to the SM Lagrangian. For charged leptons we need to add

$$\mathcal{L}^{L}_{\text{Yuk}} = -\sum_{i=\{e,\mu,\tau\}} y_i \bar{L}^i H e^i_R + \text{h.c.} \tag{1.12}$$

where $\{y_i\}$ are *Yukawa couplings*. Quark masses can be generated similarly by

$$\mathcal{L}^{Q}_{\text{Yuk}} = -\sum_{i,j=1}^{3} \left(Y^d_{ij} \bar{Q}^i H d^j_R + Y^u_{ij} \bar{Q}^i \widetilde{H} u^j_R \right) + \text{h.c.} \tag{1.13}$$

where $\widetilde{H} \equiv i\sigma_2 H^*$. In this expression, the first term generates masses for the quarks $\{d, s, b\}$, while the second term generates for the quarks $\{u, c, t\}$. After the symmetry breaking, the Higgs field H will be replaced by its VEV, $H \to \frac{m_H}{\sqrt{2\lambda_H}} = \frac{v_H}{\sqrt{2}}$. Then (1.12) generates mass

terms for the charged leptons. As an example, the mass term for the electron will be $-m_e(\bar{e}_L e_R + \bar{e}_R e_L)$, with $m_e = \frac{y_e v_H}{\sqrt{2}}$. The Yukawa terms for the quarks (1.13) become after the symmetry breaking

$$\mathcal{L}^Q_{\text{Yuk}} = -\frac{v}{\sqrt{2}}\left(\bar{d}_L Y^d d_R + \bar{u}_L Y^u u_R\right) + \text{h.c.} \tag{1.14}$$

where now Y^d and Y^u are 3×3 complex matrices with elements $\left(Y^{u,d}\right)_{ij} = Y^{u,d}_{ij}$. To obtain the quark masses, the mass terms in (1.14) need to be diagonalized. This can be achieved by introducing two diagonal matrices M_d and M_u and two unitary matrices U_d and U_u so that

$$Y_d Y_d^\dagger = U_d M_d^2 U_d^\dagger \quad \text{and} \quad Y_u Y_u^\dagger = U_u M_u^2 U_u^\dagger. \tag{1.15}$$

One can further write

$$Y_d = U_d M_d K_d^\dagger \quad \text{and} \quad Y_u = U_u M_u K_u^\dagger, \tag{1.16}$$

where K_d and K_u are again unitary matrices. Then, after a change of basis by $u_L \to U_u u_L$, $d_L \to U_d d_L$, $d_R \to K_d d_R$ and $u_R \to K_u u_R$, (1.14) in the mass basis becomes

$$\mathcal{L}^Q_{\text{Yuk}} = -\sum_i^3 \left(m_i^d \bar{d}_L^i d_R^i + m_i^u \bar{u}_L^i u_R^i\right) + \text{h.c.} \tag{1.17}$$

where $\left\{m_i^d\right\}$ and $\{m_i^u\}$ are the diagonal elements of $\frac{v}{\sqrt{2}} M_d$ and $\frac{v}{\sqrt{2}} M_u$ respectively.

This concludes our lightning review of the SM. In the next section we will discuss why we expect that this picture should change eventually.

1.2 The Standard Model as an Effective Theory

The SM is being tested continuously in collider experiments with ever-increasing precision. So far, no statistically significant deviation have been measured[1]. Despite of this, we know that there should exist physics *beyond the SM* since there are a lot of physical phenomena which cannot be explained using the framework of SM. Some of the notable ones are

- **Neutrino Masses:** Neutrinos are *massless* in the SM. Writing mass terms for them using the Yukawa interactions like in (1.12) is not possible because right-handed neutrinos do not exists in the field content of the SM; at least they have not been observed. But, we have learned from neutrino oscillations experiments that they *do* have a tiny but non-zero mass.

- **Dark Matter:** Latest cosmological observations show that the SM fields can only provide 15% of the matter in the observable universe [15]. The rest of it consists of a hypothetical substance called *dark matter*. If it is a particle, then it should be electrically neutral, weakly interacting and stable to explain all the observations. The SM does not have such a candidate.

- **Dark Energy:** The supernova observations made in 1998 showed that the universe is not only expanding but the expansion is accelerating [16,17]. The most commonly used cosmological model for explaining both dark matter and dark energy is Λ_{CDM} model which contains *cold dark matter* and a positive *cosmological constant* term. Attempting to derive this term using the SM leads to a 120 order of magnitude discrepancy known as the *cosmological constant problem*. We shall explore this further later in this chapter.

- **Matter-antimatter Asymmetry:** Our observable universe contains vastly more matter than antimatter although there is no reason that the universe should start in an

[1] They are some experimental anomalies such as the *proton radius puzzle* [10], *anomalous magnetic dipole moment muon* [11] and *B-meson decays* [12–14]. But it is still uncertain that these anomalies definitely contradicting the SM.

asymmetric state. Hence, there should be a process which occurred in the early universe and produced this asymmetry. Such a process is not possible with the ingredients of the SM [18].

In addition to all these missing pieces, the strongest hint for the incompleteness of the SM comes from the fact that an *UV complete* quantum description of gravity is missing in the SM. The phrase *UV complete* is crucial for the validity of this statement, since an *effective* description of quantum gravity is perfectly compatible with the SM and even provide testable predictions. To arrive such a description, we start with the fact that the *graviton*, which is the force carrier of the gravity, should be a massless spin-2 field. Then using the requirements of unitarity and Lorentz invariance, it is possible to show that the *unique* Lagrangian one can write is [19]

$$\mathcal{L}_g = M_{\rm pl}^2 \sqrt{-\det\left(\eta_{\mu\nu} + \frac{1}{M_{\rm pl}} h_{\mu\nu}\right)}\, \mathcal{R}\left(\eta_{\mu\nu} + \frac{1}{M_{\rm pl}} h_{\mu\nu}\right), \tag{1.18}$$

where $h_{\mu\nu}$ represents the fluctuations of the metric, i.e. $g_{\mu\nu} = \eta_{\mu\nu} + M_{\rm pl}^{-1} h_{\mu\nu}$, $M_{\rm pl} = G_N^{-1/2} \approx 10^{19}\,\text{GeV}$ with G_N being the Newton's constant, and $\mathcal{R}$ is the Ricci scalar. The scale $M_{\rm pl}$ has been introduced so that the graviton field $h_{\mu\nu}$ has mass dimension one. This is precisely the Einstein-Hilbert Lagrangian of general relativity. This shows that the Lagrangian for general relativity is the unique Lagrangian that can couple a spin-2 field to matter.

If this construction works so well, why do we say that the description of quantum gravity in the SM is not complete? The answer is related to the strength of the gravitational interaction. If we expand the Lagrangian (1.18) we find

$$\mathcal{L}_g \sim \frac{1}{2} h \Box h + \frac{1}{M_{\rm Pl}} \Box h^3 + \mathcal{O}\left(\frac{1}{M_{\rm pl}^2}\right). \tag{1.19}$$

We see that the gravitational interaction term $\Box h^3$ has the coupling constant $M_{\rm pl}^{-1}$ which has negative mass dimension. Same situation will happen if we want to couple gravity to the SM

particles. As a spin-2 field, graviton should couple to the stress-energy tensor corresponding to the SM

$$T^{\mu\nu}_{\rm SM} = -\frac{2}{\sqrt{-g}}\frac{\delta S_{\rm SM}}{\delta g_{\mu\nu}} \quad \text{with} \quad S_{\rm SM} = \int \mathrm{d}^4x\,\sqrt{g}\mathcal{L}_{\rm SM}, \tag{1.20}$$

and just from dimensional analysis the coupling should be of the form

$$\frac{1}{M_{\rm pl}} h_{\mu\nu} T^{\mu\nu}_{\rm SM}. \tag{1.21}$$

The fact that the gravity coupling has negative mass dimension makes this description of gravity *perturbatively non-renormalizable*. In these kind of field theories, one needs infinite number of counterterms to cancel all the infinities arising from the loop corrections to the model parameters. Despite of this difficulty, this description of gravity is perfectly valid and even predictive, as long as the energy scale E we are probing is much smaller than the Planck scale, $E \ll M_{\rm pl}$. In other words, the Lagrangian (1.19) together with the coupling (1.21) provides an effective theory description of quantum gravity valid up to the *cutoff scale* $M_{\rm pl}$ of the theory.

The breakdown of perturbative renormalizability does not mean that a field theory is ill-defined at higher energies. Such a field theory might be *non-perturbatively renormalizable*, if the Renormalization Group (RG) evolution of its couplings having negative mass dimensions have non-trivial fixed points in the UV. Such theories are called *asymptotically safe* [20]. It is a possibility that the gravity is such a theory, and this description holds even at higher energies [21].

However, from a historical perspective, non-renormalizable theories were generally signs of new physics and the cutoffs of these theories gave good estimates about the scale at which new physics appeared. The most well known example of a non-renormalizable theory is the Enrico Fermi's theory β-decay [22]. In this theory, the weak decays are modeled using a

Lagrangian of the form

$$\mathcal{L}_{\text{Fermi}} = G_F \bar{\psi}_p \psi_n \bar{\psi}_e \psi_\nu, \tag{1.22}$$

where $\{p, n, e, \nu\}$ are $\{\text{positron}, \text{neutron}, \text{electron}, \text{neutrino}\}$. Since each fermion should have mass dimension $3/2$, the mass dimension of G_F should be -2, thus this theory is non-renormalizable. The value of G_F can be measured using muon decays. It's latest value is [23]

$$G_F = 1.1663787(6) \times 10^{-5}\,\text{GeV}^{-2} \approx \left(\frac{1}{293\,\text{GeV}}\right)^2. \tag{1.23}$$

From an EFT point of view, this result tells us that new physics should replace the Fermi's theory around the energy scale $E \sim 293\,\text{GeV}$. We know that the replacement is the Glashow-Salam-Weinberg(GSW) model of electroweak interactions, for which we wrote down the Lagrangian explicitly in (1.6). While in the Fermi theory, the weak decays are point interactions between four fermions, in GSW model the weak decays are four fermion interactions due to exchange by a massive electroweak gauge boson, whose masses are [23]

$$m_W = 80.379(12)\,\text{GeV} \quad \text{and} \quad m_Z = 91.1876(21)\,\text{GeV}. \tag{1.24}$$

Although these numbers are smaller than our naive expectation $E \sim 293\,\text{GeV}$, they agree very well as an order of magnitude estimate. If the perturbative gravity can also be UV completed in a similar way, we can argue that the SM is an effective theory valid up to the cutoff scale Λ_{SM} given by

$$\Lambda_{\text{SM}} \lesssim M_{\text{pl}} \approx 10^{19}\,\text{GeV}. \tag{1.25}$$

Of course this bound assumes that there is no new physics between the Planck scale and

the energy scale being probed by today's colliders, which is $\sim$ TeV. It is perfectly possible, in fact expected, new physics will show up well before the Planck scale. In this case the cutoff scale of the SM will be much lower than (1.25). Whenever the new physics scale appears, and how complicated the new physics will be, it should be possible to express its effects in energies $E \ll \Lambda_{\rm SM}$ by adding non-renormalizable operators to the SM Lagrangian. Hence to study new physics, we can expand the SM Lagrangian generically as

$$\mathcal{L}_{\rm SM} \to \mathcal{L}_{\rm SM} + \sum_{\Delta=5}^{\infty} \frac{1}{\Lambda_{\rm SM}^{\Delta-4}} \mathcal{O}_\Delta, \tag{1.26}$$

where the mass dimension of the operator $\mathcal{O}_\Delta$ is $[\mathcal{O}_\Delta] = \Delta$[2].

The *higher-dimensional operators* $\{\mathcal{O}_\Delta\}$ are commonly used in attempts to explain the problems of the SM we have mentioned before. For example, to generate neutrino masses without right-handed neutrinos[3], one can use the 5-dimensional *Weinberg operator* [24]

$$\frac{1}{\Lambda_{\rm SM}} \left(\bar{L}\widetilde{H}\right) \left(L^c \widetilde{H}\right), \tag{1.27}$$

where L^c is the charge conjugate of the lepton doublet. This is the unique $\Delta = 5$ term which can be written in the SM Lagrangian. With order one coefficients, this term generates neutrino masses around $m_\nu \sim 0.1\,\text{eV}$ for $\Lambda_{\rm SM} \approx 10^{14}\,\text{GeV}$ [25]. This example shows that the EFT picture allows us to get hints about where the new physics might appear, even though we don't know the details of the new physics.

If we push ourselves to consider a situation where the SM does not get any corrections up to the Planck scale and breakdown of perturbative renormalizability of quantum gravity is saved by the asymptotic safety, there is still a problem which might prevents SM from being a UV complete theory. The problem is with the RG evolution of the $\mathsf{U}(1)_Y$ hypercharge

[2] By mass dimension we mean canonical dimension, i.e. we are ignoring anomalous mass dimensions.
[3] With right-handed neutrinos, neutrino masses can be generated with $\Delta = 4$ operators.

gauge coupling g'. At one loop, the RG evolution of g' is given by [26]

$$\frac{4\pi}{\alpha_1(E^2)} = \frac{4\pi}{\alpha_1(\mu^2)} - \frac{41}{10}\log\left(\frac{E^2}{\mu^2}\right), \tag{1.28}$$

where

$$\alpha_1 = \frac{1}{4\pi}\frac{5}{3}g'^2 = \frac{5\alpha}{3\cos^2\theta_w}, \tag{1.29}$$

with α being the *fine structure constant*. The μ^2 is an energy scale at which the coupling constant α_1 needs to be measured experimentally. We can see that due to the negative sign of the log-term in (1.28), which corresponds to a positive β-function coefficient, there is an energy scale Λ_L at which the coupling constant diverges. This scale is given by $\alpha_1^{-1}(\Lambda_L) = 0$ or

$$\frac{4\pi}{\alpha_1(\mu^2)} = \frac{41}{10}\log\left(\frac{\Lambda_L^2}{\mu^2}\right). \tag{1.30}$$

Using the fact $\alpha(m_W^2) \approx 1/128$ and $\sin^2\theta_w(m_Z^2) \approx 0.231$ [23], we get $\alpha_1(m_Z^2) \approx 0.017$ and

$$\Lambda_L \sim 10^{41}\,\text{GeV}. \tag{1.31}$$

This is called the *Landau pole* related to the $\mathsf{U}(1)_Y$ gauge coupling and represents the breakdown of predictability of the SM as a perturbative field theory. One might worry that the one-loop expression (1.28) is derived using perturbation theory but close to the Landau pole, the gauge coupling g' becomes non-perturbative and the one-loop expression looses its validity. In fact the lattice simulations of Quantum Electrodynamics (QED), which has the similar problem albeit at $\Lambda \sim 10^{277}\,\text{GeV}$, show that before reaching to its Landau pole the theory enters to a new phase at which fermions form a condensate and breaks the chiral symmetry [27–29]. But such a condensate will also break the electroweak symmetry at a

much higher scale than the weak scale which will be in conflict with the GSW model we have described in Section 1.1.

The take-away message of this section should be that although there is no *mathematically rigorous* argument which *proves* that the SM is incomplete, there are a lot of hints, both from theoretical and experimental point of view. In the rest of this dissertation, we will take the SM as an EFT with some cutoff scale $\Lambda_{\rm SM}$ as our starting point, and study what kind of hints can we get from this effective description about the physics beyond the SM.

1.3 The Relevant Operator of the Standard Model and the Hierarchy Problem

In the previous section we have argued that a good starting point for studying the beyond the SM physics is an effective description of the SM with up to some cutoff scale $\Lambda_{\rm SM}$. This cutoff scale should not be very close to the electroweak scale m_W, since the current version of the SM can reproduce the results of the collider experiments perfectly. We don't know the precise value for this cutoff, but it is pretty likely that the SM will be replaced by something else at latest at the Planck scale, so for definiteness we choose $\Lambda_{\rm SM} \lesssim M_{\rm pl}$.

Theories with a physical cutoff can be studied using the framework of *Wilsonian renormalization group* [30–34]. In contrast to the *continuum RG* picture where Λ stands for an *UV regulator* which renders the loop integrals finite, the Wilsonian RG treats Λ as a *reference scale* of the theory, like atomic spacing in a metal. The RG evolution of the coupling constants can be obtained by reducing the cutoff from Λ to Λ', where one *integrates out* the degrees of freedom $\Lambda' < p < \Lambda$, and adjusting the coupling constants so that the low-energy physics is the same.

In the Wilsonian RG and the EFT language, the operators are classified according to their mass dimensions. If d denotes the number of spacetime dimensions and Δ denotes mass dimension of the operator, then the operator is called *relevant* if $\Delta < d$, *irrelevant* if

$\Delta > d$, and *marginal* if $\Delta = d$. Classically marginal operators can get *anomalous dimensions* from quantum corrections and depending the sign of the correction they can be *relevant* or *irrelevant*, marginally so if the quantum corrections are small. If $C_{\Delta-d}$ is the (in general dimensionful) coefficient of an operator of mass dimension Δ, then it can be shown that under a RG transformation $\Lambda \to \Lambda' = b\Lambda$ with $b < 1$, $C_{\Delta-d}$ scales as [35]

$$C_{\Delta-d} \to C'_{\Delta-d} = b^{\Delta-d} C_{\Delta-d}. \tag{1.32}$$

Therefore for an irrelevant operator $C' < C$ so the coupling of this operator *decreases* towards lower energies, or *towards IR*, which implies that at lower energies $E \ll \Lambda$ this operator becomes less important. We note that the irrelevant operators correspond to the perturbatively non-renormalizable terms in the Lagrangian. This explains why non-renormalizable field theories are perfectly valid and predictive as low energy effective field theories.

On the other hand for a relevant operator $C' > C$ and the coupling *increases* towards IR. This implies that the relevant operators are *sensitive* to the UV physics. This immediately rings an alarm bell. Our aim was to consider the SM as an effective theory with the hope that its low-energy description will be independent of its UV completion, but we ended up in a situation where the UV sensitivity of our model increases as we go to lower energy scales. We would have been fine if the SM did not contain any relevant operators, but this is not the case. There is only one relevant operator in the SM[4], which is the Higgs mass parameter in the Higgs potential (1.5). This is the essence of the so called *hierarchy problem* which we will describe in detail now.

In (1.26), we added irrelevant operators to the Lagrangian by the terms of the form $\Lambda_{\text{SM}}^{-(\Delta-4)}\mathcal{O}_\Delta$ with $\Delta > 4$. By extrapolating this form to the relevant operators we can argue

[4]Here we mean "relevant" by naive power counting. There are also marginally relevant operators in the SM, like the QCD field strength squared.

that the Higgs mass term should be of the form

$$c\Lambda_{\rm SM}^2|H|^2, \tag{1.33}$$

where c is a dimensionless coefficient. We can see this formally by calculating the quantum corrections to the Higgs mass parameter of (1.5). These corrections will come from Higgs self-interactions, gauge and fermion loops. All these contributions are *quadratically divergent* so they need to be regulated with a cutoff. Since we are treating the SM as an effective theory, we can use $\Lambda_{\rm SM}$ to regulate the integrals. Then we can express the quantum corrections to the Higgs mass parameter as

$$\delta m_H^2 \approx \frac{\Lambda_{\rm SM}^2}{16\pi^2}\left[-6y_t^2 + \frac{1}{4}\left(9g^2 + 3g'^2\right) + 6\lambda_H + \cdots\right], \tag{1.34}$$

where y_t is the top-quark Yukawa coupling[5]. Thus we see although we would have chosen a small value for the bare Higgs mass parameter m_H^2, the quantum corrections will push it all the way to the cutoff scale.

Of course the bare mass parameter is not an observable and we have to choose it such that $m_H^2 + \delta m_H^2$ reproduces the experimentally measured value for the Higgs mass, which can also be defined as the *pole mass*. Since the Higgs pole mass is $m_h \approx 125\,\text{GeV}$, using (1.11) we get $(m_H^2)_{\rm pole} \approx (88\,\text{GeV})^2$. Choosing the SM cutoff $\Lambda_{\rm SM}$ to be the Planck scale $M_{\rm pl}$ we find

$$(m_H^2)_{\rm pole} = (m_H^2)_{\rm bare} + \delta m_H^2 \Rightarrow (88\,\text{GeV})^2 \approx (m_H^2)_{\rm bare} + \left(10^{19}\,\text{GeV}\right)^2, \tag{1.35}$$

where $(m_H^2)_{\rm bare}$ is the *bare* mass parameter in the Higgs potential. This result shows that

[5]We have ignored the contribution from other fermions since they will be small compared to the top-quark contribution.

the bare mass parameter should be *tuned* to a precision of

$$\frac{(m_H^2)_{\text{pole}}}{\Lambda_{\text{SM}}^2} \approx \frac{(88\,\text{GeV})^2}{(10^{19}\,\text{GeV})^2} \sim 10^{-34}. \tag{1.36}$$

This is called *fine-tuning* which means extreme sensitivity of the physical observables, such as the Higgs pole mass, to variation of model parameters. The theories which require such a precise tuning are usually called *fine-tuned* or *unnatural*.

Since the quadratic sensitivity to the cutoff scale in (1.35) comes from an UV divergent integral, it is a meaningful question to ask what would have happened if we had choose a different regularization scheme to perform the loop integrals. A commonly used regularization scheme in gauge theories is the *dimensional regularization* since it respects gauge invariance. If one evaluates the loops in (1.34) using dimensional regularization, then one finds that the quadratic divergence is replaced by a pole at $\epsilon = 0$ with $d = 4 - \epsilon$

$$(\delta m_H^2)_{\text{DimReg}} \sim \frac{1}{\epsilon} + \text{finite}. \tag{1.37}$$

As in the usual renormalization procedure, this pole can be canceled by introducing suitable counterterms and so one finds that the quantum correction to the Higgs mass is finite and does not depend on the cutoff Λ_{SM} at all.

At this point, one might think that the quadratic sensitivity to the cutoff scale in (1.34) is merely a consequence of choosing a wrong regulator, therefore it does not represent something physical. However from an effective field theory point of view, the Λ_{SM}^2 in (1.34) *not* a regulator, it is a *physical scale* which is a placeholder for new physics. Now we will show this explicitly using a toy model[6]. We consider a theory given by the Lagrangian

$$\mathcal{L} = \frac{1}{2}\partial_\mu\phi\partial^\mu\phi - \frac{1}{2}m^2\phi^2 + \frac{\lambda}{4}\phi^4 + i\bar{\Psi}(\partial\!\!\!/ - M)\Psi + y\phi\bar{\Psi}\Psi, \tag{1.38}$$

[6]The following discussion is based on the lectures given by Nathaniel Craig at the *Prospects in Theoretical Physics (PiTP) 2017* summer school available at https://www.youtube.com/watch?v=orCZeoQXXWw.

where a scalar field ϕ is coupled to a fermion Ψ with a Yukawa interaction. We assume that the mass of the scalar is much smaller than the fermion mass, so $m \ll M$. In this case, we consider an EFT with only the scalar field ϕ, where the heavy fermion Ψ has been integrated out. The Lagrangian in the effective theory is

$$\mathcal{L}_{\text{EFT}} = \frac{1}{2} Z_\phi \partial_\mu \phi \partial^\mu \phi - \frac{1}{2} \widetilde{m}^2 \phi^2 + \cdots , \tag{1.39}$$

where Z_ϕ is the *wave-function renormalization term* and $\widetilde{m}^2$ is the renormalized mass parameter. We didn't include the ϕ^4 term since we only interested in the corrections that the mass parameter will get. Now we want to perform a *matching* procedure between the full theory and the effective theory at the scale M. This can be done by matching the scalar two-point functions in both descriptions. At one loop, this matching can be done by calculating the one-loop contribution involving the heavy fermion[7]:

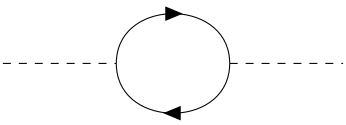

To avoid any confusion with quadratic divergences, we will use the dimensional regularization with *minimal subtraction* ($\overline{\text{MS}}$) scheme to evaluate this loop. Then the contribution of this loop to the scalar self-energy is given by

$$\Sigma_2(p^2) = \frac{4y^2}{16\pi^2} \left[\left(\frac{3}{\bar{\epsilon}} + 1 + 3 \log \left(\frac{\mu^2}{M^2} \right) \right) \left(M^2 - \frac{p^2}{6} \right) + \frac{p^2}{2} - \frac{p^2}{20 M^2} + \cdots \right] , \tag{1.40}$$

where $\bar{\epsilon}^{-1} = \epsilon^{-1} - \gamma_E + \log(4\pi)$ with γ_E being the *EulerMascheroni constant*. Then we perform the renormalization procedure by adding counterterms to cancel the $1/\bar{\epsilon}$ pole and

[7] The Feynman diagrams in this thesis are produced by the Ti*k*Z-Feynman package [36]

match at the scale $\mu = M$. After this we find the Lagrangian in the effective theory as

$$\mathcal{L}_{\rm EFT} = \left(1 - \frac{4}{3}\frac{y^2}{16\pi^2}\right)\frac{1}{2}\partial_\mu\phi\partial^\mu\phi - \left(m^2 - \frac{4y^2}{16\pi^2}M^2\right)\frac{1}{2}\phi^2 + \cdots . \tag{1.41}$$

We see that the scalar mass gets quantum corrections proportional to M^2. This toy model clearly demonstrates that the quadratic divergence in (1.34) is really a *placeholder for new physics*. The hierarchy problem is not about quadratic divergences. It is about the sensitivity to higher energy scales.

One might worry that this contribution arises due to the coupling between the heavy fermion Ψ and the Higgs, and it might be possible to avoid this contribution by not coupling the new physics to the Higgs. Let us assume that the heavy fermion Ψ is not coupled to the SM at all. But it should at least couple to gravity. Then we can write the following three-loop correction to the Higgs mass involving gravitons coupled to top quark loop and the heavy fermion loop:

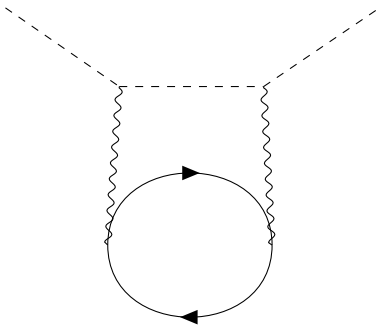

The correction to the Higgs mass due to this diagram is given by

$$\delta m_H^2 \sim \frac{6y_t^2}{(16\pi^2)^3}\left(\frac{M}{M_{\rm pl}}\right)^4 M^2. \tag{1.42}$$

If the mass of the heavy fermion is very close to the Planck scale $M \lesssim M_{\rm pl}$, then despite of the suppression coming from the loop factor, the M^2 correction to the Higgs mass does still exists. In summary, it is really hard to shield the Higgs mass from the corrections coming

from the higher energy scales.

Before concluding this section, we will mention yet another way to describe the hierarchy problem, which will make use of the symmetries. We have said that the hierarchy problem is unique to the Higgs, since it is the only relevant operator in the SM. But there is another reason why the Higgs suffers from this problem. To see this, consider the Lagrangian for Quantum Electrodynamics (QED):

$$\mathcal{L}_{\text{QED}} = -\frac{1}{4}F_{\mu\nu}F^{\mu\nu} + \bar{\psi}\left(i\not{D} - m_e\right)\psi, \tag{1.43}$$

with $D_\mu\psi = \partial_\mu\psi + ieA_\mu\psi$. Here, ψ is the electron represented as a *Dirac fermion* and m_e is the electron mass. The electron mass term looks like a relevant parameter so naively we expect the quantum corrections will push it to higher scales. But if we calculate the corrections we will find

$$\delta m_e = \frac{3\alpha_{\text{em}}}{2\pi} m_e \log\left(\frac{\Lambda}{m_e}\right), \tag{1.44}$$

where α_{em} is the fine-structure constant. We see that the quantum corrections are proportional to the electron mass itself, and instead of a quadratic divergence we get a *much weaker* logarithmic divergence. To appreciate how much weaker it is, let us imagine an alternative universe where the QED holds up to the Planck scale. Then taking $\Lambda \sim M_{\text{pl}}$, $\alpha_{\text{em}} \approx 1/137$ and $m_e \approx 0.511\,\text{MeV}$ we find

$$\frac{\delta m_e}{m_e} \sim 0.2. \tag{1.45}$$

What is the reason behind the logarithmic dependence in (1.44)? The answer is the *symmetry*. If we set the electron mass m_e to zero in (1.43), the electron gains an additional symmetry, namely the symmetry under *axial* transformations of the form $\psi \to e^{i\alpha\gamma_5}\psi$. In other words, setting the electron mass to zero *enhances* the symmetry of the theory. Since in

this case the symmetry will also be respected by quantum corrections[8], the corrections to the mass parameter should be proportional to the mass parameter itself. Then by dimensional analysis, we can conclude that the cutoff Λ can only appear inside the logarithm. In such a scenario, one usually says that the electron mass is *protected* by the chiral symmetry.

The same situation happens with the Yukawa couplings in the SM. Setting them to zero enhances the symmetry of the SM, so they are insensitive to higher energy scales. Therefore the hierarchy between various Yukawa couplings, such as $y_e/y_t \sim 10^{-5}$, is not considered to be a hierarchy problem. It is still a puzzle why such a hierarchy exists, but if it can be explained in a UV completion of the SM, then that explanation will remain valid at low energies too. Introducing a symmetry which protects the Higgs mass from quadratic divergences is the most commonly used strategy in attempts to solve the hierarchy problem, which we will briefly mention in Chapter 2.

1.4 A Relevant Operator of Cosmology and the Cosmological Constant Problem

When we wrote down the potential for the Higgs in (1.5), we didn't include a constant term V_0. Such a term does not have any effect in particle physics, but it plays a big role in cosmology. Although this term does not couple to any SM field, it will couple to gravity. If we denote the VEV of Higgs by $\phi_h = \sqrt{2}\,\langle|H|\rangle$, then the energy density of the *vacuum* will be given by

$$\left\langle T_0^0 \right\rangle \equiv \rho_V = V(\phi_h) = V_0 - \frac{m_H^4}{\lambda_H}. \tag{1.46}$$

[8] Actually the chiral symmetry is *anomalous* so quantum corrections will introduce a term of the form $F\widetilde{F}$ where $\widetilde{F}_{\mu\nu} = \epsilon_{\mu\nu\rho\sigma}F^{\rho\sigma}$. But in the case of QED the $F\widetilde{F}$ term is a total derivative so it does not contribute to the equation of motion.

We see that the energy density of the vacuum is *dependent* on the choice of V_0. The Einstein equations with the cosmological constant term is given by

$$\mathcal{R}_{\mu\nu} - \frac{1}{2} g_{\mu\nu}\mathcal{R} + \Lambda g_{\mu\nu} = \frac{8\pi}{M_{\rm pl}^2} T_{\mu\nu}, \tag{1.47}$$

where Λ is the *cosmological constant*. From this expression we can see that the vacuum energy density ρ_V contributes to the cosmological constant term, giving an effective cosmological constant expressed as

$$\Lambda_{\rm eff} = \Lambda + \frac{8\pi}{M_{\rm Pl}^2}\rho_V. \tag{1.48}$$

So total effective vacuum energy of the universe is given by

$$\langle\rho\rangle = \rho_V + \Lambda\frac{M_{\rm pl}^2}{8\pi} = \Lambda_{\rm eff}\frac{M_{\rm pl}^2}{8\pi}. \tag{1.49}$$

This value can be measured using cosmological observations: [16, 17, 37–41]

$$\Lambda_{\rm eff} \sim 10^{-52}\,{\rm m}^{-1} \tag{1.50}$$

which corresponds to a vacuum energy density of

$$\langle\rho\rangle \sim (10^{-12}\,{\rm GeV})^4. \tag{1.51}$$

We shall see now that the smallness of this value results in a fine-tuning problem which is much worse compared to the hierarchy problem. In the expression of the effective vacuum energy (1.49), all the terms were classical contributions. There will also be quantum corrections to the vacuum energy. If we consider SM with the cutoff $\Lambda_{\rm SM}$, then the sum of the

zero-point energies of all normal modes of some field of mass m will be given by

$$\int_0^{\Lambda_{\rm SM}} \frac{\mathrm{d}^3k}{(2\pi)^3}\frac{1}{2}\sqrt{k^2+m^2} \approx \frac{\Lambda_{\rm SM}^4}{16\pi^2}. \tag{1.52}$$

Notice that, this is in agreement with our expectation from the effective field theory point of view. The constant term in the Higgs potential V_0 is a $\Delta = 0$ operator, therefore it should appear in the effective theory as $c\Lambda^4 V_0$, where c is a coefficient and Λ is the cutoff. Again choosing the SM cutoff to be the Planck scale we find the natural value of the vacuum energy density should be $\langle\rho\rangle \sim M_{\rm pl}^4$. Comparing with the experimentally measured value (1.51) implies a tuning of

$$\frac{(10^{-12}\,\mathrm{GeV})^4}{M_{\rm pl}^4/(16\pi^2)} \sim 10^{-122}. \tag{1.53}$$

This is called the *cosmological constant problem*. It is the question of what kind of physical process could have cancelled the enourmous contribution coming from the zero-point energies of the quantum fields, such that the observed cosmological constant is very small.

The cosmological constant problem becomes much more interesting when we consider the phase transitions in the early universe. The potential we wrote for the Higgs field in (1.5) is at zero temperature. Since the temperature of the universe is very small today, $T \sim 3\,\mathrm{K}$, the zero temperature description is adaquate for studying the phenomena happening at present times. But at the early stages of the universe, the temperature was very high and one cannot rely on a zero temperature description. The physics of the early universe can be studied using *finite-temperature field theory*. In this framework, the classical potential $V(\phi_h)$ is replaced by the *finite-temperature effective potential*, which is the free energy density associated with the ϕ_h field. It can be expressed by

$$V_T(\phi_h) = \rho_\phi - T s_\phi, \tag{1.54}$$

where ρ_ϕ is the energy density and $s_\phi = -\partial V_T(\phi_h)/\partial T$ is the entropy density. To one loop in quantum and thermal corrections, the finite-temperature effective potential $V_T(\phi_h)$ is given by [42, 43]

$$V_T(\phi_h) = V_1(\phi_h) + \frac{T^4}{2\pi^2}\int_0^\infty \mathrm{d}x\, x^2 \log\left[1 - \exp\left\{-\sqrt{x^2 + \frac{M^2}{T^2}}\right\}\right], \tag{1.55}$$

where $M^2(\phi_h) = -m_H^2 + 3\lambda_H\phi_h^2$ and $V_1(\phi_h)$ is the zero-temperature potential including one loop quantum effects

$$V_1(\phi_h) = V_0 - \frac{1}{2}m_H^2\phi_h^2 + \frac{1}{4}\lambda_H\phi_h^4 + \frac{M^4}{64\pi^2}\log\left(\frac{M^2}{\mu^2}\right), \tag{1.56}$$

with μ being an arbitrary renormalization scale. The integral in (1.55) can be expanded in M^2/T^2 to get

$$V_T(\phi_h) = V_1(\phi_h) - \frac{\pi^2}{90}T^4 + \frac{M^2}{24}T^2 + \cdots. \tag{1.57}$$

Then using (1.56) we obtain

$$V_T(\phi_h) = \left(\widetilde{V}_0 - \frac{\pi^2}{90}T^4 - \frac{m_H^2}{24}T^2\right) + \left(\frac{\lambda_H}{8}T^2 - \frac{1}{2}\widetilde{m}_H^2\right)\phi_h^2 + \frac{\widetilde{\lambda}_H}{4}\phi_h^4 + \cdots, \tag{1.58}$$

where $\left\{\widetilde{V}_0, \widetilde{m}_H, \widetilde{\lambda}_H\right\}$ represent one-loop renormalized model parameters of the zero-temperature Higgs potential. From this expression we see that for $\widetilde{m}_H^2 > 0$, the coefficient of the ϕ_h^2 term changes sign at a critical temperature T_c given by

$$T_c \approx \frac{2\widetilde{m}_H}{\sqrt{\lambda_H}}. \tag{1.59}$$

Therefore the electroweak symmetry, which is broken at zero temperature, was unbroken when the temperature of the universe was higher than this critical temperature. Precise determination of this value requires the knowledge of the renormalized model parameters,

but as an order of magnitude estimate we can accept $T_c \sim 100\,\text{GeV} \sim m_{\text{EW}}$, where m_{EW} is the *electroweak scale*.

Now, let us investigate what will happen to the vacuum energy density after the symmetry restoration. Using (1.54) we can calculate the energy density as

$$\rho_\phi = \left(\widetilde{V}_0 + \frac{\pi^2}{30}T^4 + \frac{m_H^2}{24}T^2\right) - \left(\frac{\lambda_H}{8}T^2 + \frac{1}{2}\widetilde{m}_H^2\right)\phi_h^2 + \frac{\widetilde{\lambda}_H}{4}\phi_h^4. \tag{1.60}$$

At zero temperature, the minimum of the potential is at $\phi_h(T=0) = \frac{\widetilde{m}_H}{\sqrt{\widetilde{\lambda}_H}}$ then the vacuum energy density at zero temperature becomes

$$\rho_\phi(T=0) = \widetilde{V}_0 - \frac{\widetilde{m}_H^4}{4\widetilde{\lambda}_H}. \tag{1.61}$$

On the other hand at high temperature $T \gg T_c$ the electroweak symmetry is restored so the minimum of the finite temperature potential is at $\phi_h(T \gg T_c) = 0$. In this case the vacuum energy density is

$$\rho_\phi(T \gg T_c) = \widetilde{V}_0 + \frac{\pi^2}{30}T^4 + \frac{m_H^2}{24}T^2. \tag{1.62}$$

Therefore the change in the vacuum energy during the phase transition at $T = T_c$ is given by

$$\Delta\rho_\phi \equiv \rho_\phi(T=T_c) - \rho_\phi(T=0) \approx \frac{\pi^2}{30}T_c^4 + \frac{\widetilde{m}_H^4}{4\widetilde{\lambda}_H} \sim T_c^4, \tag{1.63}$$

where we have ignored the T_c^2 term and used (1.59). From this calculation, we conclude that a phase transition at some critical temperature T_c should be accompanied by a jump in vacuum energy density at the order of T_c^4. This result does not depend on the order of the phase transition.

We have showed that even if the vacuum energy density is very small today for some

unknown reason, it wasn't always small during the history of the universe. We know that the universe had at least two phase transitions; one is the electroweak phase transition at $T_c \sim m_{\rm EW} \sim 100\,{\rm GeV}$, the other is the QCD phase transition at $T_c \sim \Lambda_{\rm QCD} \sim 200\,{\rm MeV}$. It is a possibility that they are other phase transitions, such as the phase transition to a Grand Unified Theory (GUT), at much higher temperatures like $T_c \sim 10^{15}\,{\rm GeV}$. We don't know yet whether the vacuum energy did really behave like this, since most of the phenomena relevant to the observational cosmology, such as Cosmic Microwave Background (CMB), structure formation, nucleosynthesis, are sensitive to the temperatures well below the QCD scale. Moreover, both phase transitions are either second order or crossover, so their imprints are much weaker compared to first order phase transitions. For example, a strongly first order phase transition might have an imprint in the gravitational waves, which can be measured with future space-based interferometers such as the proposed *Laser Interferometer Space Antenna (LISA)* [44].

Despite the fact that the vacuum energy density might be large at earlier times, it should not have dominated the total energy density until very late times. During both phase transitions, the universe was always radiation dominated, except during the phase transitions. This makes the cosmological constant problem much more peculiar for the following reason. Let us assume that only electroweak and QCD phase transitions happened during the evolution of the universe at temperatures $T_c^{\rm EW} \sim 100\,{\rm GeV}$ and $T_c^{\rm QCD} \sim 200\,{\rm MeV}$ respectively. Then the universe should start with a vacuum energy density slightly larger than $T_c^{\rm EW}$, but not too much so that it can remain subdominant. After the electroweak phase transition, the vacuum energy density drops by a factor of $\sim (T_c^{\rm EW})^4$, but this decrease should be such that there is enough vacuum energy left for the QCD phase transition. In other words, the jump should satisfy

$$\rho_\phi(T \gtrsim T_c^{\rm EW}) - \rho_\phi(T \lesssim T_c^{\rm EW}) \sim \left(T_c^{\rm QCD}\right)^4 \sim (200\,{\rm MeV})^4\,. \tag{1.64}$$

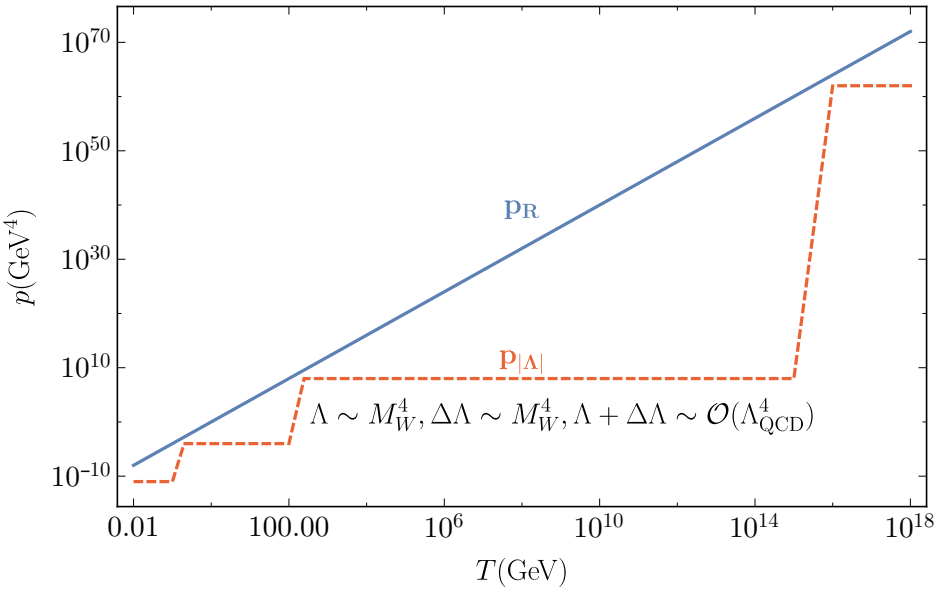

Figure 1.1: The evolution of the radiation pressure p_R and the vacuum energy density ρ_V. From left to right, the jumps in the vacuum energy density represent the electroweak, QCD and (hypothetical) GUT phase transitions. Adapted from [45].

Thus, the universe somehow *knows* when the *next* phase transition will be [45]. This behavior is shown in Figure 1.1. This strange property makes the cosmological constant problem one of most important questions in fundamental physics.

1.5 Organization of the Dissertation

In this dissertation, our aim is to describe two possible approaches for understanding the problems related to the UV sensitivity of the relevant operators. One approach will be from a model building perspective while the other one will be from a phenomenological perspective. We will try to address the hierarchy problem with the former, and the cosmological constant problem with the later.

In Chapter 2, we will explain most popular proposals for solving the hierarchy problem. In particular, we will describe models with warped extra dimensions and the AdS/CFT correspondance in detail, which are the fundamental building blocks of the model we will present in Chapter 3.

In Chapter 3, we will present an attempt for solving the hierarchy problem where we will try to relate the *critical point* of the Higgs sector to a minimum in the potential for a dynamical field. The hope of this relation is to make the Higgs criticality an attractor, so that a (classical) zero Higgs mass can be obtained for a sizable region in parameter space. We will build our model on a five dimensional geometry, where the extra dimension is a circle. The modulus field whose minimum sets the classical Higgs mass to zero will be identified with the *radion*, which corresponds to the size of the warped extra dimension. Using the AdS/CFT correspondance, we will comment on the interpretation of our model as a strongly coupled approximate conformal field theory in four spacetime dimensions.

In Chapter 4, we will argue that the behavior of the vacuum energy during phase transitions can be tested experimentally using the gravitational waves emitted by a merger of two neutron stars. Instead of a phase transition at large temperature, we will focus on a phase transition of QCD which is expected to occur at zero temperature but at very high nuclear density. Such densities are expected to be found at the cores of heavy neutron stars. If such a phase transition exists, then it will drammatically affect the *equation of state (EoS)* of neutron stars, and such an affect might have a big imprint on gravitational wave observables. Thus, neutron star mergers might provide an unique test bed for testing whether the vacuum energy really jumps during the phase transitions.

Chapter 2

Solutions to the Hierarchy Problem

In Section 1.2 we have argued that the SM *should* be treated as an effective theory, and in Section 1.3 we have shown that this treatment makes the Higgs mass extremely sensitive to the UV physics and causes the hierarchy problem. In this chapter we will briefly mention some strategies for taming this problem. Since we have also showed explicitly that the quadratic divergences are really placeholders for new physics, we take the result in (1.34) as our starting point.

2.1 Supersymmetry (SUSY)

The main property of SUSY which provides a solution to the hierarchy problem is that it imposes a relation between the elementary scalars and the fermions, so that the chiral symmetry which is protecting the fermion masses can be extended to protect the elementary scalar masses. The SUSY provides exactly this kind of relation.

The mathematical motivation of SUSY comes from the *Coleman - Mandula theorem*, which states that it is not possible to build a consistent QFT based on a non-trivial, i.e. *non-commuting*, combination of internal symmetries and spacetime symmetries [46]. However, as shown by Haag, opuszaski and Sohnius, there is one possible exception which is to use a *graded Lie algebra* whose generators are fermionic [47].

The anticommutation relation which defines SUSY is given by[1]

$$\left\{Q_\alpha, Q^\dagger_{\dot\alpha}\right\} = 2\sigma^\mu_{\alpha\dot\alpha} P_\mu \tag{2.1}$$

where Q and $Q^\dagger$ are SUSY generators, also called *supercharges*, and P_μ is the momentum operator. The $\{\alpha, \dot\alpha\} = 1, 2$ are the spinor indices[2] and

$$\sigma^\mu_{\alpha\dot\alpha} = \left\{1_{2\times2}, \sigma^i\right\} \quad , \quad \bar\sigma^{\mu\dot\alpha\alpha} = \left\{1_{2\times2}, -\sigma^i\right\}, \tag{2.2}$$

with $\{\sigma^i\}$ being the Pauli matrices and $1_{2\times2}$ is the 2×2 unit matrix. Single particle states are irreducible representations of the SUSY algebra (2.1) and are called *supermultiplets*. Each supermultiplet contains an equal number of bosonic and fermionic degrees of freedom [48]. The bosons and the fermions inside the same supermultiplet are called *superpartners* of each other. The simplest examples of supermultiplets are

- *Chiral supermultiplet:* Contains a complex scalar and a Weyl fermion.
- *Vector supermultiplet:* Contains a gauge field and a Weyl fermion.

The simplest way to make the SM supersymmetric is to assume that each SM degree of freedom is either in a chiral or in a vector supermultiplet, and introduce superpartners for them. This is known as the *Minimal Supersymmetric Standard Model (MSSM)* [49–52]. The superpartners of the SM fermions are named with a "s-" prefix, while the superpartners of SM bosons are named with a "-ino" postfix. For example the superpartner of the electron is called *selectron*, while the superpartner of the Higgs is called *Higgsino*. The particle content of the MSSM is shown in Table 2.1. Notice that there are two Higgs supermultiplets, one corresponding to the SM Higgs and another with the same SM representations but with opposite hypercharge. The reason for introducing an extra supermultiplet is to cancel the

[1] This relation can be extended to multiple supercharges $\{Q_A\}_{A=1}^{\mathcal{N}}$. In order to solve the hierarchy problem $\mathcal{N} = 1$ will be enough.

[2] In calculations with spinors, the spinor indices of conjugate spinors, like $Q^\dagger$ are written as $\dot\alpha$.

Superpartners	SM Particles	$\mathsf{SU}(3)_C$	$\mathsf{SU}(2)_L$	$\mathsf{U}(1)_Y$
$\left\{\widetilde{G}^a\right\}_{a=1}^{8}$	$\left\{G^a\right\}_{a=1}^{8}$	**Ad**	**1**	0
$\left\{\widetilde{W}^a\right\}_{a=1}^{4}$	$\left\{W^a\right\}_{a=1}^{4}$	**1**	**Ad**	0
$\left\{\widetilde{L}^i\right\}_{i=1}^{3}$	$\left\{L^i\right\}_{i=1}^{3}$	**1**	$\square$	$-\frac{1}{2}$
$\left\{\widetilde{e}_R^i\right\}_{i=1}^{3}$	$\left\{e_R^i\right\}_{i=1}^{3}$	**1**	**1**	-1
$\left\{\widetilde{Q}^i\right\}_{i=1}^{3}$	$\left\{Q^i\right\}_{i=1}^{3}$	$\square$	$\square$	$\frac{1}{6}$
$\left\{\widetilde{u}_R^i\right\}_{i=1}^{3}$	$\left\{u_R^i\right\}_{i=1}^{3}$	$\square$	**1**	$\frac{2}{3}$
$\left\{\widetilde{d}_R^i\right\}_{i=1}^{3}$	$\left\{d_R^i\right\}_{i=1}^{3}$	$\square$	**1**	$-\frac{1}{3}$
$\widetilde{H}_u = \left\{\widetilde{H}_u^+, \widetilde{H}_u^0\right\}$	$H_u = \left\{H_u^+, H_u^0\right\}$	**1**	$\square$	$\frac{1}{2}$
$\widetilde{H}_d = \left\{\widetilde{H}_d^0, \widetilde{H}_d^-\right\}$	$H_d = \left\{H_d^0, H_d^-\right\}$	**1**	$\square$	$-\frac{1}{2}$

Table 2.1: Particle content of the MSSM. The description of the representations is the same in Table 1.1. Superpartners are shown with a $\widetilde{}$. A second Higgs supermultiplet is needed to cancel the gauge anomaly.

gauge anomalies.

The degeneracy between fermions and bosons is the mechanism in SUSY which protects the Higgs mass getting quadratically divergent corrections. As an example, the Λ^2 contribution from the top quark loops will be cancelled by the Λ^2 contribution from the *stop* loops, where stop is the superpartner of the top quark. Of course this requires that both Yukawa couplings y_t be the same but since both top quark and stop live under the same supermultiplet, this is satisfied by definition in MSSM. Such cancellations occur for all the diagrams contributing to the Higgs mass to all orders in perturbation theory. An easy way to see this is to remember that SUSY introduces a degeneracy between the fermion and boson masses and as we saw at the end of Section 1.3, the fermion masses are protected by chiral symmetry.

If SUSY were a perfect symmetry of the nature, then the superpartners should have the

same masses as their SM partners, and therefore we would have discovered them long time ago. Since this is not the case, SUSY must be broken at some scale m_{SUSY}. Then following the discussion of Section 1.4, just by dimensional analysis, we can argue that the quantum corrections to the Higgs mass in a broken SUSY should have the form

$$\delta m_H^2 \sim \frac{\lambda^2}{16\pi^2} m_{\text{SUSY}}^2 \log\left(\frac{\Lambda_{\text{SUSY}}}{m_{\text{SUSY}}}\right), \tag{2.3}$$

where λ is some dimensionless coupling and Λ_{SUSY} is cutoff of SUSY. Since the SUSY breaking results in mass splittings between the SM particles and their superpartners, m_{SUSY} determines the order of these splittings. Then (2.2) tells us that irrespective of the cutoff Λ_{SUSY}, we need $m_{\text{SUSY}} \sim \mathcal{O}(\text{TeV})$ in order to get rid of the fine tuning. This condition is under tense pressure from the results of the LHC experiments [53]. Even if SUSY does exist in nature, it might not be a perfect solution for the hierarchy problem as people have thought in the beginning.

2.2 Composite Higgs Models

The main idea behind the *Composite Higgs (CH)* models [54] is to abandon the idea that the Higgs is an elementary scalar, and consider it to be a *bound state* of a strongly interacting sector. This idea is reminiscent of what happens in QCD, where spin-0 pions are bound states which arise due to condensation of quarks. Before the discovery of the Higgs, a popular way to explain the hierarchy problem was using the *technicolor* models where the electroweak symmetry breaking occurs directly via a strong condensate, not due to the Higgs [55–57]. Hence technicolor models generally do not predict a Higgs particle, after the discovery of the SM-like Higgs, such models are strongly disfavored. CH models are modifications of technicolor models, which produces the Higgs as a bound state[3].

The main ingredient of CH models is a new strongly interacting *composite* sector which

[3]This discussion of CH models is based on [25]

confines around the energy scale $f \sim \mathcal{O}(1 - 10\,\text{TeV})$. This sector emerges from an even more fundamental theory which is defined at a very high scale $\Lambda_{\text{UV}} \gg f$. The value of this scale is not important since the main goal of this construction is to make the Higgs mass insensitive to higher scales. One further assumes that at the scale Λ_{UV}, this sector sits close to a fixed point of its RG evolution and there is no strongly relevant deformations around this fixed point. The motivation behind this assumption is to generate a reasonable hierarchy between the scales f and Λ_{UV} without introducing severe tuning.

However, this is not enough. If the Higgs were a regular bound state, then its mass would be comparable to the breaking scale f. Then the composite sector would have confined around $f \sim \mathcal{O}(100\,\text{GeV})$ and this would have introduced a zoo of bound states, called *resonances*, with masses below TeV. Since these states have not been observed, the CH models should be accompanied by some mechanism which explains the mass hierarchy between the Higgs and the resonances. This is possible if the Higgs is promoted to a *Nambu-Goldstone Boson (NGB)*.

NGBs arise due to spontaneous breaking of global symmetries as a result of the *Goldstone Theorem* [58]. This theorem states that spontaneous breaking of a global symmetry G into one of its subgroups $H \subset G$ implies the existence of *massless* degrees of freedom in the broken theory which are called NGBs. The number of NGBs is equal to the number broken generators. Mathematically speaking, the NGBs *span* the *coset space* G/H. After the symmetry breaking, the broken part of the global symmetry realizes itself as *shift symmetries* for the NGBs. These shift symmetries allow only derivative interactions for the NGBs, hence quantum correction cannot generate a potential for them. This restriction can be avoided if the global symmetry G were an *approximate* symmetry which is *explicitly* broken by some terms in the Lagrangian. Then quantum corrections generate a potential for the NGBs, turning them into *pseudo NGBs (pNGBs)*.

Having all these information, the recipe to create a viable CH model is as follows: First we have the SM Lagrangian, but *without* the Higgs potential and the Yukawa interactions.

Then we have a strongly interacting composite sector with a global symmetry G which should at least contain the $\mathsf{SU}(2)_L \times \mathsf{U}(1)_Y$ subgroup. The explicit breaking of this global symmetry is done by coupling the global $\mathsf{SU}(2)_L \times \mathsf{U}(1)_Y$ conserved current of the composite sector to the electroweak gauge bosons $\{W^a\}$. This process is often described as *gauging* the $\mathsf{SU}(2)_L \times \mathsf{U}(1)_Y$ subgroup of G.

An obvious question to ask is what is the minimal possible coset G/H for a viable CH model. We have said that it should at least contain $\mathsf{SU}_L(2) \times \mathsf{U}(1)_Y$. But this is usually not enough. The strongest constraints to the BSM models come from the *electroweak precision observables*, i.e. S and T parameters. The T parameter is more constraining and it predicts

$$\rho \equiv \frac{m_W^2}{m_Z^2 \cos^2 \theta_W} = 1 \pm \mathcal{O}(1\%). \tag{2.4}$$

The reason that this value is very close to 1 is the approximate *custodial symmetry* in the SM. To see this symmetry, note that the SM Higgs potential (1.5) is invariant under a global $\mathsf{SU}(2)_L \times \mathsf{SU}(2)_R$ symmetry under which

$$H \to U_L H U_R^\dagger, \tag{2.5}$$

where $U_L \in \mathsf{SU}(2)_L$ and $U_R \in \mathsf{SU}(2)_R$. When the Higgs gets a VEV, only $\mathsf{SU}(2)_L$ part is broken. There is still a left-over $\mathsf{SU}(2)_R$ symmetry, known as the *custodial symmetry*. Although this symmetry is broken by Yukawa couplings, their contributions to (2.4) are smaller than 1%.

Therefore a good strategy for model building various BSM models is to respect this custodial symmetry. With this condition the minimal coset is $\mathsf{SO}(5)/\mathsf{SO}(4)$. Such a model is studied in [59,60], where the global symmetry of the composite sector $G = \mathsf{SU}(3)_c \otimes \mathsf{SO}(5) \otimes \mathsf{U}(1)_{B-L}$ is spontaneously broken into $H = \mathsf{SU}(3)_c \otimes \mathsf{SO}(4) \otimes \mathsf{U}(1)_{B-L}$[4]. This model is known

[4]The $\mathsf{U}(1)_B$ and $\mathsf{U}(1)_L$ are symmetries of the SM which correspond to baryon number and lepton number conservation respectively. While both symmetries are anomalous, their combination $\mathsf{U}(1)_{B-L}$ is exact.

as the *Minimal Composite Higgs Model (MCHM)*.

2.3 Large/Warped Extra Dimensions

The idea of introducing extra space dimensions in order to solve physical problems dates back to the attempts by Theodor Kaluza and Oskar Klein to unify gravitation and classical electromagnetism. Their idea was to introduce a fifth space dimension which is compactified into a circle of microscopic size [61–63]. This way both the metric of gravitation $g_{\mu\nu}$ and the vector potential of electromagnetism A^μ can be expressed in terms of a 5-dimensional metric g^5_{mn}, which is given by

$$g^5_{mn} = \left(\begin{array}{c|c} g_{\mu\nu} & A_\mu \\ \hline A_\mu & \phi_r \end{array}\right), \tag{2.6}$$

where ϕ_r is an extra scalar field which corresponds to the 55-component of the 5-dimensional metric. It is often called the *radion*.

Although this strategy didn't accomplish the unification of the gravity and the electromagnetism, most of the ideas and terminology in modern extra dimensional theories stem from the model of Kaluza and Klein. We shall now describe the basics of these models and explain why there are viable models to address the hierarchy problem[5].

The easiest example of an extra-dimensional model is to consider all the extra dimensions to be *flat* and are compactified into a circle. Let d denote the dimension of the *full* spacetime and $D = d - 4$ be the number of compactified dimensions. The line element is[6]

$$\mathrm{d}s^2 = g_{mn}\,\mathrm{d}x^m\,\mathrm{d}x^n\,, \quad m, n = 0, 1, 2, 3, 5 \tag{2.7}$$

[5]We mainly follow [64] in this section.

[6]We will use Roman letters m, n to denote the full d-dimensional spacetime indices, while reserving Greek letters μ, ν for the usual 4-dimensional spacetime indices.

where for flat extra dimensions the metric is

$$g_{mn} = \text{diag}(1, -1, -1, \ldots, -1). \tag{2.8}$$

Since all the physics we have observed so far are consistent with a four-dimensional spacetime, we assume that the extra dimensions are compactified into a D-dimensional *torus* expressed as

$$\mathbb{T}^D = \prod_{i=5}^{D+4} \mathbb{S}^1(R_i), \tag{2.9}$$

where $\mathbb{S}^1(R)$ is a circle with radius R, i.e. R_5 and R_6 are the radii of fifth and sixth dimensions respectively.

Now consider a massive real scalar field ϕ living on a 5-dimensional spacetime. Let us also denote the $4d$ spacetime coordinates by x and extra dimensional spacetime coordinate by y. Then action can be written as

$$S = \int \mathrm{d}^4x \, \mathrm{d}y \left(\frac{1}{2} \partial_m \phi(x,y) \partial^m \phi(x,y) - \frac{1}{2} m_0^2 \phi(x,y)^2 \right). \tag{2.10}$$

Since we are interested in the effects of extra dimensions on the four-dimensional physics, we should find a way to construct a $4d$ EFT out of this extra dimensional action. This can be done using a procedure called *Kaluza-Klein (KK) decomposition*. Here one solves the equation of motion (EOM) for ϕ, plug back in the action (2.10) and finally integrate over the extra dimension. This is also described as *integrating out* the extra dimension. The EOM for ϕ is

$$\left(\partial_m \partial^m + m_0^2\right) \phi(x,y) = \left(\partial_x^2 + m_0^2 - \partial_y^2\right) \phi(x,y) = 0, \tag{2.11}$$

where $\partial_x^2 \equiv \partial_\mu \partial^\mu$. The key step in the KK decomposition is to use the fact that the extra

dimensions are compactified, in order to express the scalar field $\phi(x, y)$ as a Fourier series. If the extra dimension is compactified on a circle of radius R, then the Fourier expansion of the scalar field becomes

$$\phi(x, y) = \frac{1}{\sqrt{2\pi R}} \sum_{n \in \mathbb{Z}} \phi_{(n)}(x) \exp\left\{ i \frac{n}{R} y \right\}, \tag{2.12}$$

where $\mathbb{Z}$ is the set of integers. Since ϕ is real, this sets $\phi^*_{(n)}(x) = \phi_{(-n)}(x)$. Plugging this back into the action (2.10), integrating out the extra dimension using the orthogonality relations gives

$$S_{\text{eff}} = \int \mathrm{d}^4 x \left(\partial_\mu \phi^*_{(0)} \partial^\mu \phi_{(0)} - m_0^2 \left| \phi_{(0)} \right|^2 \right) + \sum_{n=1}^{\infty} \left(\partial_\mu \phi^*_{(n)} \partial^\mu \phi_{(n)} - \frac{n^2}{R^2} \left| \phi_{(n)} \right|^2 \right). \tag{2.13}$$

So in the effective theory we have a complex scalar field $\phi_{(0)}$ with the mass m_0 plus an *infinite* number of heavy particles with masses $m_n = n/R$, which are called *KK modes*, or *KK tower*. As the radius of the extra dimension is getting smaller, the masses of KK modes become heavier.

A similar analysis can also be done for the gauge fields for which the action reads

$$S = \int \mathrm{d}^4 x \, \mathrm{d}y \left(-\frac{1}{4} F_{mn} F^{mn} \right), \tag{2.14}$$

where $F_{mn} = \partial_m A_n - \partial_n A_m$, and

$$A_m = \begin{pmatrix} A_\mu \\ A_5 \end{pmatrix}. \tag{2.15}$$

Under $4d$-Poincare transformations A_μ is a vector while A_5 is a scalar. The KK decomposition

can be done as in the scalar case. The Fourier expansion is

$$A_m(x,y) = \frac{1}{\sqrt{2\pi R}} \sum_{l\in\mathbb{Z}} A_m^{(l)}(x) \exp\left\{ i\frac{l}{R} y \right\}. \tag{2.16}$$

Plugging this into (2.14) and performing the integration over the extra dimension gives

$$\begin{aligned} S_{\text{eff}} = \int \mathrm{d}^4x \Bigg\{ & \left[-\frac{1}{4} F_{\mu\nu}^{(0)} F^{\mu\nu(0)} + \frac{1}{2} \partial_\mu A_5^{(0)} \partial^\mu A_5^{(0)} \right] \\ & + \sum_{l=1}^{\infty} \left[-\frac{1}{2} F_{\mu\nu}^{(l)} F^{\mu\nu(-l)} + \frac{l^2}{R^2} A_\mu^{(l)} A^{\mu(-l)} - i\frac{l}{R} \left(A_\mu^{(l)} \partial^\mu A_5^{(-l)} - A^{\mu(-l)} \partial_\mu A_5^{(l)} \right) \right] \Bigg\}. \end{aligned} \tag{2.17}$$

The last term suggest a mixing between $A_\mu^{(l)}$ and $A_5^{(l)}$ when $l \neq 0$. But this mixing can be removed by gauge freedom. Namely in the $5d$ *axial gauge* we can set

$$A_\mu^{(l)} \to A_\mu^{(l)} - \frac{i}{l/R} \partial_\mu A_5^{(l)}, \quad A_5^{(l)} \to 0, \quad \text{for} \quad l \neq 0, \tag{2.18}$$

which removes this mixing term. So the effective action we get is

$$S_{\text{eff}} = \int \mathrm{d}^4x \left\{ \left[-\frac{1}{4} F_{\mu\nu}^{(0)} F^{\mu\nu(0)} + \frac{1}{2} \partial_\mu A_5^{(0)} \partial^\mu A_5^{(0)} \right] + 2 \sum_{l=1}^{\infty} \left[-\frac{1}{4} F_{\mu\nu}^{(l)} F^{\mu\nu(-l)} + \frac{1}{2} \frac{l^2}{R^2} A_\mu^{(l)} A^{\mu(-l)} \right] \right\}. \tag{2.19}$$

So in the effective theory we have a massless gauge boson $F_{\mu\nu}^{(0)}$, a massless scalar field $A_5^{(0)}$ and a tower of massive gauge bosons $\left\{ A_\mu^{(l)} \right\}_{l=1}^{\infty}$. The excitations of A_5's are unphysical since they can be removed by gauge fixing.

Now consider the gauge covariant derivative in this setup. It is given by

$$D_m = \partial_m - i g_5 A_m, \tag{2.20}$$

where g_5 is the $5d$ gauge coupling. Since $[\partial_m] = 1$, from (2.14) the mass dimensions of the

field strength F_{mn} and the gauge field A_m should be $[F_{mn}] = 5/2$ and $[A_m] = 3/2$ in $5d$. But then (2.20) tells us that the $5d$ gauge coupling g_5 should be dimensionful and $[g_5] = -1/2$. We can get a dimensionless *effective* $4d$ *gauge coupling* by plugging the Fourier expansion (2.16) into (2.20). This way we find

$$D_\mu = \partial_\mu - ig_5 \left(\frac{1}{\sqrt{2\pi R}} A_\mu^{(0)} + \dots \right), \tag{2.21}$$

which says that the effective $4d$ coupling constant g_4 is

$$g_4 = \frac{g_5}{\sqrt{2\pi R}}. \tag{2.22}$$

This result can be generalized to higher dimensions by [65]

$$g_4^2 = \frac{g_{4+D}^2}{\mathrm{vol}_D}, \tag{2.23}$$

where vol_D is the total volume of the extra dimensions.

Same exercise can also be done for the gravitational coupling. The *Einstein-Hilbert action* in a flat spacetime with D extra dimensions is given by[7]

$$S_{4+D} = -M_{4+D}^{2+D} \int \mathrm{d}^{4+D}x \, \sqrt{|g_{4+D}|} \mathcal{R}_{4+D}, \tag{2.24}$$

where M_{4+D} is the analog of Planck scale in higher dimensions. For flat extra dimensions we have $\mathcal{R}_{4+D} = \mathcal{R}_4$ at linear order [65], thus after integrating out the extra dimension we get

$$S_{4+D} = -M_{4+D}^{2+D} \int \mathrm{d}^D x \, \sqrt{|g_D|} \int \mathrm{d}^4 x \, \sqrt{|g_4|} \mathcal{R}_4 = -M_{4+D}^{2+D} \, \mathrm{vol}_D \int \mathrm{d}^4 x \, \sqrt{|g_4|} \mathcal{R}_4, \tag{2.25}$$

[7] The power of the Planck scale $2 + D$ comes from the fact that the mass dimension of the Ricci scalar is $[\mathcal{R}] = 2$ in all dimensions.

Thus we obtain the Planck scale in an extra dimensional theory as

$$M_{4+D}^{2+D} = \frac{M_{\rm pl}^2}{\mathrm{vol}_D}. \tag{2.26}$$

We can now try to estimate the *natural* size of the extra dimension. The simplest assumption would be that all dimensionful parameters are set by the same physical scale and take that scale to be M_{4+D}. By generalizing the exercise following (2.20), we can find that in the case D extra dimensions $[g_{4+D}] = -D/2$, so the natural size of this gauge coupling is

$$g_{4+D} \sim \frac{1}{M_{4+D}^{D/2}}. \tag{2.27}$$

Combining this result with (2.26) and (2.23) gives

$$\mathrm{vol}^{1/D} \sim R \sim \frac{1}{M_{\rm pl}} g_4^{-\frac{2+D}{D}}, \tag{2.28}$$

where R is the average size of the extra dimensions. The result shows that the natural size of the extra dimensions would be on the order of the Planck length $l_{\rm pl} \sim 10^{-35}\,\mathrm{m}$ and the KK modes are at the Planck scale. Clearly this is not a viable phenomenological model. Moreover this model didn't help to solve the hierarchy problem at all. It is important to keep in mind that in this setup all the SM particles are propagating in the *bulk*, which is the space spanned by the extra dimensions. We shall see now the situation drastically changes if one relaxes this assumption.

Instead of letting them to propagate through the whole bulk, the fields can be *localized* by introducing the concept of *branes*. Branes are $3+1$ dimensional *hypersurfaces* with localized stress-energy tensor so that fields can be trapped on them. Mathematically one can define them as topological defects of some sort. String theories have similar objects, called *D-branes* where open strings are attached. From a BSM model building point of view, it is not important how these branes did end up there. All the models we will mention in

this section should be considered as effective field theories valid up to some cutoff scale Λ_{UV}. Proper explanation of the branes should be handled by some new physics which is expected to replace the effective description at the cutoff scale.

The simplest implementation of branes in extra-dimensional theories is the scenario of *Large Extra Dimensions*, introduced by Arkani-Hamed, Dimopoulos, and Dvali [66]. In their model, all the SM fields are localized on a brane, and only gravity can propagate through the bulk. Then, as a consequence of (2.26) one can lower the fundamental scale of gravity $M_{4+D} \equiv M_*$ considerably by choosing volume the extra dimensional space vol_D to be large. Since M_* is the cutoff which will enter to the SM calculations, lowering M_* to the TeV would solve the hierarchy problem.

If there are D extra dimensions with a similar radii R, then from (2.26) we can write

$$R \sim \frac{1}{M_*} \left(\frac{M_{\text{pl}}}{M_*} \right)^{2/D} . \tag{2.29}$$

Choosing $M_* \sim 1\,\text{TeV}$ and $M_{\text{pl}} \sim 10^{19}\,\text{GeV}$ gives

$$R \sim (1\,\text{TeV})^{-1} \times 10^{32/D} \sim 10^{(32/D-19)}\,\text{m}. \tag{2.30}$$

For $d = 1$, this gives $R \sim 10^{13}\,\text{m}$ which is on the order of the solar system and is clearly ruled out. For $d = 2$, we get $R \sim 1\,\text{mm}$. Although this might seem large too, it is very hard to experimentally test the gravity. The current bound is $R < 37\,\mu\text{m}$ [67,68] which excludes $d = 2$ with $M_* \sim 1\,\text{TeV}$, but not too much. This bound can be avoided if $M_* \gtrsim 3\,\text{TeV}$. However much stringent bounds exist from astrophysical and cosmological observations which pushes M_* to $M_* > 10 - 10^3\,\text{TeV}$ [69–71].

For larger D, the sizes of extra dimensions are within experimental limits. However this idea has one big conceptual issue. If M_* is the fundamental scale of the theory, then the size of the extra dimension should also be determined by that scale, which would imply $R \sim M_*^{-1}$. But (2.29) shows that if there is a large hierarchy between M_{pl} and M_*, which is

needed to solve the hierarchy problem, then $R \gg M_*^{-1}$. In other words, this model redefines the hierarchy problem between the weak scale and gravity to the hierarchy problem between the size of the extra dimension and the fundamental gravity scale.

An obvious next step would be to abandon the assumption flat extra dimensions and consider extra dimensions with non-trivial geometry. This is not an easy task though since it is generally very hard to find gravity solutions. Such a solution were found by Randall and Sundrum in their famous paper [72]. They showed that a metric of the form

$$\mathrm{d}s^2 = \left(\frac{R}{z}\right)^2 \left(\eta_{\mu\nu}\,\mathrm{d}x^\mu\,\mathrm{d}x^\nu - \mathrm{d}z^2\right). \tag{2.31}$$

with R being a constant, is a solution to the $5d$ Einstein equations on a $5d$ *interval* with *negative cosmological constant* Λ, bounded by two branes having tensions T_0 and T_1. These branes are called *UV* and *IR* branes respectively. (2.31) is the metric for the *5-dimensional Anti-de-Sitter* AdS_5 space and the conformal factor $(R/z)^2$ is called the *warp factor*. We will see that this warp factor will play a big role in addressing the hierarchy problem. This model and other models which are based on this one are called *Randall-Sundrum (RS) models* in the literature.

We will now calculate the effective $4d$ gravity and gauge couplings. We will assume that the branes are located at $z_0 \sim R \sim M_{\mathrm{pl}}^{-1}$ and $z_1 \sim R' \sim$ TeV. Matching the gravity coupling is slightly more involved in this case, since the extra dimension is not flat. This can be done by embedding the $4d$ graviton $h_{\mu\nu}(x)$ into the AdS_5 metric as [65]

$$\mathrm{d}s^2 = \left(\frac{R}{z}\right)^2 \left[\left(\eta_{\mu\nu} + h_{\mu\nu}(x)\right)\mathrm{d}x^\mu\,\mathrm{d}x^\nu - \mathrm{d}z^2\right]. \tag{2.32}$$

What we need to calculate is how the Ricci tensor $\mathcal{R}^{(4)}_{\mu\nu}$ calculated from $h_{\mu\nu}$ is contained in $\mathcal{R}^{(5)}_{\mu\nu}$ which is calculated from (2.32). Since both metrics differ only by a conformal factor

$(R/z)^2$ we find

$$\mathcal{R}^{(5)} \supset \left(\frac{R}{z}\right)^2 \mathcal{R}^{(4)}. \tag{2.33}$$

Then the effective gravity action becomes

$$S_{\text{eff}} = -M_*^3 \int \mathrm{d}^4x\, \mathrm{d}z\, \sqrt{|g^{(5)}|}\mathcal{R}^{(5)} \supset -M_*^3 \int_R^{R'} \mathrm{d}z \left(\frac{R}{z}\right)^3 \int \mathrm{d}^4x\, \sqrt{|g^{(4)}|}\mathcal{R}^{(4)}. \tag{2.34}$$

By performing the integral over the extra dimension, we find the effective Planck scale as[8]

$$M_{\text{pl}}^2 = M_*^3 R \left[1 - \left(\frac{R}{R'}\right)^2\right]. \tag{2.35}$$

We see that for $R \sim M_*^{-1}$, we have $M_{\text{pl}} \sim M_*$ so unlike in the large extra dimensional scenario, in warped space models there is no hierarchy between the $4d$ and the $5d$ gravity.

Let us do a similar exercise for the weak scale. For simplicity, assume that there is only the Higgs field and is localized on the TeV brane. Then we can add the following term to the $5d$ action:

$$S_{(5)} \supset \int \mathrm{d}^4x\, \mathrm{d}z\, \sqrt{-g_1}\delta(z - R')\mathcal{L}_H, \tag{2.36}$$

where g_1 is the *induced metric* on the TeV brane, $(g_1)_{\mu\nu} = (R/R')^2\eta_{\mu\nu}$, and $\mathcal{L}_H$ is the usual Higgs Lagrangian:

$$\mathcal{L}_H = \left(\partial^\mu H^\dagger\right)\left(\partial_\mu H\right) + m_H^2|H|^2 - \lambda_H|H|^4. \tag{2.37}$$

[8]There is an extra factor of 2 in this result coming from the fact that in RS models one usually considers the extra dimension to be a $\mathbb{S}_1/\mathbb{Z}_2$ orbifold. In these configurations the extra dimension starts as a circle $\mathbb{S}_1$ with a radius r_c and domain $-\pi r_c \leq y \leq \pi r_c$. The branes located at $y_0 = 0$ and $y_1 = \pi r_c$. Then one imposes a $\mathbb{Z}_2$ symmetry by $y \to -y$ so that the theory is formulated on a line segment $0 \leq y \leq \pi r_c$. However the integration over the extra dimension contains a double copy of this line, and hence we get an additional factor of 2.

The crucial part is that we have to use the induced metric to raise and lower the Lorentz indices in this expression, i.e.

$$\left(\partial^\mu H^\dagger\right)\left(\partial_\mu H\right) = g_1^{\mu\nu}\left(\partial_\mu H^\dagger\right)\left(\partial_\nu H\right) = \left(\frac{R}{R'}\right)^{-2}\eta^{\mu\nu}\left(\partial_\mu H^\dagger\right)\left(\partial_\nu H\right). \tag{2.38}$$

Now we can integrate out the extra dimension to get an effective $4d$ action

$$S_{(4)} \supset \int \mathrm{d}^4x\, \mathcal{L}_H^{(4)}, \tag{2.39}$$

where

$$\mathcal{L}_H^{(4)} = \left(\frac{R}{R'}\right)^2 \eta^{\mu\nu}\left(\partial_\mu H^\dagger\right)\left(\partial_\nu H\right) + \left(\frac{R}{R'}\right)^4 m_H^2|H|^2 - \lambda_H\left(\frac{R}{R'}\right)^4|H|^4. \tag{2.40}$$

However the Higgs kinetic term is not *canonically normalized*. We can normalize it by rescaling the Higgs by $H \to (R'/R)\,H$. After this rescaling we obtain

$$\mathcal{L}_H^{(4)} = \eta^{\mu\nu}\left(\partial_\mu H^\dagger\right)\left(\partial_\nu H\right) + \left(\frac{R}{R'}\right)^2 m_H^2|H|^2 - \lambda_H|H|^4. \tag{2.41}$$

The scaling factor in front of the Higgs mass term is the key property of RS models which makes them a popular solution to the hierarchy problem. We can see that even m_H is set by M_*, which would naturally be the case, in the $4d$ effective theory it appears much smaller provided that $R/R' \ll 1$. In particular, for $M_* \sim 10^{19}\,\mathrm{GeV}$ and $m_H \sim 10^2\,\mathrm{GeV}$, one needs $R/R' \sim 10^{-17}$. This result shows the key distinction between the large and the warped extra dimensions. In large extra dimensions, both weak and gravity scales are at TeV, but the apparent gravity scale is M_{pl} due to its *dilution* through the extra dimension. On the other hand in RS models, both weak and gravity scales are at M_{pl}, but the weak scale *warped down* by the extra dimension so its apparent $4d$ scale is TeV.

Now the question is how can we get a hierarchy of $R'/R \sim 10^{17}$ naturally? In RS model,

this needs to be set by hand since there is no mechanism which can stabilize the size of the extra dimension. A stabilizing mechanism was found by Goldberger and Wise shortly after the RS paper, and it is usually called *Goldberger-Wise (GW) mechanism* in the literature [73].

GW did consider a massive scalar field Φ living the bulk whose action is

$$S_{\text{GW}} = \frac{1}{2}\int \mathrm{d}^4x\,\mathrm{d}z\,\sqrt{g}\left(g^{mn}\partial_m\Phi\partial_n\Phi - m^2\Phi^2\right). \tag{2.42}$$

Again there are UV and IR branes, but this time they contain potentials for Φ:

$$S_{\text{brane}} = -\sum_{i=0,1}\int \mathrm{d}^4x\,\sqrt{-g_i}\lambda_i\left(\Phi^2 - v_i^2\right)^2, \tag{2.43}$$

where the subscripts 0 and 1 represent parameters for the UV and the IR branes respectively. These potentials cause the bulk scalar Φ to develop a z-dependent VEV, which can be obtained by solving the classical EOM arising from the variation of (2.42) with respect to Φ. The unique solution can be found with the help of the two boundary conditions imposed by the branes. This solution can then be put back into the action (2.42) and the extra dimension is integrated out. After all these steps one obtains a $4d$ *effective potential* for the size of the extra dimension. GW then showed that the effective potential has a minimum around

$$\log\left(\frac{R'}{R}\right) \approx \left(\frac{2}{mR}\right)^2 \log\left(\frac{v_0}{v_1}\right). \tag{2.44}$$

For $\log(v_0/v_1) \sim \mathcal{O}(1)$, a large hierarchy $R'/R \sim 10^{17}$ can be generated by a modest value of $(mR)^2 \sim (m/M_*)^2 \sim 0.1$.

In the paper of GW, the form of the metric is held constant, i.e. the *backreaction* of the scalar field Φ on the metric is ignored. The coupled scalar-gravity equations can be solved exactly for some bulk potentials, including the potential used in the GW model, using the *superpotential* method [74]. Such a calculation for one scalar field is presented in [75] while

the generalization to multiple fields is also possible [76].

2.4 AdS/CFT Correspondence

In this final section of this chapter, we will see how the CH models we have presented in Section 2.2 and RS models we have presented in Section 2.3 can be related to each other by using one of the most powerful ideas in theoretical physics in recent years, which is the *gauge-gravity duality*. The main reference for this section will be [77].

In physics, *duality* means the description of a physical system in completely different ways having entirely different degrees of freedom and interactions. As a basic intuition, one can think of a system, such as QCD, which is weakly coupled at high energies and therefore perturbative. At this energies, its degrees of freedoms are approximately free. However at lower energies this theory becomes strongly coupled, its degrees of freedom are no longer uncoupled from each other, and therefore perturbation theory breaks down. But at strong coupling, bound states of fundamental degrees of freedom might be formed and these can behave as a new set of variables which are weakly coupled to each other. So it is somehow expecting that a system should be able to described differently at different energies.

The *AdS-CFT correspondence* [78] is a special example of a general class of dualities known as *gauge-gravity dualities*. It is duality between *Type IIB string theory* on $\mathsf{AdS}_5 \times \mathbb{S}^5$ and $\mathcal{N} = 4$ *Super-Yang-Mills theory* which is a *Conformal Field Theory (CFT)* in four dimensions with the gauge group $\mathsf{SU}(N)$. The parameters on both sides of the duality are related to each other by

$$\left(\frac{R}{l_s}\right)^4 \Leftrightarrow 4\pi g_{\mathrm{YM}}^2 N, \tag{2.45}$$

where R is the AdS radius, l_s is the string scale and g_{YM} is the gauge coupling on the CFT side. In order to describe gravity on the AdS side classically, one needs $R \ll l_s$ which means on the CFT side we need $g_{\mathrm{YM}}^2 N$ which corresponds to strong coupling. The usefulness of

this duality lies in this observation. We can explain strongly coupled field theories by doing calculations with classical gravity.

The symmetry group of a conformal Poincare-invariant field theory in d dimensions is the *conformal group* $\mathsf{SO}(d,2)$. This group contains the Poincare transformations, d *special conformal transformations* and a *scale transformation* given by

$$D : t \to \lambda t, \quad \mathbf{x} \to \lambda \mathbf{x}. \tag{2.46}$$

Conformal field theories are field theories which are invariant under this transformations, hence they lack a physical scale. The main motivation behind the AdS/CFT correspondence is the fact that the *isometry group*[9] of AdS_{d+1} is also $\mathsf{SO}(d,2)$. The scale transformations in (2.45) are reflected on the AdS side as

$$D : t \to \lambda t, \quad \mathbf{x} \to \lambda \mathbf{x}, \quad z \to \lambda z. \tag{2.47}$$

The last transformation is crucial. It says that a scale transformation on the CFT corresponds to a *movement in the extra dimension*. Since scale transformation is related to RG evolution in a field theory we have

$$\text{movement in extra dimension} \Leftrightarrow \text{RG evolution in } 4d \text{ theory}.$$

Breaking one the symmetries on one side corresponds to breaking it on the other side. The branes we have encountered in Section 2.3 do break the AdS isometry, so they correspond to breaking of conformal symmetry on the CFT side.

A *global symmetry* of the field theory is realized as a *gauge symmetry* on the AdS side. But there is no such requirement for the *gauge symmetries* of the field theory. This is not surprising since gauge symmetries are not real symmetries; they are redundancies in the

[9] An *isometry* is a map between two metric spaces which preserve the distance.

description. Moreover since different gauge symmetries are characteristics of different degrees of freedom, so it is expected that they don't match. However gauge invariant quantities are physical, therefore they should match. This is indeed true. Each field on the gravity side corresponds to a *gauge invariant* operator in the field theory.

To see this explicitly, let us consider the action given in (2.42) without any branes but in $d+1$ dimensions. Close to the boundary of the AdS_{d+1}, $z \to 0$, we can express the solution to Φ as

$$\Phi(z \to 0, x) = z^{\Delta_-} \left[\alpha(x) + \mathcal{O}(z^2)\right] + z^{\Delta_+} \left[\beta(x) + \mathcal{O}(z^2)\right], \tag{2.48}$$

where $\alpha(x)$ and $\beta(x)$ are functions of the $4D$ coordinates and

$$\Delta_\pm \equiv \frac{d}{2} \pm \sqrt{\frac{d^2}{4} + m^2 R^2}. \tag{2.49}$$

Since $z \to \lambda z$ under a scaling transformation, the functions α and β should scale as

$$\alpha(x) \to \lambda^{-\Delta_-} \alpha(x) \quad \text{and} \quad \beta(x) \to \lambda^{-\Delta_+} \beta(x). \tag{2.50}$$

One of these functions should be fixed by boundary conditions. A commonly used choice is to fix α by $\alpha(x) \equiv J(x)$ for some choice of $J(x)$. This way $\beta(x)$ becomes a dynamical variable which in the field theory can be identified with an operator $\mathcal{O}(x)$ with scaling dimension Δ_+. Since $\mathcal{O}(x)$ is turned on after introducing $J(x)$, $J(x)$ is identified as a *source* for the operator $\mathcal{O}(x)$. Note that this implies the scaling dimension of $J(x)\mathcal{O}(x)$ is $\Delta_+ + \Delta_- = d$ which should be the case for a field theory in d dimensions. In summary, AdS/CFT provides a relation between the partition functions of the gravity and the field theory:

$$\mathcal{Z}[\Phi; \alpha(x) = J(x)] \Leftrightarrow \mathcal{Z}_{\text{CFT}}[\text{source for } \mathcal{O}(x) \text{ is } J(x)]. \tag{2.51}$$

Although it is expected that this relation to hold for generic models, we only know how to do classical gravity. The left hand side of this relation approaches to the classical gravity if one considers the *large-N limit* on the CFT side, i.e. when $g_{\rm YM}^2 N \gg 1$.

Since the scaling dimension of $\mathcal{O}$ is Δ_+ using (2.49) we can classify $\mathcal{O}$ as

$$\begin{cases} \text{irrelevant} & \text{if} \quad m^2R^2 > 0, \\ \text{marginal} & \text{if} \quad m^2R^2 = 0, \\ \text{relevant} & \text{if} \quad m^2R^2 < 0. \end{cases} \tag{2.52}$$

Unlike the Minkowski space, the AdS_{d+1} space allows scalar having negative masses as long as they satisfy the *Breitenlohner-Freedman (BF) bound* [79, 80]:

$$m^2R^2 \geq -\frac{d^2}{4}. \tag{2.53}$$

This sets the bound $\Delta \geq d/2$ for any operator in the CFT. However this bound can be lowered to $\Delta \geq d/2 - 1$ by modifying the gravity action with boundary terms [81].

With all these information we can build the bridge between the Composite Higgs and the Randall-Sundrum models. We will try to explain the general picture without specifying how the individual fields are related to each other, since they can be model dependent. We start with a pure AdS_5 space without any branes which is dual to a strongly coupled $4d$ CFT, and we identify this CFT with the composite sector of CH models. We will add ingredients one by one to either side and describe the related deformation on the other side, as it has been done in [82] which we shall follow closely.

Let us start by adding a UV, or Planck, brane. On the CFT side this gets translated to an *UV cutoff* $\Lambda_{\rm UV}$, at which the CFT description breaks down. Since the metric is still pure AdS, we still have an exact CFT below the cutoff. Moving the UV brane from $1/R$ to $1/\widetilde{R}$ where $\widetilde{R} > R$ corresponds to integrating out the degrees of freedom between the energy scales $\Lambda = 1/R$ and $\widetilde{\Lambda} = 1/\widetilde{R}$.

Putting an IR, or TeV, brane at $R' = 1/\Lambda'$ *strongly* breaks the conformal invariance of the composite sector at $1/\Lambda'$. If all the SM fields live on the TeV brane like in the RS model, then this would imply that all the SM fields emerge as bound states of the composite sector. So from the $4d$ point of view, the RS model is a theory where the SM is embedded inside a strongly coupled CFT above the TeV.

Now add a scalar field to the bulk as in the GW mechanism. We already know that it should correspond to an operator on the CFT side $\mathcal{O}_\Phi$ with scaling dimension

$$\Delta_+ = 2 \pm \sqrt{4 + m^2 R^2} \approx 4 + \frac{m^2 R^2}{4}, \quad \text{for small } m^2 R^2. \tag{2.54}$$

We see that for small $m^2 R^2$, the operator $\mathcal{O}_\Phi$ is marginally relevant for $m^2 < 0$ and marginally irrelevant for $m^2 > 0$. This operator is sourced by the coefficient of z^{Δ_-} term of (2.48). All these amount to *perturbing* the CFT by an operator

$$\mathcal{L}_{\text{CFT}} \to \mathcal{L}_{\text{CFT}} + J\mathcal{O}_\Psi, \tag{2.55}$$

which mildly breaks the conformal symmetry *explicitly*. The RG running of this operator is determined by the RG running of its coupling constant J, which will be Jz^{Δ_-}. Since $\Delta_- \approx -\frac{m^2 R^2}{4}$, for $m^2 < 0$ this coupling will grow towards the IR and at some point breaks the CFT, which is realized on the AdS side as the IR brane. The $m^2 > 0$ case can be thought as a mechanism for generating the UV brane. In this case the coupling will grow towards the UV and breaks the CFT at some UV scale, which is realized on the AdS side as an UV brane.

Chapter 3

Self-Organized Higgs Criticality

3.1 Introduction

The Higgs instability in the electroweak sector of the Standard Model (SM) appears thus far to be of the simplest variety, with the Higgs sector residing "unnaturally" close to a critical point seemingly unprotected by symmetry and well described by mean field theory. The Higgs sector is associated with a Landau-Ginzburg theory of a symmetry breaking phase transition. The Higgs field of the Standard Model develops a vacuum expectation value (VEV) due to a relevant operator (the Higgs mass term) having the "wrong sign" in the infrared which destabilizes the origin in field space. The naturalness issue, or the hierarchy problem, is the statement that in units of the much larger fundamental scales in the problem, i.e. the Planck or GUT scales, the bare mass must be tuned to an absurd degree to accommodate the observed value for the VEV and the mass of the Higgs particle, and that quantum corrections spread this sensitivity among fundamental parameters. That is, quantum effects make the Higgs mass similarly sensitive to, for example, the value of the top quark Yukawa coupling. As a consequence it is expected that low energy effective theories with Higgs sectors like that of the SM are extraordinarily rare when there are other large physical scales present.

Most proposed resolutions of this problem invoke new symmetries requiring new particles with fixed interactions that ameliorate the sensitivity of the Higgs mass to larger mass scales. The paucity of new particles at the TeV scale has sown growing doubt that this is the way nature has created a low electroweak scale.

In this work, we begin an investigation of the possibility that the critical point for Higgs sectors like that of the SM can arise naturally not due to symmetry, but rather because of a self-organization principle, as suggested in [83]. This is inspired by critical behavior that has been observed in a wide variety of seemingly unrelated physical systems in nature [84, 85], with the canonical example being the sandpile. In this example, a pile of sand is created and sustained by slowly pouring sand from a funnel onto a fixed point. The sand self-organizes into a cone with opening angle fixed by microscopic interactions between grains. Perturbations, even if only involving a single grain of sand, result in avalanches at all scales, following a power law distribution. After the avalanche, when the system has removed the perturbation, the cone of sand is in a new configuration, but still critical so long as sand continues to be slowly added. Such "self-tuning" is also thought to arise at earthquake fault lines, river bifurcations, and temporally near financial market crashes [86]. It has been key to describing some astrophysical phenomena as well [87]. It has been hypothesized that these phenomena of criticality at the threshold of "catastrophic failure" can be related to an instability arising from critical exponents becoming complex, corresponding to discrete scale invariance [88]. This possibly suggests an approach to the Higgs fine-tuning problem in extra-dimensional models in AdS space, where similar features appear when the Breitenlohner-Freedman (BF) bound [80] is violated, leading to complex scaling dimensions and a complete loss of conformality in a hypothetical 4D dual [89].

Typically, in the examples we have in statistical physics, criticality is "self-organized" by temporal loading of the system: the slow addition of sand grains at a pile's apex, gradual stress building at faults due to tectonic drift, etc. In relativistic theories, this slow temporal loading can be exchanged with mild spatial gradients, and in 5D, through the AdS/CFT

duality [78], spatial translation and gradients can be, in turn, related to scale transformations and renormalization group evolution. This further suggests an approach where the instability associated with complex scaling dimensions is reached dynamically through slow renormalization group evolution, or, in a 5D dual, via growth of a deformation of AdS space that leads to eventual violation of the BF bound. This has a parallel in some perturbative 4-dimensional theories where dimensional transmutation directs the Higgs potential [90]. In models such as the MSSM, the instability of the electroweak sector can be arrived at through quantum corrections [91–93]: RG flow from some microscopic theory seemingly devoid of instabilities evolves to an IR theory where a Higgs picks a non-vanishing condensate.

Stepping away from the background motivation, we can state generally that the eventual goal of this line of research is to have a zero for the Higgs mass term coinciding (or nearly coinciding) with a minimum in the potential for an extra-dimensional modulus field over a wide range of extra-dimensional input parameters. In this case Higgs criticality would be a dynamical attractor for the theory without extreme sensitivity to fundamental constants. In other words, such a 5D system *self-tunes* to the critical point of its 4D low energy effective Higgs theory. This is similar to the way in which the strong CP problem is resolved by the axion hypothesis where the axion field promotes the CP phase to a dynamical field whose potential minimum resides at the point where CP is conserved in QCD, and also to models which solve the hierarchy problem using cosmological dynamics and slightly broken shift symmetries [94].

To be properly identified as self-organization, in the most conservative application of this label, criticality near the minimum of the potential must be robust under reasonable variation of model input parameters: we are looking for a theory with a near-critical Higgs *region*. From the perspective of the low energy theory, at energy scales below the modulus VEV, the lightness of the Higgs would be in apparent violation of effective field theory principles and power counting, that is, a violation of the principle of locality of scales.[1]

[1]Such violation has been observed before in a toy model with discrete scale invariance [95], another suggestive connection to self-organized critical systems.

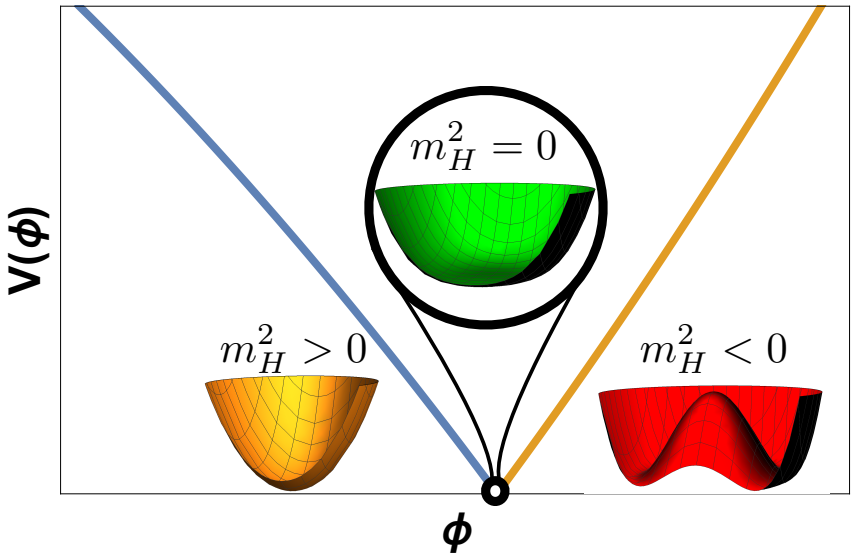

Figure 3.1: This figure exhibits a cartoon of a potential for a modulus field, ϕ, where the singular minimum matches on to a critical point at which the mass of a physical light Higgs field fluctuation passes through zero. On either side of the singular point, the Higgs boson mass is finite and positive, but on one side the mass squared for the field is negative, with the instability driving spontaneous symmetry breaking.

This could be reconciled by the fact that in a microscopic 5D theory, quantum corrections might renormalize the potential for the Higgs and modulus field simultaneously, shifting the *location* of the minimum, but not the property that the physical Higgs boson is light at that minimum. A cartoon is shown in Figure 3.1. We emphasize that this has not yet been realized in a dynamical model in this work, but rather is a longer term goal in which this paper could be a crucial first step.

To realize such a scenario, there first must be a feedback mechanism, such that when the Higgs field develops a VEV, the potential for the modulus responds, as shown in Figure 3.1. This is somewhat akin to the way thresholds can play an important role in Casimir energies, as in, for example [96]. If this feedback is itself the origin of the minimum of the potential, with the minimum being at or near the critical value at which the Higgs VEV turns on, the modulus field will be attracted to the minimum, where the mass of the Higgs fluctuation is small or vanishing.

In one "toy" and one fully dynamical construction, we investigate the mutual potential

of a modulus field (in our case, the radion of a Randall-Sundrum (RS) 2-brane model [72]) and a 5D Higgs field. The models are constructed so that the value of the modulus field vacuum expectation value influences the Higgs stability criterion. Specifically, we consider scenarios where the Higgs instability is linked to dynamical violation of the BF bound far from the UV boundary of the RS geometry through interactions with the modulus field.

The CFT dual of this picture corresponds to the theory described above: one which is conformal in the deep UV, without instabilities, and which contains a near marginal deformation that drives a slow running of the scaling dimension of an operator in this approximate CFT [82, 97]. There is an interplay between two operators, $\mathcal{O}_\epsilon$, a near marginal operator, and $\mathcal{O}_H$. Similar to the way dynamical symmetry breaking for the Higgs can occur via radiative corrections, here an analogous instability is reached in the RG flow for the dual picture, with the scaling dimension for the operator $\mathcal{O}_H$ becoming complex, and causing an "unhealthy" [98] limit cycle-like behavior in the RG flow that is terminated by condensation of operators in the approximate CFT, breaking the approximate conformal invariance spontaneously.

Curiously, in the models studied here, a nontrivial cosmology may be a common feature of the classical ground state. In the 5D picture, the metric and scalar fields must include a cosmology for the low energy 4D effective theory in order to satisfy the metric junction conditions for the two brane model, unless UV and IR brane tensions are tuned. We suspect this is due to a frustration mechanism similar to that which causes striped and other inhomogeneous phases to appear in some high T_c superconductors [99], and may lead in this case to a time-dependent vacuum state [100, 101]. Studies of holographic superconductivity have identified such phases when the BF bound is violated deep in the interior of asymptotically AdS geometries due to non-trivial gauge and gravitational field backgrounds [102]. In other words, the resolution of the RG limit cycle instability may have its imprint in the low energy theory as a limit cycle in time evolution. We have left a full exploration of the time dependence for future work, however we do speculate on the possible relevance of this

feature for cosmology [103, 104].

The chapter is organized as follows: In Section 3.2, we set the stage with a discussion of a possible effective theory for a dilaton vacuum expectation value that has features that we find in our holographic model, and which points towards a new way to set the confinement scale in an approximately conformal theory. In Section 3.3, we describe a 5D toy holographic implementation of these ideas that leaves out certain backreaction terms, with a bulk Higgs mass that is given *explicit* dependence on the extra-dimensional coordinate. In Section 3.4, we show how to promote this simplest model to a dynamical one, where the effective Higgs mass evolves due to a coupling to a "driving" scalar which picks a coordinate-dependent VEV. In Section 3.5 we discuss in more detail a possible approximate CFT interpretation of the 5D model, and make some connections to generalized BKT scaling discussed in [89]. In Section 3.6, we briefly discuss connections to self-organized critical models in statistical physics, to catastrophic failure modes of these systems, and future implementation of these ideas into an extension of the SM. Finally, we discuss aspects of the cosmology of the model, part of which involve speculation that can be more fully resolved with future work, in Section 3.7.

3.2 Preliminaries: The Frustrated Dilaton

We begin by considering an effective theory of a dilaton that has aspects of the behavior of the more detailed holographic models we consider. In an approximately scale-invariant theory that undergoes spontaneous breaking, the potential that sets the scale of that breaking is a (nearly) scale-invariant quartic: $V_{\text{dil}} = \alpha(f) f^4$, where α has some weak dependence on f that encodes the amount of explicit breaking. This potential can have a nontrivial minimum at small values of f if α obeys some basic properties.

It is important to note that in this effective theory, f is a summed total scale of conformal breaking, and relations between individual VEVs are hidden in this potential. In other

words, many operators could be simultaneously condensing which all contribute to conformal breaking. In addition, if there is some small breaking of conformal invariance, there can be nontrivial relations between these operator VEVs that are not encoded in the total dilaton potential.

Now we note that it could be the case that there is simply no solution that satisfies the relation between VEVs in the approximate CFT for a total f below some critical value, $f < f_{\text{crit}}$. How does the theory exit the CFT in this case? The dilaton is frustrated – internally, it seeks to satisfy the relations between operator VEVs, providing a lower limit to the total breaking scale. On the other hand, in the low energy theory, a smaller or vanishing f is preferred.

As a very simple example of this, we could consider two VEVs f_ϕ and f_{higgs} where at some critical value of decreasing f_ϕ, f_{higgs} begins to turn on:

$$f_{\text{higgs}}^2 = \begin{cases} -\frac{\lambda f_\phi - \mu^2}{\lambda_H} & \lambda f_\phi - \mu^2 < 0 \\ 0 & \text{otherwise} \end{cases} .$$

Such behavior occurs in the "relaxion" models of electroweak symmetry breaking. Note however, that we are not specifying a global potential for this behavior, but instead are merely providing an ad hoc relationship between operator VEVs that might arise inside of the approximate CFT. In the holographic models we consider, f_ϕ corresponds to the VEV of a marginally relevant operator, and f_{higgs} to the VEV of an operator whose scaling dimension is driven into the complex plane.

If these VEVs contribute to an effective dilaton potential as $V_{\text{dil}} \approx \alpha(f_\phi^4 + f_{\text{higgs}}^4)$ (as though they are both from operators with scaling dimension near 4), the potential will be globally minimized when $f_\phi^2 = \frac{\lambda}{2\lambda_H f_\phi} f_{\text{higgs}}^2$ if the relationship between VEVs is maintained. A large hierarchy between f_{higgs} and f_ϕ can be created by having a small value of λ_H, and the dilaton potential appears to be minimized at some f_{crit} while enforcing the relation.

We note that the dilaton potential itself does not enforce the relation between the VEVs,

which is instead specified by some dynamics that is part of the UV completion of the dilaton effective theory. This can create a puzzle from the perspective of the low energy theorist, which sees only the total breaking scale f, not the interrelations between the individual f's that contribute. The low energy observer would think that $f = 0$ should minimize the pure quartic potential, but instead the theory gets "trapped" at a larger f. Of course these relations between VEVs would require some breaking of scale invariance, and the potential would not be precisely quartics.

There may be a connection here to the concept of frustrated phase separation in condensed matter physics, a phenomenon where (for example) high T_c superconductivity is blocked due to long range Coulomb interactions, and the theory resolves the tension by creating an intermediate phase which spontaneously breaks translation invariance, creating "stripes" [99]. Here, Higgs condensation may be blocked by quasi-long range dilaton interactions, and there may be some analog of these striped phases that resolves the frustration that is important for cosmology.

With this hypothetical scenario as context and motivation, we begin our holographic studies.

3.3 Toy Model: Explicitly Varying Higgs Mass

To illustrate a basic model with the features we seek, we work in 5D asymptotically anti-de Sitter space without a UV brane, and give the Higgs a bulk mass term that varies *explicitly* with the extra-dimensional coordinate. We strongly emphasize that this is a toy model that easily illustrates some curious features that help motivate the more realistic model in Section 3.4. Specifically, this model leaves out backreaction between the Higgs and the (here unspecified) dynamics that give rise to the varying mass term, while in Section 3.4, this backreaction is taken fully into account.

The metric can be written as (setting the AdS curvature near the AdS boundary, k, to

1) [105]:

$$ds^2 = \frac{1}{z^2}\left[dx_4^2 - \frac{dz^2}{G(z)}\right]. \tag{3.1}$$

The coordinate z ranges from 0 at the AdS boundary to an IR brane at $z = z_1$, and for $z \to 0$, the function G has the asymptotic behavior $G(z) \to 1$ and $G'(z) \to 0$. Away from $z = 0$, the function G encodes the effects of gravitational backreaction due to nontrivial bulk physics such as condensates. We are restricting our ansatz for the background to solutions obeying 4D Lorentz invariance.

The action is given by

$$\begin{aligned} S = &\int d^4x dz \sqrt{g}\left[|\partial_M H|^2 + \frac{6}{\kappa^2} - m^2(z)|H|^2 - \frac{1}{2\kappa^2}R\right] \\ &- \int d^4x z^{-4} m_0^2 |H|^2\Big|_{z\to 0} - \int d^4x z^{-4} V_1(|H|)\Big|_{z\to z_1}, \end{aligned} \tag{3.2}$$

with $\kappa^2 = 1/(2M_{\rm Pl}^3)$. The bulk mass function is chosen to a have fixed value in the limit $z \to 0$, and decreases monotonically and slowly as z increases:[2]

$$m^2(z) = -4 + \delta m^2 - \lambda z^\epsilon. \tag{3.3}$$

Note that $m^2 = -4$ corresponds to the Breitenlohner-Freedman bound, and δm^2 is taken to be a positive quantity so that the $z \to 0$ limit is well-defined.[3] We note that past work explored constant Higgs bulk mass at or near the BF bound [106, 107] with interesting implications for radius stabilization. A possible relationship between the BF bound and scalars with suppressed mass in lattice studies of theories at the boundary of the conformal

[2] It is not difficult to arrange for this type of z-dependent mass term to arise dynamically, rather than through this forced explicit breaking of the isometries of AdS. We give examples in Section 3.4.

[3] If the mass is taken below the BF bound as $z \to 0$, perturbations solving the scalar equation of motion oscillate rapidly in the UV, indicating the need for an ultraviolet cutoff, such as a brane that cuts off the small z region of the spacetime [89].

window was discussed in [108]. For the IR brane potential, we take

$$V_1(|H|) = T_1 + \lambda_H |H|^2 \left(|H|^2 - v_H^2\right), \tag{3.4}$$

where T_1 is the tension of the brane. The Higgs may, for some regions of parameter space, pick a nonvanishing vacuum expectation value, $\langle H \rangle = \phi(z)/\sqrt{2}$, where the Higgs VEV has a nontrivial profile along the z-coordinate.

Restricting to solutions that obey 4D Lorentz invariance, the 5-5 component of the Einstein equations relate the metric function G to the behavior of the Higgs VEV in the bulk:

$$G = \frac{-\frac{\kappa^2}{6} V(\phi)}{1 - \frac{\kappa^2}{12}(z\phi')^2}, \tag{3.5}$$

and they can be further employed to reduce the effective potential for the classical background configuration to a pure IR boundary term [75]:

$$V_{\text{rad}} = \frac{1}{z_1^4}\left[V_1(\phi) + \frac{6}{\kappa^2}\sqrt{G}\right]. \tag{3.6}$$

There is generally a UV contribution from the brane at z_0 as well, but it vanishes as $z_0^{2\sqrt{\delta m^2}}$ in the $z_0 \to 0$ limit, with the exception of a constant term which is tuned to give vanishing effective cosmological constant. We also note that the remaining components of Einstein's equations in the bulk do not give additional information on G, being equivalent to the scalar field equation of motion for the z-dependent background, and that for the purposes of calculation of the effective potential for the size of the extra dimension, we fix the 4D portion of the metric to be flat. This amounts to satisfying vanishing variation of the action with respect to those metric components in a trivial manner, requiring that the variations themselves vanish: $\delta g_{\mu\nu} = 0$.

For small values of the Higgs VEV, or alternatively weak 5D gravity, this effective radion

potential reduces to

$$V_{\rm rad} = \frac{1}{z_1^4}\left[V_1(\phi) + \frac{6}{\kappa^2} - \frac{1}{4}m^2(z_1)\phi^2(z_1) + \frac{1}{4}z_1^2\phi'^2(z_1)\right]. \tag{3.7}$$

The scalar field equation of motion in the limit of small κ^2 is

$$\phi'' - \frac{3}{z}\phi' - \frac{1}{z^2}\frac{\partial V}{\partial \phi} = 0, \tag{3.8}$$

with energetic favorability of a nontrivial solution depending on the boundary conditions, which are (again in the small κ^2 limit):

$$z\phi'|_{z=z_{0,1}} = \pm\frac{1}{2}\frac{\partial V_{0,1}(\phi)}{\partial \phi}. \tag{3.9}$$

Near the AdS boundary $z \to 0$, the solutions are power law in z, with the expected behavior $\phi \propto z^{2\pm\sqrt{\delta m^2}}$, where the two different scaling laws correspond to two different boundary conditions or definitions of the action [81]. The scaling law z^{Δ_+} is more generic, with fine-tuning of BCs (or supersymmetry) required to obtain the scaling with power law Δ_-. The full solution for all z, including the effects of the changing bulk mass, is

$$\phi \sim \phi_\pm z^2 J_{\pm\nu}\left(\frac{2\sqrt{\lambda}}{\epsilon}z^{\epsilon/2}\right), \tag{3.10}$$

where $\nu \equiv 2\sqrt{\delta m^2}/\epsilon$. For $m_0^2 \neq 2 - \sqrt{\delta m^2}$, only the $+$ solution is relevant, while for the special case $m_0^2 = 2 - \sqrt{\delta m^2}$, the field behavior is given by the $-$ solution. Choosing the special case corresponds in the holographic picture to fine-tuning the coefficient of an operator $O_H^\dagger O_H$ to force the RG flow to go "backwards" compared to the more generic $+$ scaling solution [89, 109], or in other words, tuning so that the theory sits at a UV fixed point.

Choice of the UV boundary condition does not much affect the discussion, and we choose

to display the effects of the first of these two solutions, taking $m_0^2 = 0$.

For large values of z, and small ϵ, the asymptotics of the Bessel function exhibit log-periodicity on top of scaling when z is past the point where the BF bound is surpassed by the evolving bulk mass:

$$\phi \propto z^{2-\epsilon/4} \cos\left(\sqrt{\lambda}\log z + \gamma\right). \tag{3.11}$$

This log-periodic power law behavior may be a common feature in systems where criticality is self-organized [88].

The condition for formation of a condensate is met when the IR brane boundary condition favors a nontrivial value for the coefficients of the bulk solution:

$$\frac{1}{\epsilon}\left(\lambda_H v_H^2 - 4\right) \geq \frac{xJ'_\nu(x)}{J_\nu(x)}, \tag{3.12}$$

where $\nu \equiv 2\sqrt{\delta m^2}/\epsilon$ and $x \equiv 2\sqrt{\lambda} z_1^{\epsilon/2}/\epsilon$. Equality is associated with the presence of the exact critical point. Note that equality is satisfied at many values of z_1 due to quasi-periodicity of the right-hand side at large z_1. We label the i-th critical point as $z_{\rm c}^i$. The emergence of a massless degree of freedom at these critical points can be seen in the small momentum behavior of the bulk correlator for the Higgs fluctuations. Working in the unbroken phase, the Green's equation for scalar fluctuations is given by

$$\left[\partial_z^2 + p^2 - \frac{3}{z}\partial_z - \frac{m^2(z)}{z^2}\right] G\left(z, z'; p^2\right) = iz\delta(z - z'). \tag{3.13}$$

At the point of criticality, for small p^2, the Green's function in terms of an eigenfunction decomposition takes the form

$$G\left(z, z'; p^2\right) \approx \frac{\psi_0(z)\psi_0^*(z')}{p^2} - \sum_{i=1}^{\infty} \frac{\psi_i(z)\psi_i^*(z')}{m_n^2}, \tag{3.14}$$

where $\psi_0(z)$ solves the 5D equation of motion for $p^2 = 0$, and thus takes the same functional form as the VEV, $\phi(z)$. The m_n are the usual KK-mode masses. As we discuss in further detail below, the m_n^2 are not guaranteed to be positive at all of the critical points, and in fact only one, the smallest z_c critical point, z_c^1 has a positive spectrum.

As the Higgs VEV turns on, the character of the radion potential also changes dramatically. Of primary interest is the behavior of the radion potential near the region of z_1 where the Higgs VEV is just turning on. A linearized approximation of the Higgs contribution to the potential gives the leading contribution in the immediate neighborhood of criticality. The function for $\phi(z_1)^2$ is analytic, and near its zeros, say one at $z_1 = z_c^1$, we have

$$\phi(z_1)^2 \approx \sigma^2 \left(\frac{z_1}{z_c^1} - 1 \right), \tag{3.15}$$

where σ^2 is a positive function of the parameters of the theory:

$$\sigma^2 = \frac{-4m^2 (z_c^1) + \lambda_H v_H^2 (\lambda_H v_H^2 - 8)}{2\lambda_H}. \tag{3.16}$$

The radion potential in the regime just after the VEV turns on is given by

$$V_{\text{rad}} \approx \frac{1}{z_1^4} \left[\delta T_1 + \frac{\lambda_H \sigma^4}{8} \left(\frac{z_1}{z_c^1} - 1 \right) \right]. \tag{3.17}$$

The radion potential is thus piecewise, and if we look in the vicinity of the critical point, it takes the form

$$V_{\text{rad}} \approx \begin{cases} \frac{1}{z_1^4} \delta T_1 & z_1 < z_c^1 \\ \frac{1}{z_1^4} \left[\delta T_1 + \frac{\lambda_H \sigma^4}{8} \left(\frac{z_1}{z_c^1} - 1 \right) \right] & z_1 > z_c^1 \end{cases}, \tag{3.18}$$

where δT_1 is the mistune between the IR brane tension and the bulk cosmological constant. We note that quantum corrections will spread z-dependence from the scalar mass to the cosmological constant term, and the background will no longer be pure AdS. These small

corrections will modify the background potential away from a pure quartic - this is not, however, important for the features we draw attention to in this model. In the next section, the background potential is modified away from a pure quartic by a Golderberger-Wise type potential.

At the critical point, there is a kink discontinuity in the radion potential.[4] The contribution of the Higgs condensate to the radion potential is also positive definite. In order for the derivative of the radion potential to change sign, creating a kink *minimum*, an additional condition for the radion quartic (the IR brane mistune) must hold:

$$0 < \delta T_1 < \frac{1}{128\lambda_H}\left[4m^2\left(z_c^1\right) - \lambda_H v_H^2\left(\lambda_H v_H^2 - 8\right)\right]^2. \tag{3.19}$$

These requirements are satisfied relatively robustly under variation of the input parameters. In Figure 3.2, we show an example of the radion potential, where we have taken $\delta T_1 = 1$, $\delta m^2 = 1$, $\lambda = \epsilon = 0.1$, $v_H^2 = 0$, and $\lambda_H = 1/8$.

There are two plots in the figure: in the first, on the left, we show a close-up that focuses on the critical value of the radion VEV. On the right, we zoom out. Unsurprisingly, it appears that there are multiple such minima, and that the first one is metastable. This is due to the quasi-periodicity of the Higgs VEV solution at large values of z. Closer examination of the theory in these regions shows that there are unresolved tachyon instabilities associated with Higgs fluctuations. In these regions, no VEVs are formed, but there are solutions to the scalar equation of motion with negative mass squared, as we show in the next subsection.

Before studying the instabilities, it is worthwhile to explore the behavior of the effective potential under variations of the fundamental parameters. Crucial to the success of the model as one of self-organized Higgs criticality is the existence of a broad critical region, over which the Higgs remains light. In Figure 3.3, we examine the behavior of the radion potential under variations of the IR brane Higgs mass squared, encoded in v_H^2. We see that

[4] We note that this kink feature is due to the fact that we are deliberately ignoring backreaction between the Higgs and the dynamics that creates the varying mass term. The properties of the critical point differ in complete models, and we begin a study of an explicit example in Section 3.4.

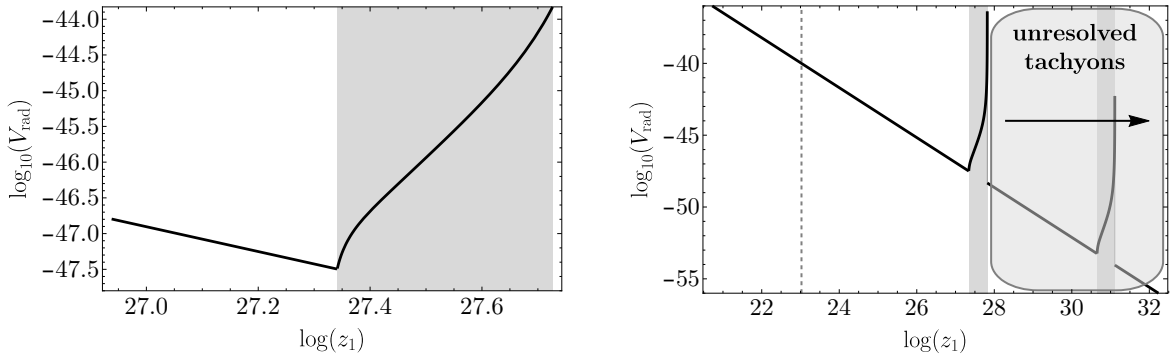

Figure 3.2: Here we display the radion potential, $V_{\rm rad}(z_1)$. In the white region, the Higgs VEV is vanishing, and the radion potential is a pure quartic. In the gray region, $\phi(z_1) \neq 0$, and the contribution of the Higgs to the radion potential causes a kink-like minimum to appear at the critical points. In the first plot, we have zoomed in on the first minimum, corresponding to the smallest z_1 for which the criticality conditions are met. In the second plot, we zoom out, showing other potential minima. These are unhealthy, in that the theory at this point contains unresolved tachyons. The dashed vertical line in the second plot corresponds to the value of z at which the evolving bulk Higgs mass passes the BF bound.

with changing v_H^2, the location of the minimum is relatively constant, however there is a crucial value of v_H^2 past which the location of the minimum moves away from the kink in the potential. The region of parameter space where the minimum resides at the kink is a critical region, as there is a zero mode Higgs for all values of $v_H^2 < v_H^2(\text{crit})$.

In the next subsection, we comment on properties of this kink minimum in the effective radion potential, in particular those related to the metric ansatz that we have enforced.

3.3.1 Metric Boundary Conditions

In calculating the radion potential in Eq. (3.7), we have imposed the boundary conditions for the scalar fields, but we have neglected the metric junction conditions on the branes, which enforce

$$\sqrt{G(z_0)} = \frac{\kappa^2}{6} V_0, \qquad \sqrt{G(z_1)} = -\frac{\kappa^2}{6} V_1. \tag{3.20}$$

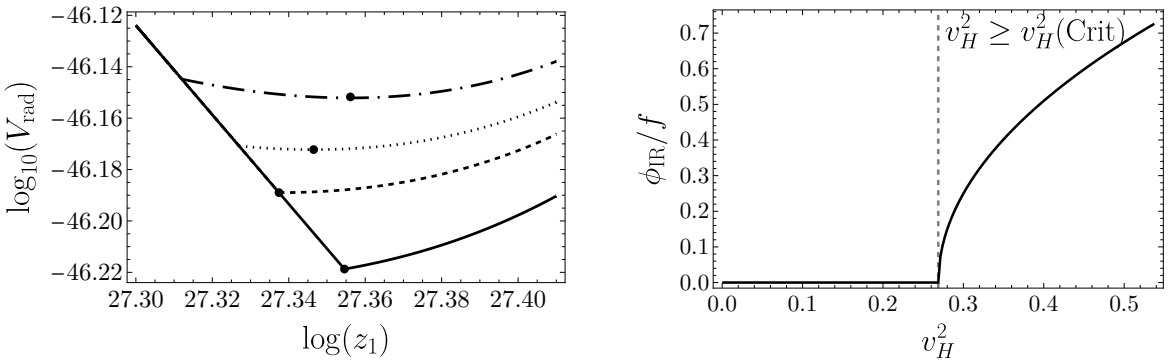

Figure 3.3: Here we show, on the left, the dependence of the potential on the IR brane parameter v_H^2 in the vicinity of the first critical point. The curves correspond to $v_H^2 = -1$ (solid), $v_H^2 = v_H^2(\text{crit})$ (dashed), $v_H^2 = 1$ (dotted), and $v_H^2 = 2$ (dot-dashed). The dots indicate the minimum of the potential. The minimum moves into the region where the Higgs VEV is nonzero after some critical point $v_H^2(\text{crit})$. On the right, we show the value of the Higgs field on the IR brane in units of the scale $f = z_{\rm min}^{-1}$, where $z_{\rm min}$ is the location of the minimum of the radion potential. The VEV (and Higgs mass/inverse of the correlation length), which is proportional to $\phi_{\rm IR}$, is vanishing below $v_H^2(\text{crit})$, and grows quickly after the critical point is exceeded.

This is equivalent to having the UV brane and IR brane contributions to the effective potential separately vanish [110, 111]:

$$\begin{aligned} \widetilde{V}_{\rm UV} &= V_0 - \frac{6}{\kappa^2}\sqrt{G_0} = 0, \\ \widetilde{V}_{\rm IR} &= V_1 + \frac{6}{\kappa^2}\sqrt{G_1} = 0, \end{aligned} \tag{3.21}$$

where we have defined $V_{\rm rad} = \frac{1}{z_0^4}\widetilde{V}_{\rm UV} + \frac{1}{z_1^4}\widetilde{V}_{\rm IR}$. In fact, these conditions are not satisfied for any values of z in the above potential. These conditions should be interpreted as consistency conditions for our metric ansatz, in which we have forced the metric to exhibit 4D Lorentz invariance so that we can interpret the result as a Lorentz-invariant 4D effective potential for the modulus field. In terms of variation of the scalar-Einstein-Hilbert action, we have satisfied vanishing variation of the action by keeping the variations of the 4D metric components $\delta g_{\mu\nu}$ themselves to be zero, and in so doing, Eq. (3.20) is no longer a constraint on the solution.

In the usual Goldberger-Wise scenario, the second of the two conditions in Eq. (3.20) is met automatically at the minimum of the potential, with the value of the size of the extra dimension being set by its solution. The first is then arranged for by tuning (equivalent

to the usual tuning of the bare cosmological constant to small values). From this, we can roughly interpret the time dependence away from the minimum of the usual Goldberger-Wise potential as a combination of cosmological acceleration and oscillations of the stabilized radion. The situation is quite different in the case of the potential described above. At the kink minimum generated by the Higgs contribution, these junction conditions cannot both be met unless two tunings are performed – both the bare cosmological constant and the mistune in the IR brane tension.

This doesn't necessarily mean that the region where the kink is a minimum is forbidden, but rather tells us that once inside this region, a dynamical geometry is unavoidable, and must be included in a fully consistent calculation of the spectrum of the low energy theory. In other words, in a theory with fully dynamical gravity, the ansatz for the background *must* be relaxed to include a nontrivial 4D cosmology. In Section 3.7, we discuss this issue of a dynamic cosmology further, and speculate on its resolution and interpretation.

We further note that the same behavior occurs in the case of the dynamical scalar model considered in Section 3.4, although the kink feature is absent.

3.3.2 Instabilities

Here we briefly examine the stability of fluctuations for different values of the position of the IR brane. Summarizing the results first: the minimum for smallest z_c and neighboring values of the radion VEV is always a "healthy" minimum where there are no unresolved tachyonic states. However, past the first region where the Higgs VEV resolves the tachyon, there are apparently instabilities without condensates to rectify them, or the condensates are insufficient to prevent all of them. In this case, the approximation of a static 5D description is not a good one, and the theory must resolve the tachyon with some more dramatic dynamics. We comment briefly on this in Section 3.6, and a more complete analysis of this region is part of future work.

We can inspect the tachyon instabilities through examination of the spectrum of Higgs

fluctuations. The equation of motion for these, presuming a vanishing Higgs VEV, is given by

$$h''(z) - \frac{3}{z}h'(z) - \frac{1}{z^2}\left(-4 + \delta m^2 - \lambda z^\epsilon\right) h(z) = -m^2 h(z), \tag{3.22}$$

with IR boundary condition given by

$$h'(z_1) = \frac{1}{2z_1}\lambda_H v_H^2 h(z_1). \tag{3.23}$$

The UV boundary condition we impose is that the solution must asymptote to the behavior given in Eq. (3.10), on the + branch. Equivalently, one could impose $z_0 h'(z_0) = m_0^2 h(z_0)/2$ for some non-tuned value of m_0^2, and subsequently take the limit as $z_0 \to 0$. The result is similar.

Solving the boundary value problem gives the spectrum of states. In Figure 3.4, we display the lowest eigenvalue, expressed as the ratio $(m_h/f)^2$, where $f^{-1} = z_1$. The region where the Higgs VEV resolves the tachyon is shaded, and there Higgs fluctuations are massive. At larger z_1, outside the gray region where there is no Higgs condensate, there is a tachyon that persists. It appears that the condensate can rectify the tachyon so long as the mode is not *too* tachyonic. For larger z_1, the problem grows still worse: in the neighborhood of the n-th critical value of z_1, there are $n-1$ unresolved tachyons.

Due to the presence of unresolvable tachyons for larger z_1, we focus our main attention on values of z_1 where there is either no tachyon, at $z_1 < z_c^1$, or there is a single tachyon that is resolved by the vacuum expectation value for the Higgs field, $z_1 \gtrsim z_c^1$.

It is interesting that the first minimum appears metastable, with other minima at larger values of z_1, but lower effective potential energy, as seen in Figure 3.2. We comment further on this in Section 3.6. However, we must not take this region of large z_1 too seriously. For one, the vacuum expectation value for the Higgs diverges at the end of the first condensate region, and the theory cannot be trusted there, where gravitational backreaction will be very

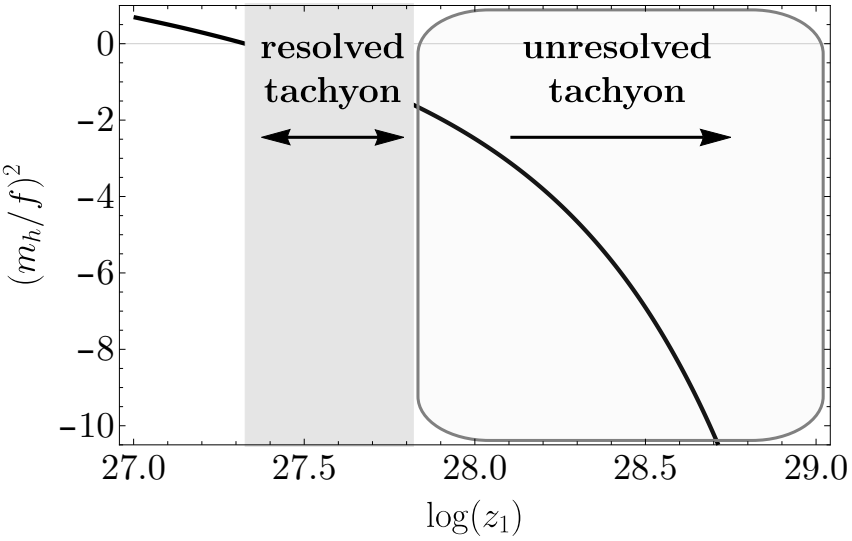

Figure 3.4: Here we show the lowest eigenvalue associated with the Higgs fluctuations, the solutions to Eq. (3.22) with the boundary conditions associated with the IR brane-localized Higgs potential. The region where the Higgs VEV resolves a single tachyon is shaded, and the physical Higgs fluctuation here is in fact massive. This is the first critical region, where there is only one tachyon to be resolved. An unresolved tachyon emerges for larger z_1, when the Higgs VEV turns off, indicating a fundamental instability.

large. It is not obvious that the geometry can be considered at all past this point.

Additionally, as discussed in the previous subsection, we have not taken into account the required time dependence in the solution. It is not obvious that the same instabilities will be present once the ansatz for the background is relaxed to allow for a dynamical background.

Finally, we have enforced a rigid dependence of the mass on the z-coordinate, which is not likely to be possible in a self-contained fully dynamical model. It is likely that this rigidity of the mass profile is responsible for the kinked behavior of the potential at the critical point. Backreaction between the dynamics that drives the mass and the Higgs VEV may smooth out the potential. This is confirmed in a fully dynamical model explored in the next section.[5]

[5]We thank Prashant Saraswat and Michael Geller for useful comments on the first version of this pre-print that led us to more fully explore the details of the dynamical model.

3.4 Dynamical Model

In the previous section, the varying bulk mass for the Higgs was taken as an input, breaking the isometries of AdS explicitly, and we took the UV brane to the AdS boundary. In this section we show how similar physics can be derived in a dynamical and more realistic model with a UV brane where the interplay of a Goldberger-Wise-like scalar field and a bulk Higgs on an AdS background generates a similar physics result. This model has the benefit of being fully dynamical, of having a possible CFT dual that is easier to interpret, and having a modulus potential that does not exhibit the kink of the previous toy model. The 5D Higgs profile can no longer be solved for analytically, and so we perform a numerical study.

This model has two bulk scalar fields, a real scalar, $\phi_{\rm d}$, the "driving scalar", in addition to a Higgs scalar. The fields are coupled in such a way that a varying VEV of the scalar $\phi_{\rm d}$ drives the effective bulk mass of the Higgs, making it a function of the extra-dimensional coordinate. The 5D action is given by

$$\begin{aligned} S = \int d^4x dz \sqrt{g} \left[|\partial_M H|^2 + \frac{1}{2}(\partial_M \phi_{\rm d})^2 + \frac{6}{\kappa^2} - \left(m_H^2 - \lambda \phi_{\rm d}\right)|H|^2 - \frac{1}{2} m_{\phi_{\rm d}}^2 \phi_{\rm d}^2 - \frac{1}{2\kappa^2} R \right] \\ - \int d^4x z^{-4} V_0(\phi_{\rm d}, |H|)\Big|_{z\to z_0} - \int d^4x z^{-4} V_1(\phi_{\rm d}, |H|)\Big|_{z\to z_1} . \end{aligned} \tag{3.24}$$

The brane potentials are assumed to take the form $V_{0,1} = \delta T_{0,1} + V_{0,1}^{\phi_{\rm d}} + V_{0,1}^{H}$. For the brane Higgs potentials, we take

$$V_0^H = m_0^2 |H|^2, \qquad V_1^H = \lambda_H |H|^2 \left(|H|^2 - v_H^2\right). \tag{3.25}$$

The potential here is quite similar to that in [94], however in this model, there are no very small parameters, and this is a 5D bulk potential – the effective bulk potential in the 4D theory is of course related, but not in one-to-one correspondence. There is a mild approximate shift symmetry in the bulk for the $\phi_{\rm d}$ scalar – a slightly suppressed bulk mass parameter as utilized in the Goldberger-Wise stabilization mechanism [73], and a perturbative bulk

interaction with the 5D H field.

The equation of motion for $\phi_{\rm d}$ is given by

$$\phi_{\rm d}'' - \frac{3}{z}\phi_{\rm d}' - \frac{1}{z^2}\left(m_{\phi_{\rm d}}^2\phi_{\rm d} - \frac{\lambda}{2}\phi_h^2\right) = 0, \tag{3.26}$$

which is a simple linear non-homogeneous equation for a given Higgs background, ϕ_h, and the solution is given by

$$\phi_{\rm d} = z^\epsilon\left(\phi_\epsilon + \frac{\lambda}{4(2-\epsilon)}\int_{z_0}^{z}\phi_h^2(\widetilde{z})\widetilde{z}^{-1-\epsilon}d\widetilde{z}\right) + z^{4-\epsilon}\left(\phi_4 - \frac{\lambda}{4(2-\epsilon)}\int_{z_0}^{z}\phi_h^2(\widetilde{z})\widetilde{z}^{-5+\epsilon}d\widetilde{z}\right), \tag{3.27}$$

where $\epsilon = 2 - \sqrt{4+m_{\phi_{\rm d}}^2}$. We take ϵ to be small and positive, but not tiny, e.g. $\epsilon = \mathcal{O}(0.1)$, corresponding to a small tachyonic bulk mass for $\phi_{\rm d}$. There are two contributions to the solution – the solution to the homogeneous part of Eq. (3.26), and the integrals that solve the nonhomogeneous part from a non-vanishing Higgs VEV.

The Higgs equation of motion is given by

$$\phi_h'' - \frac{3}{z}\phi_h' - \frac{1}{z^2}\left(m_H^2 - \lambda\phi_{\rm d}\right)\phi_h = 0, \tag{3.28}$$

which can, in principle, be expressed as a single nonlinear integro-differential equation by inserting the solution to the $\phi_{\rm d}$ boundary value problem.

The radion potential, again assuming small gravitational backreaction, now takes contributions from both fields, and is given in general by

$$\begin{aligned} V_{\rm rad} &= \frac{1}{z_0^4}\left[V_0 - \frac{6}{\kappa^2}\sqrt{G_0}\right] + \frac{1}{z_1^4}\left[V_1 + \frac{6}{\kappa^2}\sqrt{G_1}\right] \\ &\approx \frac{1}{z_0^4}\left[\delta T_0 + V_0^{\phi_{\rm d},0} + V_0^H + \frac{1}{4}m_H^2(z_0)\phi_{h,0}^2 - \frac{1}{4}z_0^2\phi_{h,0}'^2 + \frac{1}{4}m_{\phi_{\rm d}}^2\phi_{{\rm d},0}^2 - \frac{1}{4}z_0^2\phi_{{\rm d},0}'^2\right] \\ &\quad + \frac{1}{z_1^4}\left[\delta T_1 + V_1^{\phi_{\rm d},1} + V_1^H - \frac{1}{4}m_H^2(z_1)\phi_{h,1}^2 + \frac{1}{4}z_1^2\phi_{h,1}'^2 - \frac{1}{4}m_{\phi_{\rm d}}^2\phi_{{\rm d},1}^2 + \frac{1}{4}z_1^2\phi_{{\rm d},1}'^2\right]. \end{aligned} \tag{3.29}$$

Using the analytic solution for $\phi_{\rm d}$ in terms of the function ϕ_h from Eq. (3.27), supplemented

by the boundary conditions for $\phi_{\rm d}$, one can express the entire radion potential purely in terms of the solution to the ϕ_h equation of motion.

We first specify to a model where much can be done analytically to show some basic results in this model. We take the IR brane potential for the $\phi_{\rm d}$ scalar to be a localized mass term, $V_1^{\phi_{\rm d}} = -\epsilon\phi_{\rm d}^2$. If we assume this value for the mass, and if the Higgs VEV is taken to be zero, the solution is $\phi_{\rm d} = v_0(z/z_0)^\epsilon$. Without the Higgs contribution, the radion potential is just a scale-invariant quartic. We then assume a UV brane potential that fixes v_0 to some value (a stiff-wall-type boundary condition). In this background, ignoring the nonhomogeneous part of $\phi_{\rm d}$ in the Higgs equation of motion, the solution for the Higgs VEV is the same as described in the previous section.

Also, in the case of the model under consideration, there are considerable simplifications of the radion potential. Specifically, all of the $\phi_{\rm d}$ terms in the IR brane contribution cancel after imposing the boundary condition $z\phi_{\rm d}' = \epsilon\phi_{\rm d}$, which arises from the boundary potential we have chosen for $\phi_{\rm d}$.

The radion potential, expressed purely in terms of the boundary values of and integrals over the solution to the Higgs equation of motion, is

$$\begin{aligned} V_{\rm rad} = \frac{1}{z_0^4}\Bigg[&\delta\widetilde{T}_0 + \frac{m_0^2}{2}\phi_{h,0}^2 + \frac{1}{4}\left(m_H^2 - \lambda v_0\right)\phi_{h,0}^2 - \frac{1}{4}\left(z_0\phi_{h,0}'\right)^2 - \frac{1}{2}\epsilon v_0 z_0^{4-\epsilon} I_4 - \frac{1}{4}\left(z_0^{4-\epsilon} I_4\right)^2\Bigg] \\ &+ \frac{1}{z_1^4}\Bigg[\delta\widetilde{T}_1 - \frac{1}{4}\left\{m_H^2 - \lambda\left(\frac{z_1}{z_0}\right)^\epsilon\left(v_0 + \frac{z_0^\epsilon}{2(2-\epsilon)}I_\epsilon - \frac{z_0^{4-\epsilon}}{2(2-\epsilon)}I_4\right)\right\}\phi_{h,1}^2 \\ &+ \frac{1}{4}\lambda_H\phi_{h,1}^2\left(\phi_{h,1}^2 - 2v_H^2\right) + \frac{1}{4}\left(z\phi_{h,1}'\right)^2\Bigg], \end{aligned} \tag{3.30}$$

where I_ϵ and I_4 are the following integrals:

$$\begin{aligned} I_\epsilon =& \frac{\lambda}{2}\int_{z_0}^{z_1}\phi_h^2(\widetilde{z})\widetilde{z}^{-1-\epsilon}d\widetilde{z}, \\ I_4 =& \frac{\lambda}{2}\int_{z_0}^{z_1}\phi_h^2(\widetilde{z})\widetilde{z}^{-5+\epsilon}d\widetilde{z}. \end{aligned} \tag{3.31}$$

This expression is exact up to contributions from gravitational backreaction, which we are

here neglecting.

We note that one can show analytically by expanding the solution near the critical point that the kink of the previous section is removed by the backreaction of the Higgs VEV onto the driving scalar [112].

In the limit of tiny Higgs VEV, the Higgs background is well approximated by the solution that assumes $\phi_{\rm d} = v_0(z/z_0)^\epsilon$, which was explored in the previous section:

$$\phi_h = z^2 \left(\phi_+ J_\nu \left(z^{\epsilon/2} \frac{2\sqrt{\lambda v_0}}{\epsilon} \right) + \phi_- J_{-\nu} \left(z^{\epsilon/2} \frac{2\sqrt{\lambda v_0}}{\epsilon} \right) \right), \tag{3.32}$$

where $\nu = 2\sqrt{\delta m^2}/\epsilon$, with $\delta m^2 = m_H^2 + 4$. This is sufficient for determining the critical point, however, for the purposes of evaluating the effective potential, a full numerical solution is necessary. That is, past the critical point, the Higgs background looks similar to this profile, but the differences due to the nonlinearities need to be incorporated in order to correctly determine the radion potential.

In the next subsection, we embark on a full numerical analysis of the coupled equations, working with a more common setup for the $\phi_{\rm d}$ scalar, where its boundary values are set to $v_{0,1}$ on the UV/IR branes.

3.4.1 Still Wall Model

In the stiff wall limit, the boundary conditions for $\phi_{\rm d}$ are $\phi_{\rm d}(z_{0,1}) = v_{0,1}$. Thus, the value of the bulk Higgs mass varies from $m_H^2(z_0) = m_H^2 - \lambda v_0$ on the UV brane to $m_H^2(z_1) = m_H^2 - \lambda v_1$ in the IR. It is not difficult to arrange for the effective Higgs mass to vary such that it crosses the BF bound somewhere in the bulk, and evolves from power law behavior in the UV to a log-periodic power law in the IR. For small values of z_1, the AdS tachyon is not reached, however, for larger values, the tachyon eventually must emerge and be resolved by condensation of some sort. In order to understand this process fully, we embark on a numerical exploration of solutions to the scalar equations of motion.

We note that the bulk equations governing the behavior of $\phi_{\rm d}$ and ϕ_h are nonlinear, and that one must take care in seeking out solutions to the scalar equations of motion. Existence and uniqueness are not guaranteed in the case of the general nonlinear boundary value problem. Due to this complication, we do not search for solutions with fixed z_1, but rather search for solutions with varying values of the Higgs VEV. We note that there is always a solution with $\phi_h = 0$ – the solution to the linear Goldberger-Wise problem with just the $\phi_{\rm d}$ scalar.

To numerically investigate the solutions, we generalize the bulk equations to accommodate a sort of shooting method. That is, we search for solutions to the boundary value problem at hand by scanning over a range of initial value problems until we find a global solution. To do so, we write the solution to the Higgs as $\phi_h = h_0 f_h(z)$ with $f_h(z_0)$ set to some arbitrary value. The coefficient h_0 does not appear explicitly in the Higgs equation of motion, as for fixed $\phi_{\rm d}$, that equation is linear. It does, however, appear in the $\phi_{\rm d}$ equation:

$$\begin{aligned} &f_h'' - \frac{3}{z} f_h' - (m_H^2 - \lambda\phi_{\rm d}) f_h = 0, \\ &\phi_{\rm d}'' - \frac{3}{z}\phi_{\rm d}' - (\epsilon^2 - 4\epsilon)\phi_{\rm d} + \frac{\lambda}{2} h_0^2 f_h(z)^2 = 0. \end{aligned} \tag{3.33}$$

We shoot from the UV brane, enforcing the UV brane boundary conditions for f_h and $\phi_{\rm d}$, which in our cases of study are $f_h'(z_0) = m_0^2 f_h(z_0)/(2z_0)$ and $\phi_{\rm d}(z_0) = v_0$. We then use a prechosen value of h_0 to define each solution. The magnitude of h_0 closely tracks the low energy effective Higgs VEV as a fraction of the KK scale. As $f_h(z_0)$ is fixed arbitrarily, the only remaining condition is on $\phi_{\rm d}'$, the correct value for which will be determined by shooting. The value of z_1 for a $\phi_{\rm d}'$ guess is chosen by finding the point in the bulk at which the IR brane boundary condition for the Higgs is met: $h_0^2 = 1/f_h(z)^2 \left(v_H^2 - \frac{2f_h'(z)}{\lambda_H z f_h(z)}\right)$. Of course at that z_1, it will not usually be the case that the IR boundary condition for $\phi_{\rm d}$ is met, so we repeat the process by shooting with different values of $\phi_{\rm d}'$ until both the Higgs and $\phi_{\rm d}$ boundary conditions are solved at the same value of z_1. In summary, for a given input Higgs VEV, we obtain a value for z_1 and the associated bulk profiles for ϕ_h and $\phi_{\rm d}$.

It is useful to characterize each solution in terms of some parameter with physical meaning to a low energy observer, and we choose the effective Higgs VEV, evaluated by integrating the Higgs solution squared over a hypothetical flat zero-mode gauge boson wave function with appropriate metric factors:

$$\left(\frac{v_{\text{eff}}}{f}\right)^2 = z_1^2 h_0^2 \int_{z_0}^{z_1} \frac{1}{z^3} f_h^2(z) dz. \tag{3.34}$$

We find that the types of solutions one obtains can be divided into two classes based on the value of the IR brane-localized Higgs mass, determined by taking different values for v_H^2. If v_H^2 is taken to be very negative, corresponding to a non-tachyonic brane-localized Higgs mass squared, there is no solution for nonzero Higgs VEV with $z_1 > z_{\text{c}}$. Instead, with increasing Higgs VEV (roughly h_0 in our numerical analysis), the solution requires *smaller* values of z_1. This then means that for a given value of $z_1 < z_{\text{c}}$, there may be two solutions, one with positive effective 4D Higgs mass squared/vanishing VEV, and the other with nonvanishing Higgs VEV. For more positive values of v_H^2, a different behavior is possible, e.g. where the value of z_1 at first increases as the Higgs VEV is turned on, and then turns around, so that at some particular z_1 value, there are two possible values of the effective Higgs VEV.

None of this should be too surprising from the perspective of the 4D CFT dual. The value of z_1 represents some total scale of conformal breaking through the relation $z_1 \sim 1/f$ where f should be some additive combination of all vacuum expectation values in the system that break approximate conformal invariance spontaneously. The bulk $\phi_{\text{d}}|H|^2$ interaction has enforced a relationship between the multiple f's (in this case, dual to the ϕ_{d} and ϕ_h scalar solutions), and lifted the constraint of uniqueness present in theories without bulk scalar interactions. In other words, the nonlinearity of the boundary value problem has allowed for multiple solutions for a given z_1, and thus different ways for the bulk theory to produce a given total $f \sim 1/z_1$. In Figure 3.5, we show for two different values of v_H^2 that are close to

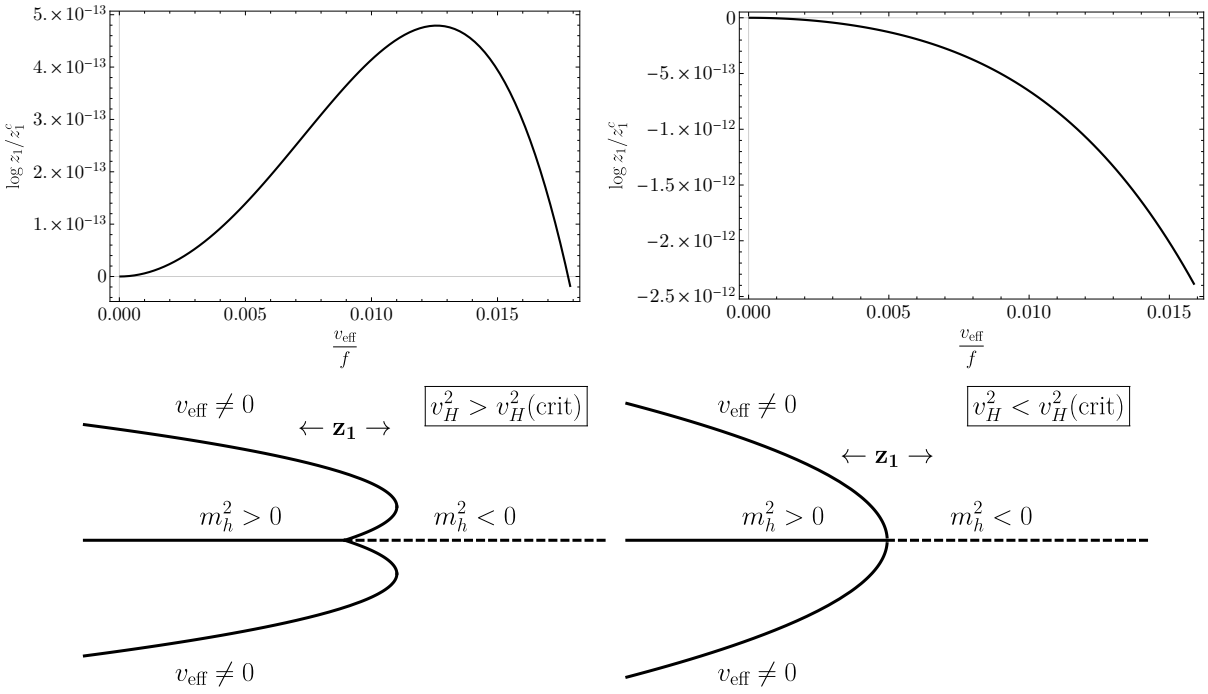

Figure 3.5: In this plot, we show the effective VEV as a function of z_1. On the left, we show it for a value of v_H^2 that is very close to "critical," but with $v_H^2 > v_H^2(\text{crit})$. In this case, for small Higgs vev, $z_1 > z_c$. On the right, we display it for v_H^2 more negative than the critical value, and in this case, for all values of the Higgs VEV, we find $z_1 < z_c$. We also sketch the "bifurcation" diagrams for each of these scenarios as a function of z_1, where the solid lines represent the stable scalar configurations and the dashed line represents the background solution with unresolved tachyon(s). The branching point corresponds to $z_1 = z_c$.

a critical value (but on either side) the relationship between z_1 and the effective VEV. We note that the Higgs VEV grows extremely fast near the critical point.

This matches onto the first part of our preliminary discussion of the dilaton effective theory in Section 3.2. Extremization of the scalar part of the action corresponds in the dual picture to sorting out the correct relationship between the vacuum expectation values of operators in the approximate CFT. This relationship must now be fed into the total radion effective potential.

Now we consider the radion potential for this model. Plugging in the results from the numerical solutions, we find that for $v_H^2 > v_H^2(\text{crit})$, there are solutions to the scalar equations of motion and boundary conditions with $z_1 > z_c$. For all $v_H^2 < v_H^2(\text{crit})$, there is a minimum in the effective radion potential *at* $z_1 = z_c$, the value of z_1 where the Higgs fluctuation is

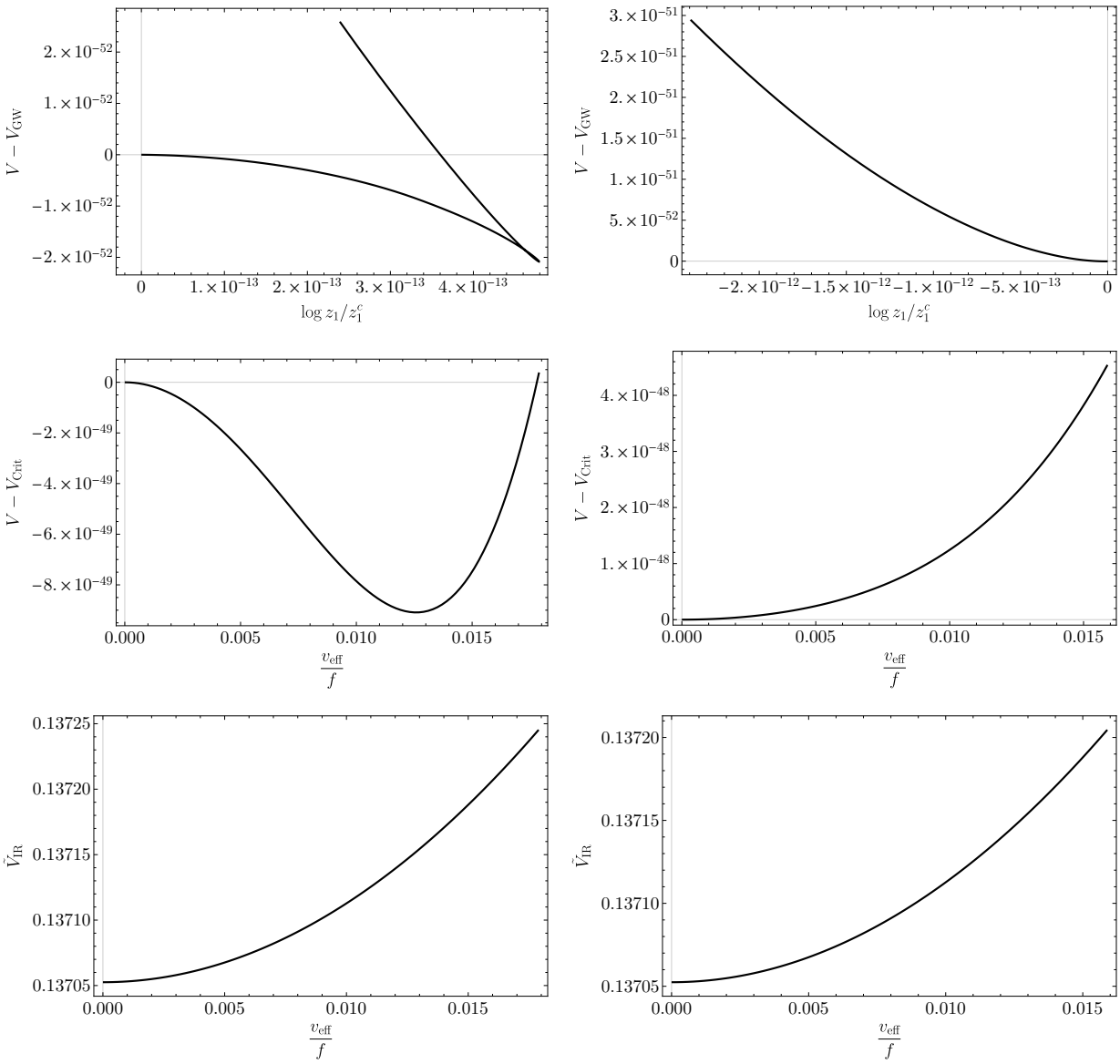

Figure 3.6: In this plot, we show the radion potential for two different values of v_H^2 near $v_H^2(\text{crit})$. In the column on the left, $v_H^2 > v_H^2(\text{crit})$. We have taken $\epsilon = v_0 = 1/10$, $m_H^2 = -3.9$, $v_0 = 1$, $\delta T_1 = -1/10$, $\lambda = 1/3$, $m_0^2 = 4.1$, and $\lambda_H = 1/8$. The critical point is between $v_H^2 = -16.5830$ and $v_H^2 = -16.5831$, and the two columns correspond respectively to these two values of v_H^2 that straddle $v_H^2(\text{crit})$. In descending order, the plots display: the difference between the radion potentials with and without a Higgs VEV as a function of $\log z_1/z_1(\text{crit})$, the same potential with $V_{\rm crit}$ being its value at the critical z_1, but instead as a function of $v_{\rm eff}/f$, and finally the value of $\widetilde{V}_{\rm IR}$, defined in Eq. (3.21), indicating the degree of mismatch of the metric junction condition on the IR brane. There is no discernible difference in these two plots on either side of the critical value of v_H^2, and there is certainly no zero.

massless. We note that this is under the constraint that values of z_1 where there is an

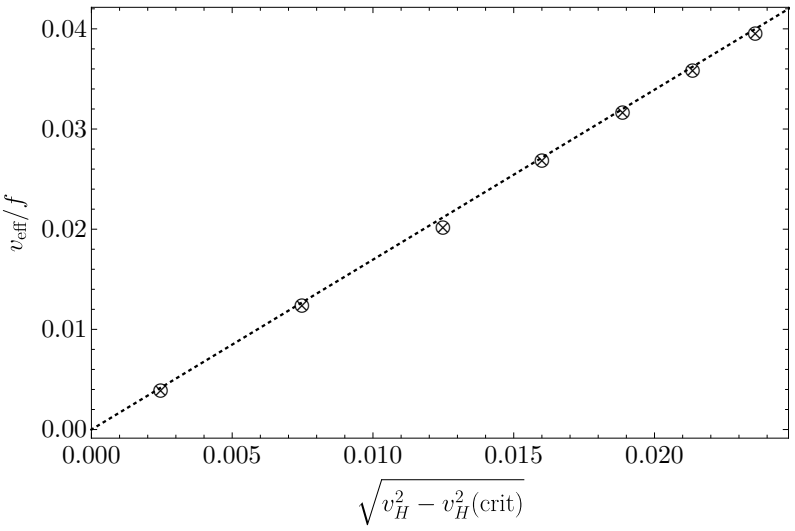

Figure 3.7: In this plot, we display the behavior of $v_{\rm eff}/f$ at the minimum of the radion potential for subcritical $v_H^2 > v_H^2(\rm crit)$ as it approaches the critical region. The dashed line is a linear fit to the numerical data forced to pass through the origin by adjusting $v_H^2(\rm crit)$. The critical value is determined in this manner to be $v_H^2(\rm crit) = -16.58305605$

unresolved tachyon are disallowed. [6]

In Figure 3.6, we display the results of the radion potential for two values of v_H^2 near the critical value. We show the potential both as a function of z_1 and as a function of $v_{\rm eff}/f$. In this plot, $V_{\rm GW}$ denotes the GW contribution to the radion potential, while $V_{\rm crit}$ is the radion potential at the critical z_1. For the subcritical case, the location of the potential minimum is at an energy which is lower than if the Higgs VEV is turned off – symmetry breaking is the preferred configuration for that value of z_1.

One can now make contact with the dilaton effective potential discussed in Section 3.2. The value of $1/z_1$ for a given solution corresponds to the total scale of symmetry breaking, with the KK-mode masses of the extra-dimensional theory corresponding to its value. Larger values of z_1 have scalar instabilities. Ignoring this region, the radion potential is minimized at the largest value of z_1 that accommodates a solution to the scalar equations of motion.

[6] Dynamics of the system *will* move the IR brane into this region - the true vacuum is not simply one in which the brane rests at z_c. Going past the critical value of v_H^2, there is likely a phase transition of the system that cannot be encapsulated under the static ansatz that was the starting point for this analysis. We speculate on its nature in Section 3.7, leaving a full analysis of the $v_H^2 < v_H^2(\rm crit)$ region for future work.

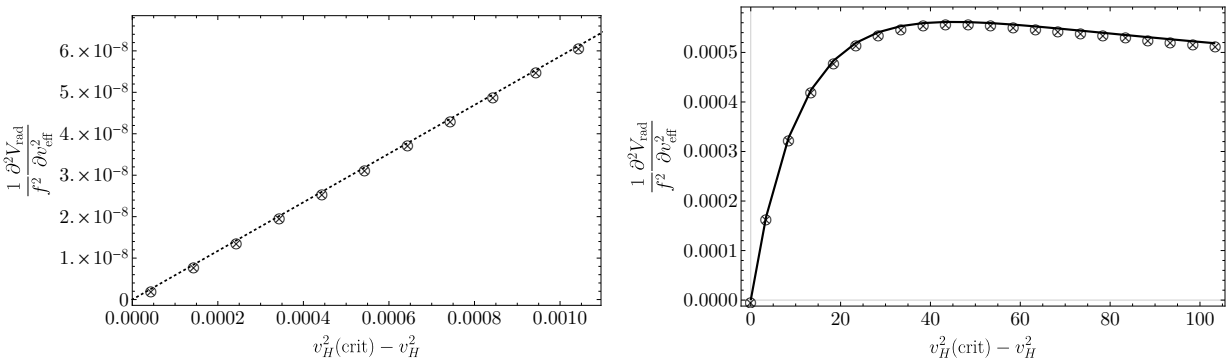

Figure 3.8: In this Figure, we display the curvature of the radion potential as a function of the effective Higgs VEV for $v_H^2 < v_H^2(\text{crit})$. In the plot on the left, we focus on v_H^2 close to the critical value, while on the right, we display the curvature for a wider range of $v_H^2 < v_H^2(\text{crit})$. Near the critical v_H^2, the behavior is well described by a line intersecting with the origin, with the critical value here determined to be $v_H^2(\text{crit}) = -16.58305645$, apparently consistent with the value determined on the sub-critical side in Figure 3.7 up to numerical errors in the solving routine.

In Figure 3.7, we display the behavior of the model with subcritical v_H^2, focusing on the value of the Higgs VEV in the approach to Higgs criticality. The Higgs VEV, roughly the inverse correlation length in the low energy theory, appears to depend linearly on $\sqrt{v_H^2 - v_H^2(\text{crit})}$ in the approach.

In Figure 3.8, we display the behavior of the model with supercritical values of v_H^2, focusing on the value of the second derivative of the radion potential at the minimum. The second derivative remains positive for all v_H^2 values less than the critical one, and so the minimum of the potential along the line where the Higgs boundary conditions are met coincides with the Higgs critical point.

While the radion potential has a smooth minimum (as a function of the effective Higgs VEV) in this dynamical model on either side of the critical value of v_H^2, we again find that it does not generally satisfy the $\mu\nu$ components of Einstein's equations, specifically the metric junction conditions $\sqrt{G_{0,1}} = \pm\frac{\kappa^2}{6}V_{0,1}$.

Of course one could fine-tune both tensions to meet both metric junction conditions, as is done in the original unstabilized Randall-Sundrum model, however one should first ask what physical phenomena occur when such tuning is not performed. In the RS model, the

mistunes lead to either collapse or runaway of the branes, however in this case, it seems unlikely that the same behavior occurs, as the potential does not exhibit obvious runaway directions. What seems more likely is that the background solution obtained after relaxing the metric ansatz to include bent branes (e.g. nontrivial time dynamics). This is discussed further in Section 3.7.

3.5 CFT Interpretation

Here we comment on the 4-dimensional CFT interpretation of this model. The dual of this picture has a parallel in weakly coupled models where electroweak symmetry breaking is driven radiatively, as is the case in the MSSM [91]. In such cases, the electroweak scale arises via dimensional transmutation, with renormalization group effects creating the instability that is rectified by the vacuum expectation value of the Higgs in spite of the microscopic theory having no explicit scales.

In the picture under consideration, a similar instability is reached when the scaling dimensions of operators in a quasi-conformal theory are pushed towards and potentially into the complex plane through renormalization group flow. Such complex scaling dimensions are a usual part of the description of theories with a discrete scale invariance, thus we have a picture where a theory evolves off of a standard nontrivial UV fixed point and begins to exhibit discrete scale invariance in the IR. Discrete scale invariance is found in the IR behavior of the Higgs profile, where the Higgs behaves approximately as

$$\phi \propto z^{2-\epsilon/4} \cos\left(\sqrt{\lambda}\log z + \gamma\right). \tag{3.35}$$

The solution is simple scaling under the discrete transformation $z \to z\exp\left(2\pi/\sqrt{\lambda}\right)$, corresponding to a discrete scale transformation $\mu \to \mu\exp\left(-2\pi/\sqrt{\lambda}\right)$. While at first glance interesting, discrete scaling behavior is forbidden in the deep IR [98], and is expected to be terminated in some way – likely by the formation of condensates and a transition scale past

which RG flow resumes more standard behavior. Indeed, the study of the scalar fluctuations in Section 3.3 shows that if one tries to continue the bulk too far into the regime of log-periodic behavior, additional tachyons emerge that are, at least in the toy 5D theory of Section 3.3, unresolved.

In the dynamical model of Section 3.4, the driving scalar field $\phi_{\rm d}$ plays the role dual to an operator whose coupling runs slowly, slightly deforming the CFT, with the deformation growing in the infrared. This running backreacts, in general, on the theory, and can generate a running for scaling dimensions of other operators in the theory. The bulk trilinear coupling between the Higgs and the scalar $\phi_{\rm d}$ is the pathway for this backreaction.

The running scaling dimension of the operator associated with the bulk Higgs is dual to the 5D z-dependence of the effective 5D mass of the Higgs in the background of the scalar, $\phi_{\rm d}$, and the instability associated with complex scaling dimensions and discrete scale invariance is dual to supersaturation of the Breitenlohner-Freedman bound. Since the effective mass begins above the BF bound, the far UV behavior is that of a normal CFT without instabilities, where the operators have normal real scaling dimensions. It is only in the IR behavior, where scaling dimensions become complex, that an instability emerges.

This class of instability, without the dynamical aspect we explore, was investigated in work by Kaplan, Lee, Son, and Stephanov [89] along with a proposed AdS dual. In this work, it was conjectured that the loss of conformality as a function of some descriptor of the theory, such as the number of massless QCD flavors, can be thought of as due to the annihilation of two fixed points (UV and IR) under variations of that parameter. They posit that such a theory could contain some operator O that has different scaling dimensions at the two fixed points, $\Delta_{\rm UV,\,IR}$, and these scaling dimensions smoothly merge and become complex when the external descriptor is moved past some critical value. It was pointed out in this work that the behavior of the theory under this transition is closely similar to scaling behavior associated with finite temperature topological phase transitions of the sort studied by Berezinskii, Kosterlitz, and Thouless (BKT) [113,114]. In these models, there is a

critical line, with the theory being conformal for a finite range of descriptor, and with a gap turning on smoothly past the point where conformality is lost. These two scaling dimensions, $\Delta_{\mathrm{UV,\,IR}}$, correspond in the 5D AdS dual to the two solutions to the scalar equations of motion in the $z \to 0$ region, each of which has different scaling properties given by Δ_{UV} and Δ_{IR}. In 5D, the loss of conformality corresponds to the merging of these two scaling solutions at the Breitenlohner-Freedman bound as the bulk mass is taken through $m^2 = -4$. Below the BF bound, the theory requires a UV cutoff, and also predicts an IR scale associated with rectification of a tachyon instability through condensation of bulk fields, corresponding in the holographic picture to a VEV for the operator O.

The 5D model we have described has given dynamics to this picture, where what was an external parameter has been promoted to a coupling in the theory which has nontrivial RG evolution. In Figure 3.9, we give a cartoon of what the model we explore achieves. In [89], in the case that parameters are chosen to put the theory in a conformal window, there are explicit UV and IR fixed points, both nontrivial. Moving in and out of the conformal window is achieved by varying those external parameters, with the fixed points merging at its threshold. In the case of our model, the idea is that the theory begins at or flows quickly to an IR fixed point which has been demoted by a slightly relevant deformation of the theory to a quasi-fixed point. The theory tracks this IR quasi-fixed point until it disappears after annihilating its associated UV quasi-fixed point. Under further RG flow, scaling dimensions become complex with a corresponding discrete scaling law, the theory becomes unstable, and the instability is potentially resolved by condensates. The theory can also begin and remain near the UV quasi-fixed point, in principle, corresponding to taking the tuned boundary condition for the bulk scalar that picks out the other slower-growing solution.

When the instability is rectified by condensates, the approximate conformal invariance is broken spontaneously. There are different options for this breaking. The Higgs itself can form a vacuum expectation value, likely along with condensates of the operator that is driving the theory towards the instability. This option gives a Higgs mass and 4D effective

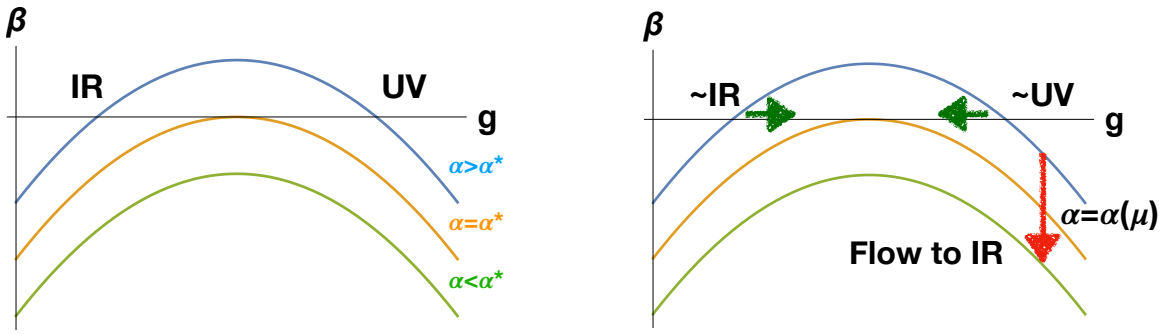

Figure 3.9: Here we show a cartoon of an approximate CFT dual of our 5D model. On the left is the picture of fixed points annihilating under continuous variation of some descriptor of the theory, as explored in [89]. On the right is our picture of quasi-fixed points annihilating under renormalization group evolution.

VEV that is not typically suppressed in comparison with the 5D KK scale or its dual picture compositeness scale. There are other options, however. It is known that the phase structure of superconductivity can be quite rich, allowing for condensates with inhomogeneous spatial configurations such as stripes or crystalline structure, and this has been reproduced in the holographic context [102].

A dynamical dilaton field, corresponding to the condensates of operators in the CFT and fluctuations about these points in field space, has a potential that depends on which operators take on VEVs, and its potential selects the most attractive channel for resolving the tachyon. The extra-dimensional modulus field, the radion, is the dual to this dilaton. Finding the classical extrema of the 5D effective potential corresponds to identifying the vacuum state of the dual CFT.

When sourced operators with nontrivial scaling dimension take on vacuum expectation values, approximate conformal invariance is spontaneously broken, and the dilaton potential is nontrivial (more than a scale-invariant quartic). If the potential has a nontrivial minimum, the resulting mass of the dilaton particle is proportional to the degree of explicit breaking of conformal symmetry. In our picture, as a function of the gap of the CFT associated with a VEV of a marginally relevant operator O_ϵ, an IR tachyon instability eventually emerges for smaller values of $\langle O_\epsilon \rangle$, in the regime of discrete scale invariance. At this point the VEV

$\langle O_H \rangle$ turns on in addition to $\langle O_\epsilon \rangle$.

The kink in the toy model of Section 3.3, or its cousin, the non-existence of solutions with nonvanishing Higgs VEV past some critical z_1 in the dynamical model of Section 3.4, are the most curious features of this setup. These behaviors appear to be strongly tied to the type of instability that is dominant in the model. The tachyon that emerges due to the renormalization group instability/violation of the BF bound appears to be a necessary component for novel behavior of the potential. This hypothesis is supported by what is observed in Figure 3.3, and in the behavior of the scalar solutions in Section 3.4. Taking, for example, v_H^2 to be large, giving a large 4D tachyonic mass to the Higgs on the brane, gives a more standard kind of picture where a Higgs condensate turns on and determines the brane location. However, for smaller or negative v_H^2, when there is no longer a 4D brane-localized tachyon, there is a turnaround in the behavior of the solutions. For v_H^2 below the critical value, it is the bulk mass falling below the BF bound that is the more important component of the instability.

3.6 Discussion

3.6.1 Connections to Condensed Matter and Statistical Physics

The construction we explore potentially gives a new way to think about self-organized criticality in the fields where it was first explored and named [84]. The scaling of perturbations ($1/f$ flicker noise in the literature), and the instabilities associated with catastrophic failure and its possible connection to an emergent discrete scale invariance have their signatures in the purported holographic dual we have proposed. The $1/f$ so-called "flicker" noise (in fact $1/f^\alpha$, where α can depend on the system under consideration) is simply the signature of criticality itself [85] – a fixed point where perturbations exhibit scaling laws. There should be CFTs describing the coarse-grained effective theory of such systems where criticality is self-organized, and there could be AdS dual descriptions of such theories. The scaling laws

associated with the self-organized critical point are associated in this case to the scaling behavior of field solutions in AdS space. The above discussion applies to any critical point, not just self-organized ones. However, the particular 5D picture we have presented here appears to have features which place it close to systems with self-organization. These share the commonality that the systems in question are brought to the point of some sort of failure mode that leads to time dynamics, typically a form of adjustment. It has been suggested that the development of the adjustment behavior can be associated, in the coarse-grained theory, with scaling dimensions of the critical point being driven into the complex plane, and creating a discrete scale invariance, with fluctuations obeying a log-periodic power law. In the context of quantum field theory, it is known that such scaling laws are not allowed, and have instabilities associated with them [98]. In our picture these instabilities map to the region in the radion potential in which there are unresolved tachyons. Should the system be placed at these points of instability, it is, at the moment, unknown what the response of the system will be.

3.6.2 Incorporation of the Standard Model

The eventual goal is to embed this class of Higgs sector into a theory which accommodates the rest of the SM field content, and where the Higgs resides not precisely at the point of criticality, but instead picks a VEV and breaks the electroweak gauge symmetry spontaneously. This may occur as a result of finite radiative corrections, or perhaps through nontrivial feedback due to explicit breaking of conformal invariance in the SM (for example, from confinement and chiral symmetry breaking in QCD), or in extensions of it (as in [94]). If the SM can accommodate such a Higgs sector, a key calculation will be the Higgs cubic coupling in the context of the manner in which its potential is generated, as this will be eventually probed by colliders. As we will discuss in the next section, cosmology of such an extension of the SM could be very interesting. As we have emphasized, we have not yet fully identified the vacuum state, which we argue must be time-dependent unless tuning is

performed.

3.7 Speculation: Cosmology

The phenomenology of this scenario, if employed by nature in creating a low electroweak scale, is expected to be quite novel. Cosmology stands out as a particularly interesting area, due to the interplay between the radion and the Higgs. Metastability of the self-organized critical state is a vital consideration, although possibly resolved trivially by details of the deformation that drives self-organization or by a more complete model without a hard wall. A very interesting possibility is that dynamics of the radion could "rock" the early universe across the electroweak phase transition, sourcing a stochastic gravitational wave background, and creating an era of the early universe with an exotic equation of state (leading to modified constraints on inflationary scenarios and/or moduli masses) [115]. This may be interesting also from the standpoint of baryo- and leptogenesis.

Even more curious features are likely to emerge under a full calculation of the classical background, which we have left for future work. As we have emphasized, in writing down a 4D Lorentz-invariant radion potential, we have been required to do some violence to the theory. That is, we have calculated the potential under the presumption that the metric slices are flat. However, at the minima we have identified, the consistency conditions for a flat metric ansatz on the boundaries of the space, that both the UV and IR contributions to the radion potential separately vanish at the minimum, cannot be met without tuning. Bent 4D slices thus appear to be an integral part of the full solution to the theory at or near Higgs criticality. The theory is telling us that, as part of the resolution of the AdS tachyon, it breaks Lorentz invariance spontaneously at long distances. It is interesting to speculate at the form that this takes without (at least in this work) undertaking a detailed calculation.

Pessimistically, we might imagine that the solution could be a runaway. This seems unlikely from the following consideration of the dynamical model discussed in Section 3.4:

one could imagine adjusting the bulk cubic coupling λ between $\phi_{\rm d}$ and the Higgs, increasing it starting from some small value. The system would then reside at the minimum of the Goldberger-Wise potential created by the VEV of the $\phi_{\rm d}$ scalar, and the Higgs would have positive mass squared. One would in this case start in an unbroken phase with a massive Higgs field near the KK scale, and a completely static geometry (presuming the usual single tuning of the UV brane tension). Increasing the coupling would move the turn-on of the Higgs VEV ever closer to the minimum of the Goldberger-Wise potential, the critical z_1 value approaching the minimum from large z_1. The lowest-lying Higgs excitation would then gradually move to the bottom of the spectrum. There is a fine-tuned value of λ where the Higgs extremum coincides exactly at the minimum of the GW potential. The theory at this point, as the usual solution to the theory at the Goldberger-Wise minimum tells us, has a massive radion. Due to the adjustment of λ, it also has a (finely-tuned) massless Higgs. The only nearby instability in the low energy theory seems like the usual one associated with the Higgs phase transition. Further increase in λ either results in a Higgs VEV and symmetry breaking of the usual sort, or a more novel transition. It would appear the latter is a good possibility in some fraction of the parameter space of the model.

We have shown that the change in the radion potential due to the Higgs contribution creates a new minimum and for large negative v_H^2, there appears to be an onset of a novel type of transition that does not satisfy the usual metric junction condition. This means that the transition is not likely a normal Higgs one, but rather could be a transition to a spontaneously Lorentz-violating dynamical background. The radion should still be stabilized by its mass if we remain close to the boundary of the critical region. Therefore if it moves, it likely oscillates rather than runs away, acting "trapped" [116].[7] Amusingly, such a "trapped" modulus, the oscillating radion field, might look cosmologically similar to non-relativistic matter from the standpoint of the low energy theory: a Bose-Einstein condensate of radion particles. Deeper into the critical Higgs region, as the metric junction conditions become further from being

[7]We thank Ofri Telem for suggesting the possibility of an oscillating radion background.

satisfied, this time dependence may become very complicated, involving a mixture of the many degrees of freedom in the model. A simulation including full backreaction may be needed. It will be interesting to see more clearly what the low energy theory looks like with further study.

In short, the resolution of the IR-emergent AdS tachyon appears to require a spontaneous breakdown of 4D Lorentz invariance possibly a time-dependent oscillatory vacuum state. In the language of condensed matter physics and superconductivity literature, the theory would be resolving the instability by entering a "striped phase" at long distances with oscillations of the radion state breaking time translation invariance. The generic phenomenon of classical spontaneous breakdown of time translation invariance was investigated in [100], with a quantum mechanical version explored in [101]. These striped phases in condensed matter systems appear to arise in the presence of a frustration in the system where competing phenomena strive to set the vacuum state. In the case of our radion model, there are two competing "minima" of the potential: one where the radion is at a global minimum set by the Goldberger-Wise mechanism, but the Higgs is unstable, and the other where the Higgs field is stabilized, but the 5D gravity sector is not at an extremum of the action. The outcome in some condensed matter systems is to resolve such tension by entering a translation invariance-breaking striped phase, and we are suggesting similar physics may be at work in resolution of this AdS tachyon, although the breaking could be of time-translation invariance. A picture of these competing extrema is shown in Figure 3.10.

This sort of time dependent vacuum state and its application to cosmology was first explored in [103], with important recent followup work concerning stability of this scenario in [104].

In the 4D CFT language, there may be strongly coupled quasi-conformal 4D theories with a dynamically generated gap that have aspects of matter-Λ cosmology built into their ground state at long distances due to frustration of the dilaton. Classical breaking of time-translation invariance in the 5D theory corresponds to its quantum mechanical counterpart

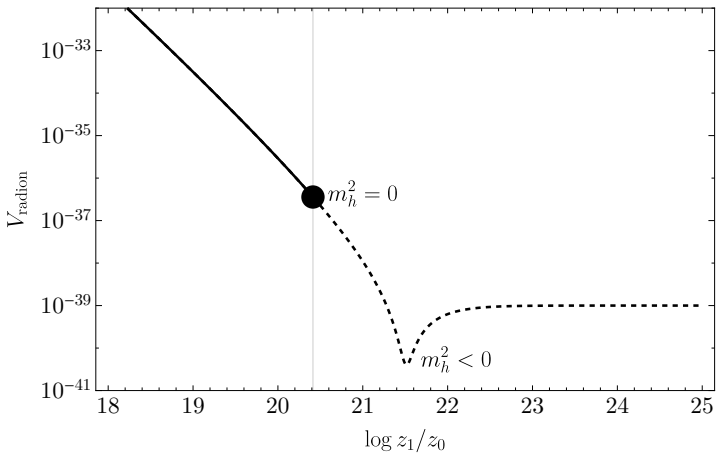

Figure 3.10: Here we show the radion potential. The dashed line is the potential if the Higgs VEV is left vanishing. There is a minimum of this potential where the metric ansatz for the IR brane is satisfied, but it corresponds to an unstable Higgs configuration. The solid line is the region where the effective Higgs mass squared in the low energy theory is positive. At the dot, the mass vanishes, and if $v_H^2 < v_H^2(\text{crit})$, the potential of the radion is minimized if the unstable Higgs region is forbidden. The gravity sector is not extremized here – the metric junction condition on the IR brane is not met.

in the 4D dual. The apparent puzzle of the light and seemingly unprotected Higgs in the critical region may be that it is the Goldstone boson of this breaking, a type of phonon, perhaps making the lightness of the Higgs directly connected to the presence of a cosmology with non-relativistic matter and dark energy content.

A better understanding of the dynamical aspects of this class of Higgs model is definitely required to make these statements more firm, but there seem to be some quite promising avenues to pursue.

3.8 Conclusions

We have discussed a new possible approach to the Higgs hierarchy problem. The model is in part inspired by attempts to model aspects of self-organized criticality in condensed matter systems in which it has been hypothesized that some classes of these critical states on the brink of catastrophic failure contain critical exponents that are becoming complex under

loading of the system, leading to discrete scale invariance and instabilities.

We have explored 5D constructions that have features that are similar to the behavior just described. It has made us directly confront the AdS tachyon, associated with violation of the Breitenlohner-Freedman bound, and search for the manner in which field theory might resolve it. In this model, the resolution takes the form of an IR brane with characteristics that depend on the 5D fundamental parameters. We found that there is are large regions of the parameter space where a novel type of transition appears to be taking place.

A dynamical cosmology is an unavoidable consequence of the model when placed inside or near this region. Time evolution appears crucial to resolution of the AdS tachyon in this model. This could be a feature rather than a bug, tying together puzzling aspects of fundamental particle physics with puzzling features of cosmology in a novel way. It remains to be seen what the Higgs vev and spectrum will be once this time evolution is completely taken into account, and whether its effective mass and/or vacuum expectation value are tied in some interesting way to aspects of the cosmology.

Top priorities are to further investigate the cosmological dynamics, determine whether this type of setup can be utilized as an extension of the Standard Model, study its novel phenomenological implications and constraints if so, and to seek an embedding in a more complete microscopic theory.

Chapter 4

Testing Vacuum Energy Using Neutron Star Mergers

4.1 Introduction

The recent observations of gravitational waves (GW's) from the merger of neutron stars (NS's) by LIGO/Virgo [117] along with the corresponding electromagnetic observations of the resulting kilonova have reverberated across most areas of physics and astronomy. From the point of view of particle physics the most important consequence of GW170817 and future merger events is our new ability to directly examine the properties of the QCD matter forming the inner layers of NS's, allowing us to use NS's as laboratories for fundamental physics [118–120]. This might also open up new avenues to testing the gravitational properties of vacuum energy (VE) which may also get at the heart of some of the deepest puzzles in fundamental physics [45].

It has long been speculated that there may be a new phase of nuclear matter at the core of the NS's [121]. If such a phase indeed exists it is expected to be accompanied by a jump in VE [122] of order $\Lambda_{\rm QCD}^4$ (where $\Lambda_{\rm QCD} \sim 200\,{\rm MeV}$ is the usual QCD scale) making NS's the only known objects where VE might make up a non-negligible fraction of the total mass.

Therefore studies of the interior structure of NS's can also probe the gravitational properties of VE, possibly shedding light on some of the most interesting open questions in physics: it could provide verification of the equivalence principle for VE. This would be the first test independent of those obtained from the cosmic acceleration of the Universe. Acceleration of the Universe provides information on VE in the low-temperature low density phase of the SM, while NS's could probe a low temperature but very high density phase if it exists in their cores. This could allow us to isolate the QCD contribution to ordinary VE and probe its gravitational properties.

Alongside the exciting advent of the gravitational wave observation era shepherded in by LIGO/Virgo, the Neutron star Interior Composition ExploreR (NICER) mission will soon measure masses and radii of several millisecond pulsars [123]. These measurements as well as the chirps from the inspiral of merging neutron stars can provide information about the equation of state (EoS) of dense nuclear matter. The chirps in particular are sensitive to the tidal deformability of NS's as they approach each other [124–128]. There has already been considerable work on constraining the EoS using the new LIGO/Virgo data [129–133].

There exists an extensive literature focused on trying to put bounds on the nuclear EoS at high densities from neutron star measurements (see for example [134–137]). Some recent theoretical work has focused on modeling possible new phases at the cores of neutron stars by using quasi-particle quarks rather than neutrons to provide the simplest description of the microscopic physics [138–144]. Further work has been done using NS's to constrain "beyond the Standard Model" physics [118–120].

In this paper we will assume that there is only Standard Model physics involved in the composition of neutron stars, and we will not try to model the microphysics of the putative new phase. Our main goal is to investigate the observable effects of the presence of VE on the GW signal as well as the mass versus radius curve of NS's, possibly providing new experimental probes of VE. To achieve this we will parameterize the effect of the new phase with a jump in the ground state energy due to a QCD phase transition assumed at the

core [45, 144–146]. This new phase would appear at a critical pressure of order $p_c \propto \Lambda_{QCD}^4$, and is expected to also lead to a change of VE [122] of order $\Delta\Lambda \propto \Lambda_{QCD}^4$. We will follow the conventional models for NS's where the EoS is divided into 7 layers, but we modify the innermost layer to take the effect of the phase transition and the appearance of VE at the core into account. Previous studies treat all 7 layers as simple polytropic fluids, but this is expected to be a poor fit to an inner core exhibiting the physics of a new phase of QCD, where the vacuum energy does not vanish. We will then evaluate the tidal Love numbers for such models, varying over the value of the vacuum energy at the core. One important consequence of the new phase (along with the presence of vacuum energy) is that the jump conditions at the boundary of the inner core have to be modified from those traditionally used in NS simulations [144–146]. We will explore the effect of a difference in energy densities of the two phases that includes a discontinuous, density independent term reflecting the absence of the low density QCD contribution to VE [45]. We will present several models of NS cores and estimate the effect of VE on tidal Love numbers. We find that VE can have a significant effect on NS merger waveforms with high chirp masses, so that such events serve as a probe of the physics of vacuum energy.

While vacuum energy is found to have a significant effect on waveforms, there are currently significant uncertainties both in terms of experimental waveform data and in terms of theoretical expectations for parameters describing the equation of state. Disentangling the effect of the QCD vacuum energy from other high density physics is currently not yet possible, however, the future of gravity wave observation holds great promise in terms of obtaining multiple independent measurements of neutron star observables, significantly tightening constraints on the equation of state of QCD. Additionally, progress may be made on the theory side – QCD is a complete microscopic theory, therefore its high density behavior can be uniquely determined from first principles. The ultimate goal is to use neutron stars as new astrophysical laboratories for studying physics at the density frontier, and determining whether the SM (plus classical gravity) agrees with data, or whether new exotic

(gravitational or particle) physics is necessary to explain the observations.

The chapter is organized as follows. In Section 4.2 we present the models we use for nuclear matter in the interior of NS's, along with a detailed discussion of the treatment of the phase transition at the boundary of the innermost layer. Section 4.3 contains the description of the tidal deformability of NS's. The results of our simulations and the effects of VE on the NS observables are given in Section 4.4: we show the mass versus radius curves and the tidal deformabilities for three different well-studied NS models and the effects of VE on those observables. Finally we conclude in Section 4.5.

4.2 Modelling High Density QCD

The main difference between our work and that of previous studies of tidal deformability of NS's is that we will fully account for a phase transition to an exotic phase of QCD in the innermost core region of NS's. Crucially, we take into account the Standard Model expectation that there is a constant shift Λ, independent of baryon number density, in the ground state energy relative to the surrounding layers parametrizing the change in VE due to the phase transition. In the ordinary phase of QCD the nonperturbative condensates of quarks and gluons make contributions [122] of order $(100\,\mathrm{MeV})^4$ to the VE. These contributions, along with those from other sectors of the SM, are canceled by the "bare" cosmological constant down to the observed cosmological constant of order $(\mathrm{meV})^4$:

$$\Lambda_{\mathrm{QCD}}^{\mathrm{SM\,vac}} + \Lambda_{\mathrm{SM\,other}} + \Lambda_{\mathrm{bare}} \simeq (10^{-3}\ \mathrm{eV})^4 \ . \tag{4.1}$$

The origin of the mechanism leading to this cancelation remains unknown. In an exotic phase of QCD the QCD contributions to the VE will have order one modifications and hence the precise cancelation will no longer apply:

$$\Lambda_{\mathrm{QCD}}^{\mathrm{exotic}} + \Lambda_{\mathrm{SM\,other}} + \Lambda_{\mathrm{bare}} \simeq \Delta\Lambda \ , \tag{4.2}$$

where $\Delta\Lambda$ is the shift in the QCD vacuum energy due to the phase transition. Hence in the absence of a dynamical adjustment mechanism, Standard Model physics predicts a density independent shift in the energy of the exotic phase compared to the ordinary phase, which will serve as a new effective cosmological constant term for this phase. An estimate of the difference between the VE of the exotic phase and the ordinary vacuum is given by nuclear saturation density: $|\Delta\Lambda| \sim \Lambda_{\rm QCD}^4$ [45]. Such a phase change is strongly suspected to occur at high chemical potential, with theoretical evidence arising from truncated diagrammatic expansions and other approximate methods [139, 140]. The phase change is in fact part of the standard picture of the QCD phase diagram. For many plausible descriptions of the matter in the outer portions of the star, nuclear saturation density is approached near the core of the densest NS's, making it quite possible that the most massive NS's contain cores with an exotic phase. In this section, we give a description of how one can model the QCD equation of state at various pressures, with particular attention paid to the phase transition that may occur in the innermost region.

4.2.1 Modeling the Outer Layers

The physics of neutron stars is an extremely rich field, and there are many details that go into modeling the different regions of NS's. Such an analysis is well beyond the scope of this work, however there are methods for coarse-graining these complexities to obtain an approximate equation of state for nuclear matter up until the phase transition we are interested in. Such an approximation is sufficient for the purposes of making predictions for gravitational wave signals. The most common methodology for modeling the high density nuclear physics region outside the exotic phase core is to separate the neutron star into multiple layers, with each layer satisfying a non-relativistic polytropic equation of state. The parameters of the polytrope are fixed either by matching conditions or by fitting results from more detailed studies.

We follow this established methodology and model the nuclear fluid and its corresponding

EoS as a piecewise polytrope where the boundaries between each layer are set by a given value of the pressure. Following previous work [136, 137] we will parametrize the EoS with a total of 7 layers. The Israel junction conditions [147, 148] require that the pressure must always be continuous between layers, even if each side of the boundary is separated by a first order phase transition. It is traditional to parameterize the EoS by assuming that the pressure is given by a power of the mass density $\rho(r) = m_n n(r)$ rather than a power of the energy density (as would be natural for a high-density, relativistic fluid). Since we want to efficiently compare our results with the existing state of the art simulations (some of which have been used as benchmarks for the LIGO/Virgo analysis) we will bow to this tradition and parametrize the EoS as

$$p = K_i \rho^{\gamma_i} \ , \qquad p_{i-1} \leq p \leq p_i \ , \tag{4.3}$$

where $i \in \{1, \ldots, 7\}$ for K_i, γ_i and $i \in \{1, \ldots, 6\}$ for p_i. The pressures, p_i, dividing the various layers have a one to one correspondence with the boundaries in the mass density: ρ_i. The Einstein equations contain the energy density, which is related to the mass density via the first law of thermodynamics: $d(\epsilon/\rho) = -p\, d(1/\rho)$. Integrating the first law together with (4.3) yields the corresponding energy density:

$$\epsilon = (1 + a_i)\rho + \frac{K_i}{\gamma_i - 1}\rho^{\gamma_i} \ , \tag{4.4}$$

where the a_i are integration constants. Note that the appearance of the a_i parameters is a consequence of using a polytropic ansatz for the mass density. Naively, one would think that using a relativistic polytropic ansatz for the energy density would have led us to a relation with one less free parameter. However another thermodynamical condition, continuity of the chemical potential, would have forced us to reintroduce the baryon number density, and therefore to bring back another parameter. So these simply correspond to different parametrizations of the EoS, and we adopt the one described above in order to follow the

traditional approach.

By using 7 layers we have introduced a large number of parameters (γ_i, K_i and a_i). Most of those can be determined by continuity of various quantities at the layer boundaries. For the outer 6 layers we assume the continuity of the energy density at the boundaries, which allows us to determine the a_i's:

$$a_i = \frac{\epsilon(\rho_{i-1})}{\rho_{i-1}} - 1 - \frac{K_i}{\gamma_i - 1}\rho_{i-1}^{\gamma_i - 1} \ . \tag{4.5}$$

If the K_1 constant for the outermost layer is known, then the other K_i values (except for the innermost layer) can be determined by the continuity of the pressure:

$$K_i = K_{i-1}\rho_{i-1}^{\gamma_{i-1}-\gamma_i} \ , \qquad i \in \{2, \ldots, 6\} \ . \tag{4.6}$$

For the outermost layer, the "crust", we have $p_0 = 0$. Requiring that $\lim_{\rho\to 0} \frac{\epsilon}{\rho} = 1$ (physically this means that the edge of the star is ordinary non-relativistic matter) implies that $a_1 = 0$. Thus the parameterization of the EoS of the NS for the outer layers will require us to specify the critical pressures p_i, all the polytropic exponents γ_i as well as the outermost polytropic constant K_1, while all other parameters will be determined by the continuity conditions.

4.2.2 Modeling the Core and the Effect of VE

For the last layer, we use an equation of state that incorporates physics associated with a change in the QCD vacuum state due to high density. There are two effects expected at this phase transition: a vacuum energy term Λ in the fluid that is independent of baryon number density, and a jump in energy density across the boundary. Unlike in the outer layers, in the exotic phase the nature of the baryonic states may be very different from the usual zero temperature baryons. Since QCD conserves baryon number, for the innermost layer it is more natural to use baryon number density n in place of the mass density as the variable parametrizing the EoS for the central core ($p > p_6$). In this case, the equation of state can

be written as:

$$p = \widetilde{K}_7 n^{\gamma_7} - \Lambda \ , \tag{4.7}$$

$$\epsilon = \widetilde{a}_7 n + \frac{\widetilde{K}_7}{\gamma_7 - 1} n^{\gamma_7} + \Lambda \ . \tag{4.8}$$

Note that the vacuum energy appears with the opposite sign in the energy density and pressure, just as with the cosmological constant. Our goal is to see how sensitive neutron star observables are to the VE shift Λ.

To keep the form of the EoS unchanged in the various layers we can introduce the density $\rho = m_n n$ where m_n is the ordinary neutron mass, and use this rescaled number density for the innermost layer. We can easily see that in terms of this rescaled density the EoS will have the same form as for the outer layers:

$$p = K_7 \rho^{\gamma_7} - \Lambda \ , \tag{4.9}$$

$$\epsilon = (1 + a_7)\rho + \frac{K_7}{\gamma_7 - 1} \rho^{\gamma_7} + \Lambda \ , \tag{4.10}$$

where $K_7 = \widetilde{K}_7 / m_n^{\gamma_7}, (1 + a_7) = \widetilde{a}_7 / m_n$ are just redefinitions of the unknown constants parametrizing the EoS for the inner layer. We adopt this notation in order to stay close to the standard formalism used in the literature.

Let us now examine in detail the continuity (or jump) of the various quantities at the phase boundary between the sixth and the seventh (innermost) layer. The Israel junction conditions [147, 148] still require that the pressure be continuous:

$$K_7 \rho_+^{\gamma_7} - \Lambda = K_6 \rho_-^{\gamma_6} = p_6 \ , \tag{4.11}$$

but due to the appearance of the Λ term this now requires a jump in $\rho(r)$ from ρ_+ to ρ_- (where $\rho_- = \rho_6$) and consequently also in $\epsilon(r)$ from ϵ_+ to ϵ_-. Since QCD conserves baryon number, another quantity that we need to require to be continuous is the chemical potential

μ (that is we are assuming chemical equilibrium at the phase boundaries with conserved baryon number). The chemical potential at zero temperature is given by

$$\mu = \frac{\epsilon + p}{n} \ , \tag{4.12}$$

where n is again the baryon number density. This relation holds even if the VE is nonzero. Therefore the jumps from ϵ_+ to ϵ_- and from ρ_+ and ρ_- (in our convention $\rho_+ = m_n n_+$ and $\rho_- = m_n n_-$) are related to each other by

$$\frac{\epsilon_+ + p_6}{\rho_+} = \frac{\epsilon_- + p_6}{\rho_-} \ . \tag{4.13}$$

The convexity of the free energy $\left(\frac{\partial^2 F}{\partial V^2}\right)_{T,N} > 0$ can be translated to $\left(\frac{\partial p}{\partial n}\right)_{T,N} > 0$. This latter form implies that the number density increases with pressure, yielding $\rho_+ \geq \rho_-$. This condition together with the continuity of the chemical potential tells us that the jump in energy density should also be positive, i.e. $\epsilon_+ \geq \epsilon_-$.

A typical phase transition will have both $\Delta\epsilon$ and Λ non-vanishing, and this scenario is the focus of our studies. We choose to parametrize the jump in energy density such that it is proportional to the absolute value of the shift in VE:

$$\epsilon_+ - \epsilon_- = \alpha|\Lambda| \ . \tag{4.14}$$

For each value of γ_7, α, and Λ, this condition, together with continuity of the chemical potential, fixes the values of K_7 and a_7. This parametrization of the phase transition has the advantage that the $\Lambda = 0$ limit reproduces the results obtained in the literature since both the mass density and the energy density become continuous in this case. In principle, α could be taken to be zero, isolating the effects of vacuum energy from a jump in the energy density, corresponding to a second order phase transition. Here we will assume that the phase transition is first order with an accompanying jump in most quantities across the

phase boundary and take $\alpha > 0$. A final consistency condition is that both the full pressure and the partial pressure of the fluid, $K_7\rho^{\gamma_7}$, must be positive. This implies that Λ must satisfy $-p_6 < \Lambda$.

4.3 Modeling Neutron Stars

After presenting the relevant physics of the dense QCD matter forming the interior of the NS we are now ready to review the usual method for calculating the structure of the interior of the NS. GW emission observed by LIGO/Virgo originates from the inspiral phase, when the stars are far apart relative to their radii. In this stage of the merger, the NS's are still well approximated by nearly spherically symmetric static objects, with deviations described by a linear response in an expansion in spherical harmonics. In this paper we will ignore the effects of NS angular momentum but plan to further investigate that in a future publication. First we briefly review the equations relevant for the spherically symmetric solution and then present an overview of the perturbations due to the gravitational field of the other NS.

4.3.1 Spherically Symmetric Solutions

At lowest order, the stars are spherically symmetric, and their mass distribution is given by the solution to the Tolman-Oppenheimer-Volkoff (TOV) equations [149]. These equations are easily derived by starting with a spherically symmetric metric ansatz

$$ds^2 = e^{\nu(r)}dt^2 - \left(1 - \frac{2Gm(r)}{r}\right)^{-1} dr^2 - r^2 d\Omega^2 \ , \tag{4.15}$$

and using the associated Einstein equations assuming a spherically symmetric fluid distribution with pressure $p(r)$ and energy density $\epsilon(r)$. The resulting TOV equations are:

$$m'(r) = 4\pi r^2 \epsilon(r) \ , \tag{4.16}$$

$$p'(r) = -\frac{p(r)+\epsilon(r)}{r\left(r-2Gm(r)\right)} G\left[m(r)+4\pi r^3 p(r)\right] \ , \tag{4.17}$$

$$\nu'(r) = -\frac{2p'(r)}{p(r)+\epsilon(r)} \ , \tag{4.18}$$

where $'$ denotes differentiation with respect to the radial coordinate r. The TOV metric provides the unperturbed solution around which the gravitational field of the second star will introduce perturbations that can be dealt with using a multipole expansion. From the solution to these equations, one obtains the internal structure of the star: the mass as a function of radius, as well as the thicknesses and masses of the various layers.

4.3.2 Tidal Distortion and Love Numbers

In a neutron star binary, each neutron star experiences gravitational tidal forces due to the other. This force squeezes the stars along the axis passing through both of their centers, and deforms the stars, inducing a quadrupole moment. The size of this induced quadrupole moment is determined by the structure of each neutron star, which can be characterized by its compactness and the stiffness of the EoS. These in turn depend on the physical properties of the dense QCD matter as described by its EoS discussed in the previous section. The effect of the induced quadrupole on gravitational wave data is to change the power emission as a function of time and frequency. Thus LIGO data on NS inspirals contains information about this tidal deformability, which depends on the equation of state of the matter making up the stars.

A common way to describe the deformability of a star is through the Love number. Love numbers were originally introduced in the study of Newtonian tides [150]. The application of Love numbers to gravitational waves produced in neutron star inspirals was initiated

in refs. [124, 125], and further generalized in [151]. Detailed studies of the prospects for gravitational wave detection were provided in [126–128].

In the local rest frame of one star a small tidal field can be described in terms of a Taylor expansion of the Newtonian gravitational potential, or the time-time component of the metric tensor. There are two contributions, one from the effect of the distant star, and the other from the induced quadrupole moment. At large distances (using Cartesian coordinates, x^i) g_{tt} takes the form [126]

$$\frac{1+g_{tt}}{2} \approx \frac{GM}{r} + \frac{3GQ_{ij}}{2r^5}x^i x^j - \frac{1}{2}\mathcal{E}_{ij}x^i x^j \ldots \tag{4.19}$$

Here $\mathcal{E}_{ij}$ parametrizes the external tidal gravitational field, and Q_{ij} is the induced quadrupole moment. Both matrices are traceless and symmetric. To linear order in the response, the induced quadrupole is determined by the tidal deformability, λ, defined by

$$Q_{ij} = -\lambda\,\mathcal{E}_{ij}\ . \tag{4.20}$$

One can then define a dimensionless quantity k_2 by

$$k_2 = \frac{3}{2}\frac{G\lambda}{R^5}\ , \tag{4.21}$$

where R is the radius of the neutron star. This is referred to as the $l = 2$ tidal Love number, and is the main physical observable. The advantage of this parametrization is that the Love number does not vary much with the size of the star, with typical Love numbers ranging from $k_2 = 0.001$ to $k_2 = 1$ as masses and equations of state are varied.

In order to determine k_2, one performs the perturbative expansion of the solutions to the Einstein equations in the presence of an external gravitational field assuming a multipole expansion. Thus inside and near the star we will write the metric perturbation as an expansion in spherical harmonics Y_l^m. Due to the axial symmetry around the axis connecting the cen-

ters of the two stars, m is zero, and since the tidal deformation is dominantly quadrupolar, with no dipole, the leading contribution is at $l = 2$ [126]. Hence the full perturbed metric $g_{\alpha\beta} + h_{\alpha\beta}$ (where $g_{\alpha\beta}$ is the metric from (4.15)) is written as

$$h_{\alpha\beta} = \text{diag}\left(e^{\nu(r)}H(r), e^{\mu(r)}H(r), r^2K(r), r^2\sin^2\theta K(r)\right) Y_2^0(\theta,\phi) \ , \tag{4.22}$$

where $e^{\mu(r)}$ and $e^{\nu(r)}$ are the functions in the solution to the unperturbed spherically symmetric metric (4.15):

$$e^{\mu}(r) = (1 - 2Gm(r)/r)^{-1} \ , \tag{4.23}$$

$$\nu'(r) = -\frac{2p'(r)}{p(r) + \epsilon(r)} \ , \tag{4.24}$$

and the Einstein equations relate the functions K and H:

$$K'(r) = H'(r) + H(r)\nu'(r) \ . \tag{4.25}$$

Inserting the perturbed metric into Einstein's equations results in a second order differential equation for $H(r)$:

$$\begin{aligned} H'' = 2He^{\mu}&\left\{-2\pi G\left[5\epsilon + 9p + \frac{d\epsilon}{dp}(\epsilon + p)\right] + \frac{3}{r^2} + 2G^2e^{\mu}\left(\frac{m(r)}{r^2} + 4\pi rp\right)^2\right\} \\ &+ \frac{2}{r}H'e^{\mu}\left\{-1 + \frac{Gm(r)}{r} + 2\pi Gr^2(\epsilon - p)\right\} . \end{aligned} \tag{4.26}$$

To find solutions, one starts with a series expansion of H very near the core of the star, at small r:

$$H(r) = a\,r^2 + \mathcal{O}\left(r^4\right) . \tag{4.27}$$

The linear term drops out since the solution must be regular at $r = 0$. The size of the

coefficient a is linearly proportional to the size of the external perturbation, $\mathcal{E}_{ij}$, and is not an intrinsic property of the star, as is clear from the fact that it is simply a normalization coefficient for the solution to the linear ODE for H. One can thus pick this coefficient arbitrarily in numerically solving for H. The $l = 2$ tidal Love number, on the other hand is an intrinsic property, and the value for a drops out in calculating it. The value for k_2 can be calculated once H is found, and matched at large r onto the metric ansatz in Eq. (4.19). It is given by

$$\begin{aligned} k_2 = {} & \frac{8C^5}{5}(1-2C)^2[2+2C(y-1)-y] \\ & \times \big\{2C[6-3y+3C(5y-8)] + 4C^3[13-11y+C(3y-2)+2C^2(1+y)] \\ & + 3(1-2C)^2[2-y+2C(y-1)]\log(1-2C)\big\}^{-1} \ , \end{aligned} \tag{4.28}$$

where C is the compactness parameter GM/R, and y is obtained from the solution to H evaluated on the surface of the star:

$$y = \frac{RH'(R)}{H(R)} \ . \tag{4.29}$$

Another dimensionless quantity, known as the dimensionless tidal deformability, is often found in the literature. It is obtained from the definition of k_2 by factoring out the C^5 in front:

$$\bar{\lambda} = \frac{2k_2}{3C^5} = \frac{\lambda}{G^4M^5} \ . \tag{4.30}$$

4.4 Results and Fits

We are now ready to present our results for the effects of adding a VE component to the innermost layer. We will use several different benchmark EoS's for modeling the NS's and investigate the consequences of the presence of VE in each of those cases. Two of the EoS's are

more "conservative" in the sense that the maximum stable NS mass that can be achieved just barely goes above $2M_\odot$ (the maximum NS mass observed thus far is $M = (2.01 \pm 0.04)M_\odot$). The two more conservative models are the AP4 [152] and SLy [135] EoS's, which were also used as benchmarks by LIGO/Virgo [117]. We also consider the less restrictive model of Hebeler et al. [137] which permits larger masses, up to nearly $3M_\odot$. For the AP4 and SLy models we use the piecewise polytropic parametrization for all 7 layers provided by Read et al. [136]. We have tabulated the corresponding parameters in Table 4.1. While the model of Hebeler et al. also uses a piecewise polytropic EoS for the innermost three layers, for the outer four layers corresponding to the crust they use a semi-analytic expression. In their parametrization, the outer crust is modeled by the BPS EoS [153] assuming β equilibrium[1], followed by a layer for which chiral EFT (valid up to the nuclear saturation density around 0.18 baryons/fm^3) is used to obtain the EoS. This semi-analytic expression is consistent with the piecewise polytropic approach of AP4 and SLy.

Varying the EoS leads to more or less compact NS's, whose deformability will also change. The compactness of the NS can be characterized by the radius of a NS with a fixed mass. The deformability describes how much the NS reacts to the presence of the gravitational field of the second NS in the binary merger event and is characterized by the tidal deformability. In the first subsection, we present our results for the mass versus radius, $M(R)$, curves of neutron stars with different nuclear EoS's including the effect of VE, while in the second, we study the tidal deformability and comment on the potential for LIGO/Virgo to discern between models with different assumptions about the change in VE in exotic phases of QCD.

4.4.1 M(R) Results

We first present the results for the mass versus radius curves for the three different benchmark equations of state, whose parameters are displayed in Table 4.1. These three benchmarks cover a realistic range of possible EoS's, with a wide variation in the maximum possible

[1] β-equilibrium corresponds to equal rates of neutron decay and proton capture of electrons.

	SLy	**AP4**	**Hebeler**
K_1	9.27637×10^{-6}		See [137]
p_1	$(0.348867)^4$		See [137]
p_2	$(7.78544)^4$		
p_3	$(10.5248)^4$		
p_4	$(40.6446)^4$	$(41.0810)^4$	$(72.2274)^4$
p_5	$(103.804)^4$	$(97.1544)^4$	$(102.430)^4$
p_6	$(176.497)^4$	$(179.161)^4$	$(149.531)^4$
γ_1	1.58425		See [137]
γ_2	1.28733		
γ_3	0.62223		
γ_4	1.35692		
γ_5	3.005	2.830	4.5
γ_6	2.988	3.445	5.5
γ_7	2.851	3.348	3

Table 4.1: The parameters used for each EoS. The exponents γ_i are dimensionless, the various pressures have units of MeV^4, and K_1 is in units of $\mathrm{MeV}^{4-4\gamma_1}$. The Hebeler et al. parametrization [137] uses a semi-analytic expression which is not piecewise polytropic in the outer region of the star, and thus cannot be displayed in the table.

stable neutron star mass. We take care not to violate basic constraints on the behavior of high density QCD matter. For example, when pressures near the center of the star become very large, and relativistic effects dominate, one must ensure that the equation of state does not violate causality. Causality requires that the speed of sound in the fluid does not exceed the speed of light:

$$v_{\mathrm{s}} = \sqrt{\frac{dp}{d\epsilon}} \leq 1 \ . \tag{4.31}$$

However, using simple EoS models this condition is often violated for very large central pressures. Such violation does not imply the instability of the NS, but is rather an indication

that the ansatz for the EoS is no longer a good approximation of the underlying nuclear physics in that region. Such causality violation would never arise in the true QCD equation of state at very high densities.

The true stability condition for the central pressures that a neutron star can support is given by

$$\frac{\partial M}{\partial p_{\text{center}}} > 0 \ . \tag{4.32}$$

This constraint arises from considerations of radial pulsation modes of the star, and is directly associated with stability of the fundamental mode of oscillation [154]. The relation in Eq. (4.32) above can be violated when the jump in the energy density is too large [145]:

$$\epsilon_+ - \epsilon_- \geq \frac{1}{2}\epsilon_- + \frac{3}{2}p_6 \ . \tag{4.33}$$

Above this bound, the mass of the NS no longer increases with increasing core pressure, and the NS is unstable [142, 143, 145, 146, 155]

We note that the condition in Eq. (4.32) can be satisfied for two stars of the same mass, but different internal pressures [156–158], corresponding to different phases in the core of the star. In such cases, the critical energy density jump exceeds that in Eq. (4.33) at the transition. However, even with this instability, one sometimes finds for $p > p_6$, that there is a disconnected class of solutions that does not exceed the bound in Eq. (4.32). The possibility then arises that some of the exotic, disconnected solutions have the same masses as some of the normal, lower pressure solutions.

Which of the two conditions, causality or monotonicity, will limit the central pressure depends on the EoS. For AP4 and SLy, the limit is set by causality. This bound can be avoided by modifying the EoS via a "causal extension" [137] into the regions where the pressure exceeds the maximal value set by the causality bound. For the models we are working with, we have found that this extension simply flattens out the curves at the point

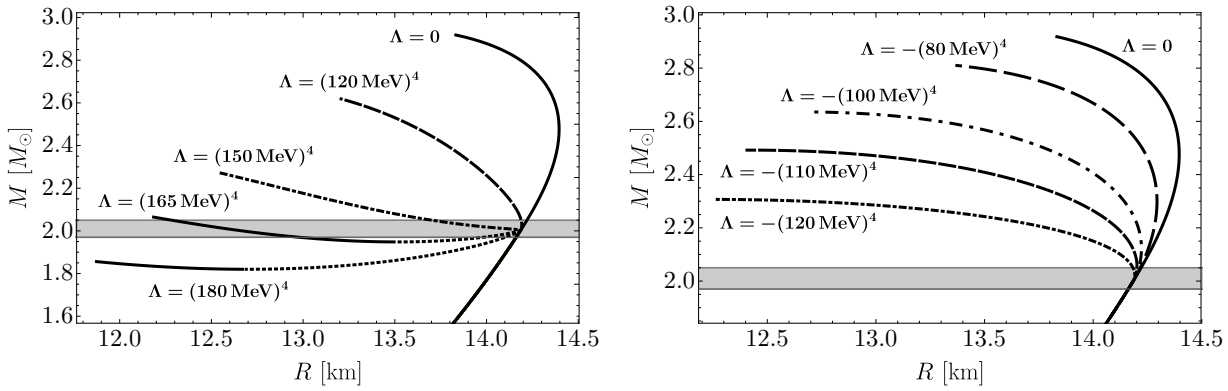

Figure 4.1: Mass versus radius curves corresponding to the stiff parametrization of Hebeler et al. [137] with $\alpha = 3$. Dotted curves in the plot on the left correspond to unstable configurations violating Eq. (4.32). Positive values of Λ are shown in the plot on the left, and negative ones on the right.

where causality is violated, and hence does not change the value of the maximum mass significantly. For this reason we have chosen not to make this modification and ended the curves at the point where the speed of sound reaches unity.

The $M(R)$ curve and the effect of VE for the Hebeler et al. EoS [137] are shown in Fig. 4.1. Each curve is obtained by varying the pressure at the center of the star but keeping all of the other parameters fixed. We have fixed $\alpha = 3$ in this plot, as well as all those that follow.[2] When the central pressure is greater than p_6, the value of Λ becomes relevant and the other curves depart from the behavior of the $\Lambda = 0$ case. Dotted parts of the curves correspond to unstable regions, i.e. solutions of the TOV equations in which the stability condition (4.32) is violated. The shaded region represents the most massive neutron star measured to date, with a mass of $(2.01 \pm 0.04) M_\odot$ [159]. Notice that for some positive values of Λ, i.e. when the jump in energy density is big enough according to Eq. (4.33), we find a second stable region which is disconnected from the main branch, as discussed above. This means that for a given mass, there are two possible types of stars, one with no exotic phase in the core, and another with a significant portion of the star in the new phase. This gives rise

[2]Taking α to be small reduces the change in the curves relative the $\Lambda = 0$ case, however small values of α are not representative of most phase transitions, which are typically accompanied by a change in the energy density as well as the vacuum energy.

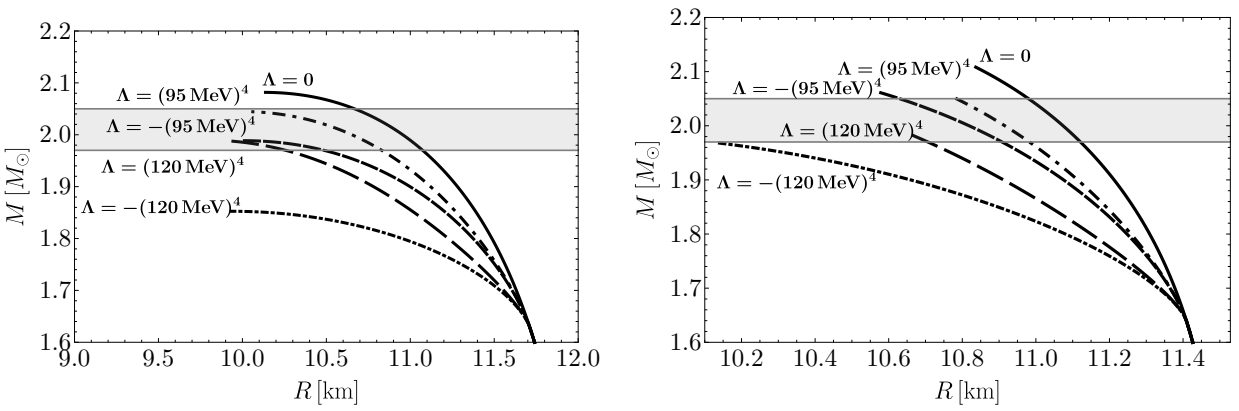

(a) SLy EoS

(b) AP4 EoS

Figure 4.2: $M(R)$ curves for the SLy and AP4 equations of state for various Λ values on the seventh layer. For all the curves, the proportionality constant α in the jump equation (4.14) is chosen to be $\alpha = 3$. The gray region shows the allowed mass range of the heaviest neutron star, with mass $(2.01 \pm 0.04)M_\odot$.

to interesting effects, both for $M(R)$ curves and in GW observables. For example, assuming that the $\Lambda = (165\,\mathrm{MeV})^4$ curve is the correct one, it would be possible to observe two $2M_\odot$ neutron stars with significantly different radii. That is, there are two stable configurations for stars with the same mass. It is quite interesting that the physics of QCD may allow for a plethora of different compact objects, with population numbers depending on the conditions of their formation.

Our procedure for introducing the VE for this model is the following. In order to make sure that all values of Λ considered here are compatible with a neutron star mass of $(2.01 \pm 0.04)M_\odot$, we stop the next-to-innermost polytropic region as soon as the mass reaches $2.00M_\odot$. This corresponds to choosing a critical pressure $p_6 \approx (150\,\mathrm{MeV})^4$. Once the critical pressure is reached, we transition into the innermost polytropic region with a nonzero VE, and we allow for the central pressure to be as high as possible without violating the causality bound.

Next we present results for the AP4 [152] and SLy [135] EoS models. The $M(R)$ curves for the AP4 and SLy models with different values of the VE in the innermost layer are shown in Fig. 4.2. One can again see that up to a certain critical mass, the curves corresponding

to different Λ's in the innermost layer do coincide with each other. The reason for this is that below this mass the central pressure is not high enough to enter the exotic high density phase of QCD. The critical pressure for the phase transition to occur is set by p_6 which is an input of the model. For the AP4 and SLy models, $p_6 \approx (179\,\mathrm{MeV})^4$ and $p_6 \approx (176\,\mathrm{MeV})^4$ respectively which correspond to a critical mass of approximately $1.6 M_\odot$ for both models.

The plots for all three EoS's show that the maximal mass of the neutron star decreases for both positive and negative values of VE. This is a generic feature of neutron star models with phase transitions with vacuum energy in our study, and is due to the jump in the energy density across the phase transition. This conclusion is similar to that obtained in previous works that study phase transitions without vacuum energy [160].

4.4.2 Tidal Deformabilities and LIGO/Virgo

Let us now discuss NS observables from GW's emitted during the merger of NS's. The frequency versus time behavior of the waveform of the emitted gravitational wave, usually expressed in terms of the "gravitational wave phase" appearing in the Fourier transform of the chirp, can be determined by an expansion in relativistic effects, starting at Newtonian order, and proceeding to post-Newtonian corrections in the velocity. At dominant Newtonian order, where the two NS's are approximated by point masses, the waveform depends only on a particular combination of the masses called the chirp mass:

$$\mathcal{M} = \mu^{3/5} M_{\mathrm{tot}}^{2/5} = \frac{(M_1 M_2)^{3/5}}{(M_1 + M_2)^{1/5}} \,, \tag{4.34}$$

where μ is the reduced mass of the system [161]. For the recently observed merger event, GW170817, the chirp mass was measured to be $\mathcal{M} = 1.188^{+0.004}_{-0.002} M_\odot$.

Since this is the dominant contribution to the waveform, the chirp mass can be determined quite accurately. However, the individual masses must be extracted from higher order velocity corrections to the waveform, and are thus more difficult to constrain. At

higher order, spin-couplings are important as well, and without information about the stars' rotational speeds and axes, precise extraction of the masses is impossible. This information is in principle retrievable from measurements of the waveform, but is difficult as it relies on data near the end of the inspiral, where current experiments lose sensitivity, and where full numerical simulation of the merger event may be necessary [162].

At present, the individual masses can only be estimated by using the chirp mass and some assumptions for the angular rotation frequency of the stars. For GW170817 in the low-spin case, the estimated mass range is 1.36–1.60$M_\odot$ for the heavy star and 1.17–1.36$M_\odot$ for the light star, while for the high-spin case, there is considerably more possible variation in the masses: 1.36–2.26$M_\odot$ for the heavy star and 0.86–1.36$M_\odot$ for its less massive partner.

Similarly, it is not yet possible to measure individual tidal deformabilities. However, it is possible to constrain a weighted combination of the individual masses and deformabilities through their contribution to the gravitational wave phase at order v^5. This so-called "combined dimensionless tidal deformability" is defined as

$$\widetilde{\Lambda} = \frac{16}{13}\frac{(M_1 + 12M_2)M_1^4\bar{\lambda}_1 + (M_2 + 12M_1)M_2^4\bar{\lambda}_2}{(M_1 + M_2)^5} \ . \tag{4.35}$$

For the recent event GW170817, the current constraint placed on $\widetilde{\Lambda}$ is ≤ 800 for the low-spin assumption and ≤ 700 for the high-spin case. In the low-spin case, the neutron star masses are probably too low to contain an exotic QCD phase, and thus event GW170817 would not contain information about VE. Of course, this may not be the case for future merger events, which may involve heavier NS's. In the high-spin case, however, the inner core could be in the exotic phase, and the constraints from GW170817 are relevant for studying VE.

The rest of this section contains our results for the effects of VE on the tidal deformabilities, which will be presented in a series of plots. Each plot will be presented both for the Hebeler et al. EoS, which allows for larger NS masses and hence larger effects from VE, as well as for the AP4 and SLy EoS's, which cut NS masses off at $2M_\odot$ and thus have smaller

VE effects.

- Fig. 4.3 shows the individual tidal deformabilities of both NS's and the effect of VE using the Hebeler et al. EoS.

- Fig. 4.4 translates the effects of VE into a fractional shift of the combined tidal deformability $\widetilde{\Lambda}$. This plot shows that the effect of VE can be as large as 70% and is generically sizable for the case of the Hebeler et al. EoS.

- Figs. 4.5, 4.6, 4.7 repeat the same analyses for the AP4 and SLy EoS's, where we see that the deviations are generically smaller, but can still reach 25–30% for larger chirp masses.

- Figs. 4.8, 4.9 emphasize the role of the chirp mass: they show the maximal achievable effect of VE as the chirp mass is increased. We can see that observing events with chirp masses above 1.6–1.8$M_\odot$ will be key to observing the effects of VE.

- Fig. 4.10 shows the effect of VE on GW170817 (assuming the Hebeler EoS) where it can significantly change the allowed region of NS masses one would infer from the constraint on the tidal deformability.

The EoS parametrization of Hebeler et al. [137] allows for large possible deviations in the tidal deformability when a VE term is added to the central core in the new phase. In Fig. 4.3, we show the effect of varying the VE term for a selection of three different input chirp masses. The curves are obtained by fixing the chirp mass $\mathcal{M}$ at a few representative values and then scanning over the mass of the heaviest star, M_1. Typically it is found that the heavier the star, the smaller the tidal deformability. This is largely due to the fact that more massive stars typically have smaller radii, and thus respond less to external tidal fields.

We note that the $\Lambda = (165\,\mathrm{MeV})^4$ curve in the third plot is composed of two separate branches, corresponding to the two separate stable stars with equal masses but different radii as explained in the previous section. The branch with the highest values of $\bar{\lambda}_2$ corresponds

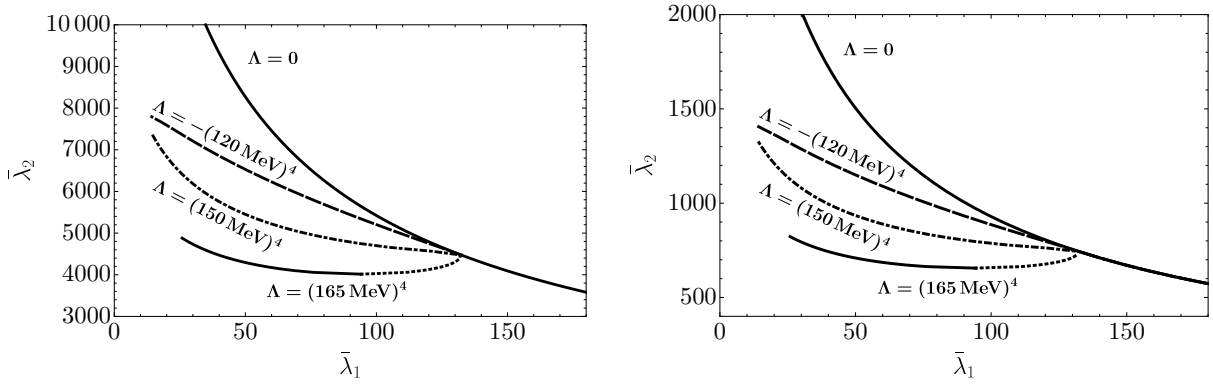

(a) $\mathcal{M} = 2^{-1/5}1.4M_\odot \approx 1.22M_\odot$ (b) $\mathcal{M} = 2^{-1/5}1.7M_\odot \approx 1.48M_\odot$

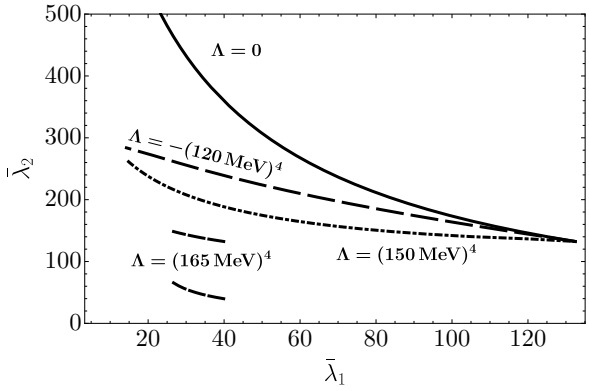

(c) $\mathcal{M} = 2^{-1/5}2.0M_\odot \approx 1.74M_\odot$

Figure 4.3: Tidal deformabilities for the Hebeler et al. parametrization with $\alpha = 3$. Each plot corresponds to a different chirp mass. Dotted parts of the curves with $\Lambda = (165\,\mathrm{MeV})^4$ correspond to unstable configurations. In all cases, the deviation from the $\Lambda = 0$ curve is significant.

to only the most massive star laying in the disconnected branch of the $M(R)$ curve, while in the other case both stars in the binary would come from the disconnected branch. Part of the reason why the deviations from the $\Lambda = 0$ curve are significant here can be found directly in Fig. 4.1. Since there the maximum mass for the $\Lambda = 0$ curve is close to $3M_\odot$, the curves that correspond to a nonzero Λ can depart significantly without being excluded by the measurement of the most massive neutron star, $(2.01 \pm 0.04)M_\odot$.

As we are most interested in the changes brought about by considering non-vanishing VE, it is useful to introduce a variable that quantifies the relative shift in $\widetilde{\Lambda}$ due to VE:

$$\delta \equiv \frac{\widetilde{\Lambda} - \widetilde{\Lambda}_0}{\widetilde{\Lambda}_0} \ , \tag{4.36}$$

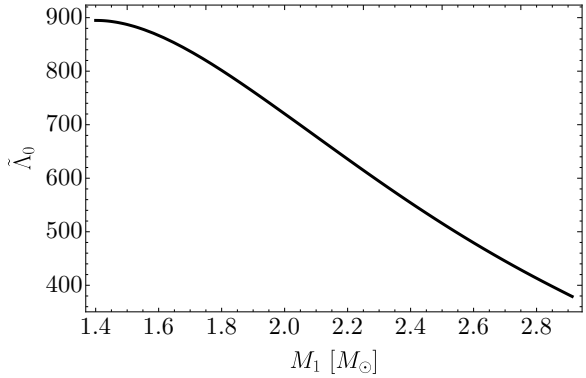

(a) $\mathcal{M} = 2^{-1/5}1.4M_\odot \approx 1.22M_\odot$

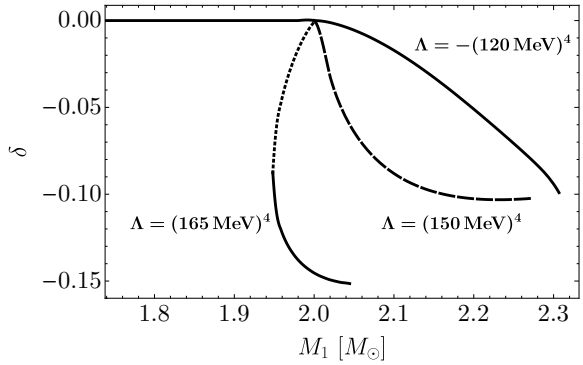

(b) $\mathcal{M} = 2^{-1/5}1.4M_\odot \approx 1.22M_\odot$

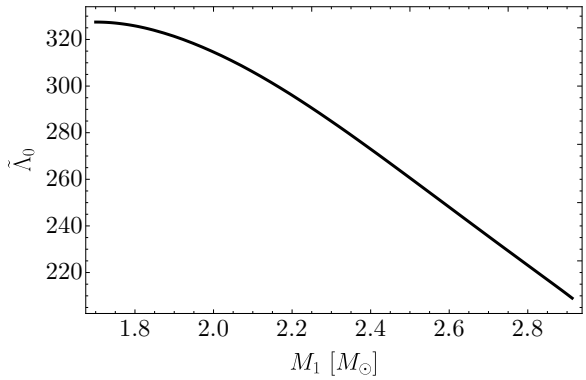

(c) $\mathcal{M} = 2^{-1/5}1.7M_\odot \approx 1.48M_\odot$

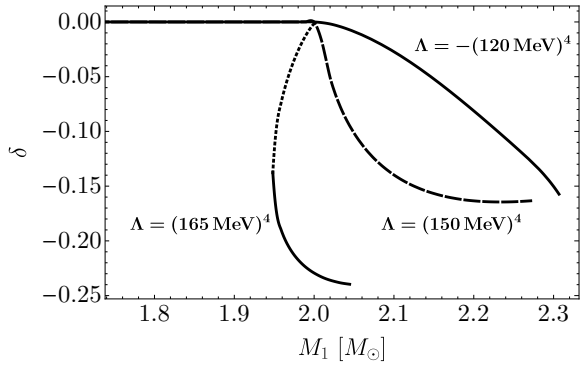

(d) $\mathcal{M} = 2^{-1/5}1.7M_\odot \approx 1.48M_\odot$

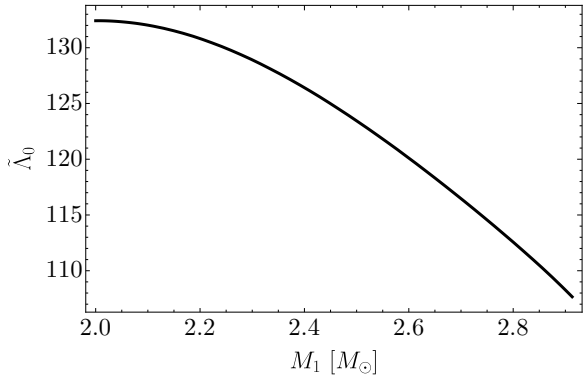

(e) $\mathcal{M} = 2^{-1/5}2.0M_\odot \approx 1.74M_\odot$

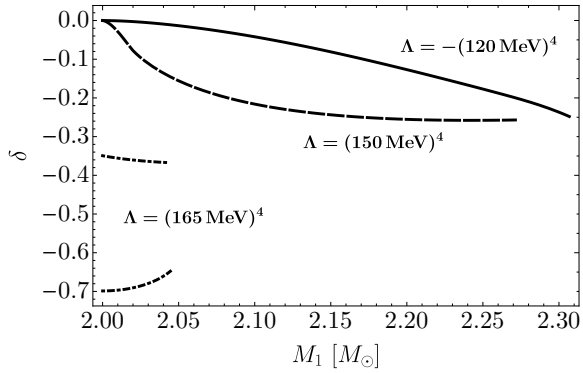

(f) $\mathcal{M} = 2^{-1/5}2.0M_\odot \approx 1.74M_\odot$

Figure 4.4: Plots on the right show the relative deviation of the combined dimensionless tidal deformability, $\widetilde{\Lambda}$, as a function of the heaviest star mass for the Hebeler et al. parametrization with $\alpha = 3$ for various values of the chirp mass. Plots on the left show $\widetilde{\Lambda}$ for vanishing VE for the same chirp masses. Dotted parts of the curves correspond to unstable configurations. The disconnected branches associated with two stable NS configurations allow for the largest deviations.

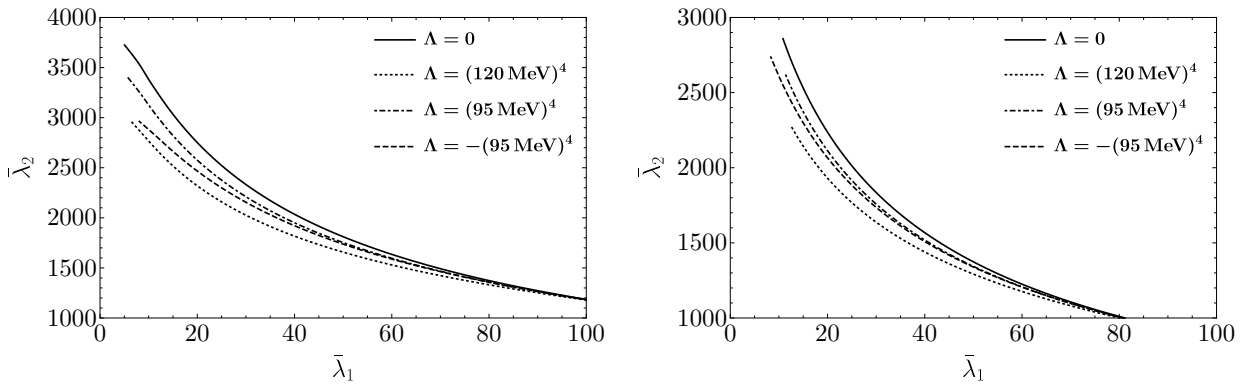

(a) SLy EoS (b) AP4 EoS

Figure 4.5: Tidal deformability curves for a neutron star binary with SLy and AP4 EoS's. The chirp mass is taken to be $\mathcal{M} = 1.188 M_\odot$, which is the same value as in GW170817. $\bar{\lambda}_1$ and $\bar{\lambda}_2$ correspond to the dimensionless tidal deformability parameters for the heavy and light stars, respectively. Each curve is obtained by varying the heavy star mass while holding the chirp mass fixed. The α-parameter of (4.14) is chosen to be $\alpha = 3$.

where $\widetilde{\Lambda}_0$ is the value of $\widetilde{\Lambda}$ obtained by taking the VE term to zero.

The deviation as a function of the heavy star mass, M_1, for the Hebeler et al. parametrization is shown in Fig. 4.4. The negative values for δ mean that introducing a VE term lowers the value of $\widetilde{\Lambda}$. In order to isolate as much as possible the effects that a nonzero value of Λ has on the internal structure of the stars, we are comparing each point in a given curve with the corresponding event on the $\Lambda = 0$ curve that has the same neutron star masses. Therefore, any deviation in the value of $\widetilde{\Lambda}$ comes entirely from the change in the tidal deformabilities, $\bar{\lambda}_i$.

Even with the more conservative SLy and AP4 models one still finds large deviations in $\widetilde{\Lambda}$ for events with larger chirp masses. The case of the (smaller) chirp mass corresponding to GW170817 is displayed in Fig. 4.5, and the deviations in deformability are small. This is because the combined deformability is typically dominated by the contribution from the less massive star, which does not contain a core in the new phase where VE plays a role. However for higher chirp masses the effect of vacuum energy can be sizable even for the SLy and AP4 EoS's, as shown in Figs. 4.6 and 4.7. As the chirp mass increases more of the star contains the new phase, and eventually both stars typically contain cores in the new phase,

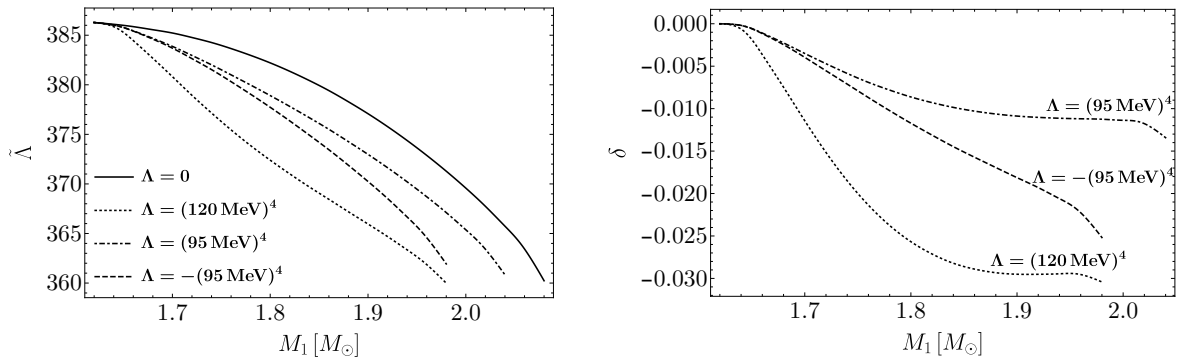

(a) $\mathcal{M} = 1.188 M_\odot$

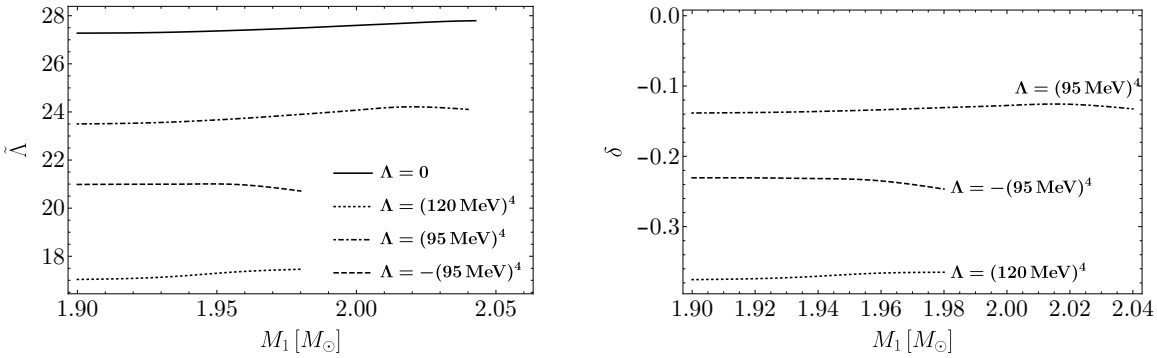

(b) $\mathcal{M} = 1.65 M_\odot$

Figure 4.6: Plot of the deviation of the combined dimensionless tidal deformability as a function of the heavy star mass for the SLy EoS with different values for the chirp mass. $\mathcal{M} = 1.188 M_\odot$ is the same as the one of GW170817, while $\mathcal{M} = 1.65 M_\odot$ corresponds to a chirp mass where if the two NS masses are equal they have a mass of $1.9 M_\odot$. For the smaller chirp mass the effect is rather small, however for a higher chirp mass the effect can be as large as 38%. The α-parameter of (4.14) is again chosen to be $\alpha = 3$.

yielding the increased sensitivity to VE. The high chirp mass we have chosen for these figures corresponds, if the stars are of equal mass, to individual masses of $1.9 M_\odot$, approaching that of the most massive NS observed to date. One can see that for this case the deviation can be as large as 37%, even for these more conservative equations of state.

Since the chirp mass is the most accurately measured property of the NS merger, it is worthwhile to examine the dependence of δ (characterizing the sensitivity to VE) on the chirp mass. In Figs. 4.8 (Hebeler) and 4.9 (AP4 and SLy) we plot $\widetilde{\Lambda}_0^{\max}$ and $\delta^{\max}$ as a function of the chirp mass. The superscript expresses the fact that, when evaluating the quantities in Eqs. (4.35) and (4.36), the mass of the heavy star is kept fixed at the maximal value allowed

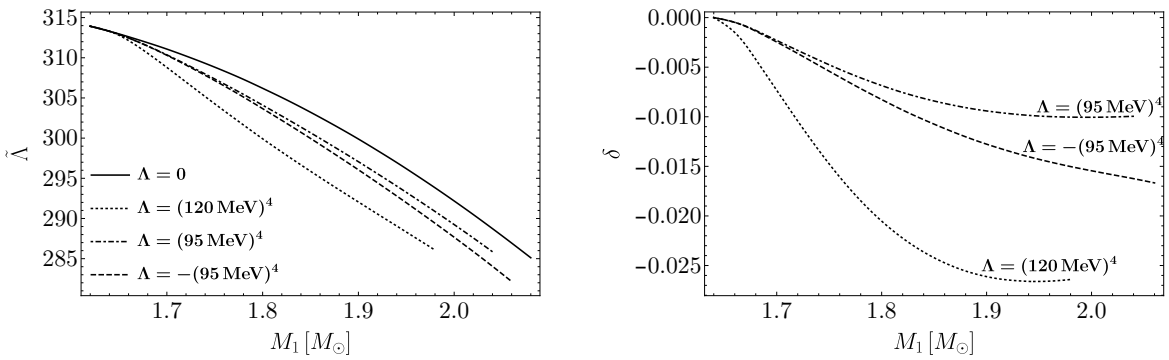

(a) $\mathcal{M} = 1.188 M_\odot$

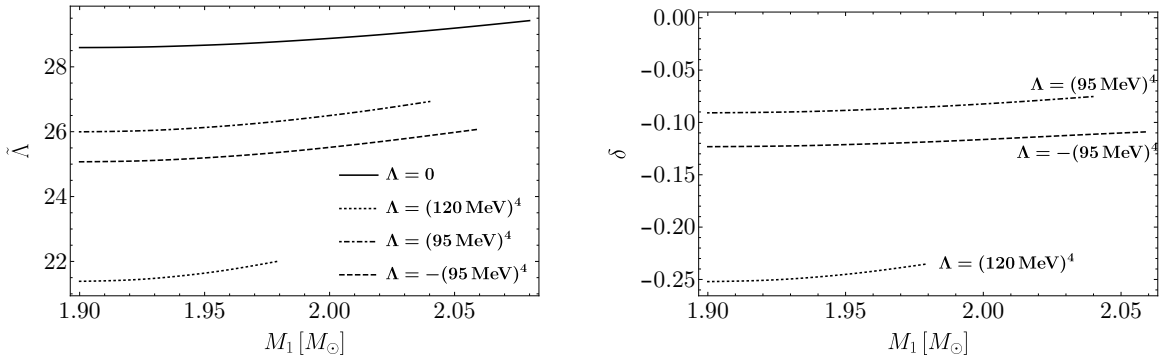

(b) $\mathcal{M} = 1.65 M_\odot$

Figure 4.7: Plot of the deviation of the combined dimensionless tidal deformability as a function of the heavy star mass for the AP4 EoS with different values for the chirp mass. Plots on the left show the value of $\widetilde{\Lambda}$, while plots on the right show the fractional deviation, δ. The chirp mass $\mathcal{M} = 1.188 M_\odot$ is the same as the one of GW170817, while $\mathcal{M} = 1.65 M_\odot$ corresponds to a chirp mass where if the two NS masses are equal they have a mass of $1.9 M_\odot$. For the smaller chirp mass the effect is rather small, however for a higher chirp mass the effect can be as large as 25%. Again the α-parameter of (4.14) is chosen to be $\alpha = 3$.

by the corresponding fixed value of Λ. Fixing one of the stars to have maximal mass will generically (though not always) give the largest VE effect on $\widetilde{\Lambda}$. The important result of the plots is that the deviation increases substantially above a certain chirp mass denoted by the vertical gray line in the plots. This threshold corresponds to the chirp mass for which the lighter star mass also reaches the critical mass for the phase transition. Therefore, the large deviation can be understood from the fact that both stars are in the new phase.

In our final plot in Fig. 4.10, we display the limits that GW170817 places on VE assuming the Hebeler et al. parametrization. In particular, we note that including a VE term

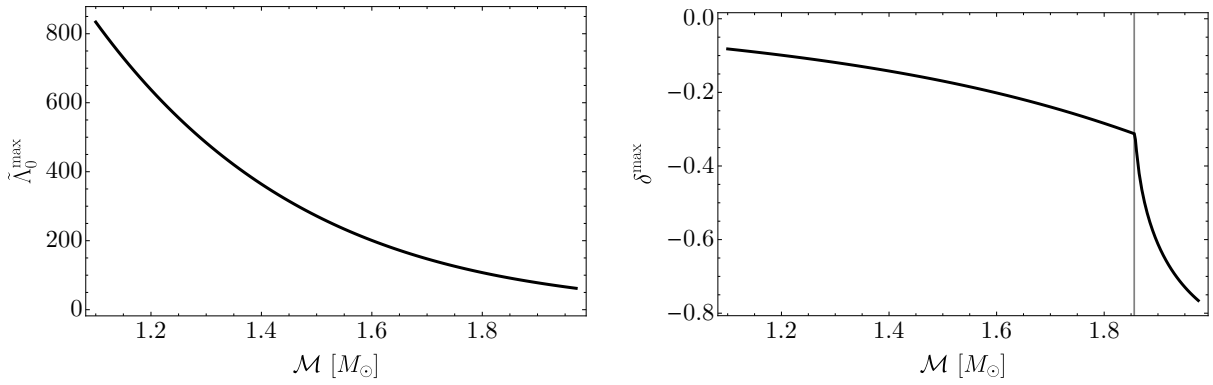

Figure 4.8: Dependence on the chirp mass in the Hebeler et al. parametrization, keeping the heaviest star mass fixed at $M_1 = 2.27 M_\odot$ (the maximum value for the $\Lambda = (150\,\mathrm{MeV})^4$ curve). The left plot shows the corresponding value of the combined tidal deformability for the $\Lambda = 0$ curve. The right plot represents the relative deviation of the combined tidal deformability by turning on $\Lambda = (150\,\mathrm{MeV})^4$ and is a measure of how the effect of VE potentially increases with the chirp mass.

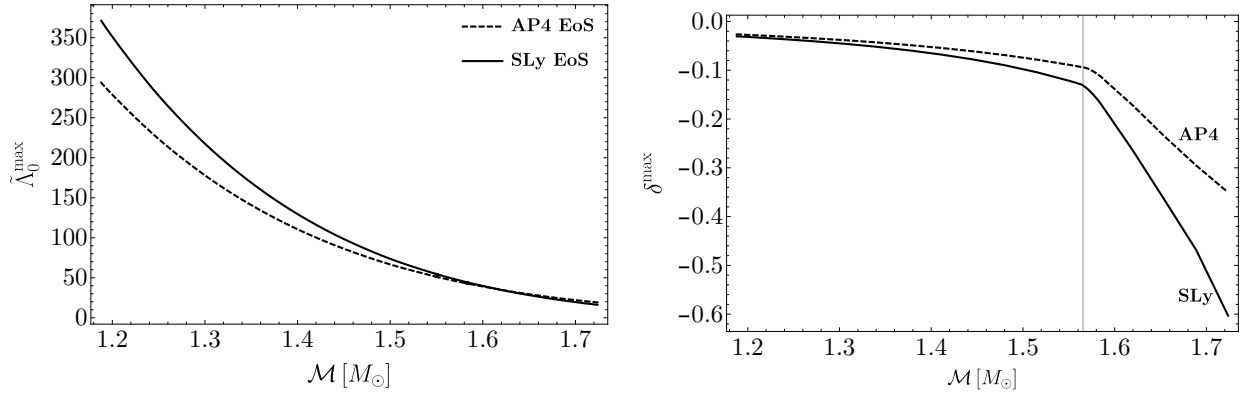

Figure 4.9: Dependence on the chirp mass in the AP4 and SLy parametrizations, keeping the heaviest star mass fixed at $M_1 = 1.98 M_\odot$ (the maximum value for the $\Lambda = (120\,\mathrm{MeV})^4$ curve). The chirp mass range is from $\mathcal{M} = 1.188 M_\odot$ to $\mathcal{M} \approx 1.72 M_\odot$, where the latter corresponds to the case when both stars have masses $M_{1,2} = 1.98 M_\odot$. The left plot shows the corresponding value of the combined tidal deformability for the $\Lambda = 0$ curves. The right plot represents the relative deviation of the combined tidal deformability and is a measure of how the effect of VE potentially increases with the chirp mass. The vertical gray line denotes the chirp mass at which the light star mass reaches the critical mass for the phase transition.

significantly changes the allowed range of the individual masses for the high-spin assumption. The effect is less pronounced for the SLy and AP4 models. As more data on NS mergers are collected with some of those corresponding to mergers of more massive stars, strong limits could be placed on the EoS of dense nuclear matter. This will especially be true once the sensitivities for probing the tidal contributions to the gravitational wave phase further

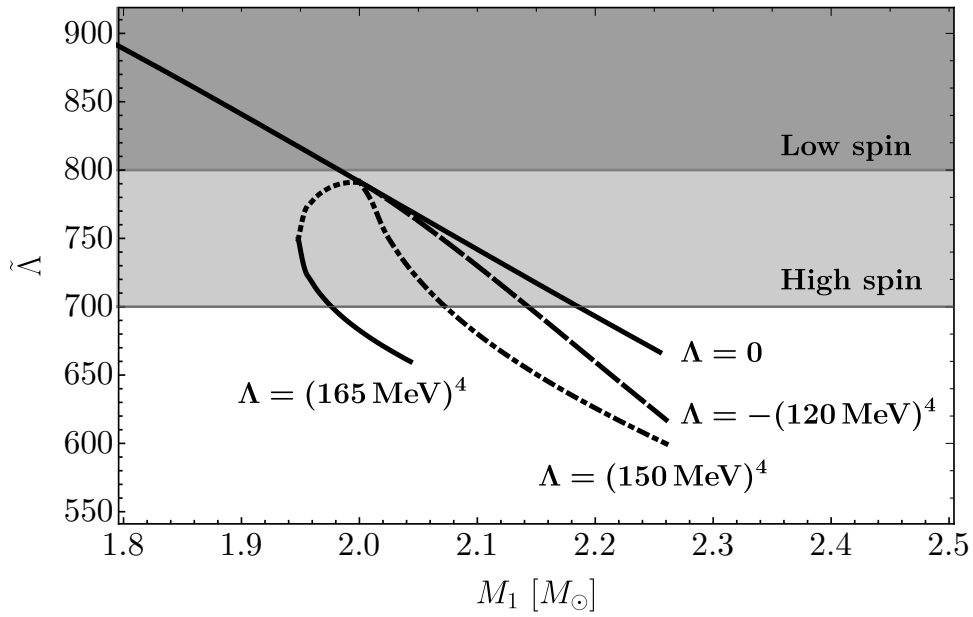

Figure 4.10: Combined tidal deformability $\widetilde{\Lambda}$ as a function of the heavy star mass M_1 for the Hebeler et al. parametrization with $\alpha = 3$. The chirp mass is the same as in the event GW170817. The figure shows the upper bounds set by the LIGO/Virgo analysis and demonstrates how a nonzero value of Λ can affect the allowed mass range.

improve.

The future outlook is difficult to extrapolate, but promising. At present, due to the sensitivity of the experiments, the limited statistics, and the number of parameters involved in the simulations, it is not possible to precisely and unambiguously determine from NS measurements the vacuum energy contribution to the QCD equation of state. However, the constraints that are placed in the coming years will depend strongly on currently uncertain characteristics of NS binaries or NS-black hole mergers that will be captured by upcoming data-taking runs at LIGO and other GW observatories [163]. Constraints will depend upon masses, spins, and branch populations in cases where there are multiple configurations with the same mass. In addition, the sensitivities of the experiments will evolve, and may be able to better capture higher order contributions to the waveforms. This will help single out the different contributions to the observable quantities, for example distinguish the effects of vacuum energy from the rest of the EoS parameters, once the uncertainties on

masses, radii and tidal deformabilities are reduced. Finally, utilization of neutron stars as laboratories to study very high density physics and VE depends crucially on a precise theoretical calculation of the QCD equation of state at high densities [164]. Such a calculation is certainly very difficult, mainly due to technical challenges rather than conceptual ones. Taking an optimistic viewpoint on these issues leads us to the conclusion that neutron star mergers can tell us about the interface of gravity and quantum field theory in a regime never before tested.

4.5 Conclusions

In this chapter, we have argued that neutron star mergers can be a valuable tool for testing new phases of QCD at large densities, in particular for finding the contribution of a VE term in exotic high density phases. To study the effects of such a new phase on neutron star observables, we have started with the conventional 7-layer parametrization of the EoS, then assumed a nonzero value for the VE in the innermost layer leading to a jump in the energy density.

For the three benchmark models we have chosen, we have calculated the $M(R)$ curves and tidal Love numbers for different values of the VE. By using those results, we have obtained individual tidal deformabilities and calculated the combined dimensionless tidal deformability parameter which can be constrained by neutron star mergers observed in gravitational wave observatories. We have found that for larger chirp masses, the nonzero VE at the innermost core can have an $\mathcal{O}(1)$ effect on the combined dimensionless tidal deformability parameter, hence future observations of neutron star merger chirps can place strong limits on the EoS of dense nuclear matter. We have also shown that for some parameters, introducing a nonzero VE can create a disconnected branch of stable neutron star solutions allowing the possibility of having two neutron stars of the same mass with significantly different radii. This possibility is unique to EoS's which have a phase transition at the core, hence it is a

smoking gun for new phases of QCD.

Bibliography

[1] ATLAS collaboration, G. Aad et al., *Observation of a new particle in the search for the Standard Model Higgs boson with the ATLAS detector at the LHC*, *Phys. Lett.* **B716** (2012) 1–29, [1207.7214].

[2] CMS collaboration, S. Chatrchyan et al., *Observation of a new boson at a mass of 125 GeV with the CMS experiment at the LHC*, *Phys. Lett.* **B716** (2012) 30–61, [1207.7235].

[3] G. S. Guralnik, C. R. Hagen and T. W. B. Kibble, *Global conservation laws and massless particles*, *Phys. Rev. Lett.* **13** (Nov, 1964) 585–587.

[4] P. W. Higgs, *Broken symmetries and the masses of gauge bosons*, *Phys. Rev. Lett.* **13** (Oct, 1964) 508–509.

[5] F. Englert and R. Brout, *Broken symmetry and the mass of gauge vector mesons*, *Phys. Rev. Lett.* **13** (Aug, 1964) 321–323.

[6] A. Salam and J. C. Ward, *Weak and electromagnetic interactions*, *Il Nuovo Cimento (1955-1965)* **11** (Feb, 1959) 568–577.

[7] S. Weinberg, *A model of leptons*, *Phys. Rev. Lett.* **19** (Nov, 1967) 1264–1266.

[8] S. L. Glashow, *The renormalizability of vector meson interactions*, *Nucl. Phys.* **10** (1959) 107–117.

[9] E. Wigner, *On unitary representations of the inhomogeneous lorentz group*, *Annals of Mathematics* **40** (1939) 149–204.

[10] C. E. Carlson, *The Proton Radius Puzzle*, *Prog. Part. Nucl. Phys.* **82** (2015) 59–77, [1502.05314].

[11] T. Blum, A. Denig, I. Logashenko, E. de Rafael, B. L. Roberts, T. Teubner et al., *The Muon (g-2) Theory Value: Present and Future*, 1311.2198.

[12] B. Capdevila, A. Crivellin, S. Descotes-Genon, J. Matias and J. Virto, *Patterns of New Physics in $b \to s\ell^+\ell^-$ transitions in the light of recent data*, *JHEP* **01** (2018) 093, [1704.05340].

[13] LHCb collaboration, R. Aaij et al., *Measurement of the ratio of branching fractions $\mathcal{B}(\bar{B}^0 \to D^{*+}\tau^-\bar{\nu}_\tau)/\mathcal{B}(\bar{B}^0 \to D^{*+}\mu^-\bar{\nu}_\mu)$*, *Phys. Rev. Lett.* **115** (2015) 111803, [1506.08614].

[14] BaBar collaboration, J. P. Lees et al., *Evidence for an excess of $\bar{B} \to D^{(*)}\tau^-\bar{\nu}_\tau$ decays*, *Phys. Rev. Lett.* **109** (2012) 101802, [1205.5442].

[15] Planck collaboration, N. Aghanim et al., *Planck 2018 results. VI. Cosmological parameters*, 1807.06209.

[16] Supernova Cosmology Project collaboration, S. Perlmutter et al., *Measurements of Omega and Lambda from 42 high redshift supernovae*, *Astrophys. J.* **517** (1999) 565–586, [astro-ph/9812133].

[17] Supernova Search Team collaboration, A. G. Riess et al., *Observational evidence from supernovae for an accelerating universe and a cosmological constant*, *Astron. J.* **116** (1998) 1009–1038, [astro-ph/9805201].

[18] D. E. Morrissey and M. J. Ramsey-Musolf, *Electroweak baryogenesis*, *New Journal of Physics* **14** (dec, 2012) 125003.

[19] M. D. Schwartz, *Quantum Field Theory and the Standard Model*, ch. 8, pp. 135–139. Cambridge University Press, University Printing House, Cambridge CB2 8BS, United Kingdom, 1 ed., 2014.

[20] S. Weinberg, *ULTRAVIOLET DIVERGENCES IN QUANTUM THEORIES OF GRAVITATION*, in *General Relativity: An Einstein Centenary Survey*, pp. 790–831. 1980.

[21] R. Percacci, *Asymptotic Safety*, 0709.3851.

[22] F. L. Wilson, *Fermi's theory of beta decay*, *American Journal of Physics* **36** (1968) 1150–1160, [https://doi.org/10.1119/1.1974382].

[23] Particle Data Group collaboration, M. Tanabashi, K. Hagiwara, K. Hikasa, K. Nakamura, Y. Sumino, F. Takahashi et al., *Review of particle physics*, *Phys. Rev. D* **98** (Aug, 2018) 030001.

[24] S. Weinberg, *Baryon- and lepton-nonconserving processes*, *Phys. Rev. Lett.* **43** (Nov, 1979) 1566–1570.

[25] G. Panico and A. Wulzer, *The Composite Nambu-Goldstone Higgs*, vol. 913 of *Lecture Notes in Physics*, ch. 1, pp. 2–17. Springer, Springer International Publishing Switzerland 2016, 11, 2015.

[26] D. I. Kazakov, *Beyond the standard model: In search of supersymmetry*, in *2000 European School of high-energy physics, Caramulo, Portugal, 20 Aug-2 Sep 2000: Proceedings*, pp. 125–199, 2000, hep-ph/0012288.

[27] M. Gockeler, R. Horsley, V. Linke, P. E. L. Rakow, G. Schierholz and H. Stuben, *Is there a Landau pole problem in QED?*, *Phys. Rev. Lett.* **80** (1998) 4119–4122, [hep-th/9712244].

[28] J. B. Kogut, E. Dagotto and A. Kocic, *New phase of quantum electrodynamics: A nonperturbative fixed point in four dimensions*, *Phys. Rev. Lett.* **60** (Feb, 1988) 772–775.

[29] M. Göckeler, R. Horsley, V. Linke, P. Rakow, G. Schierholz and H. Stüben, *Resolution of the landau pole problem in qed*, *Nuclear Physics B - Proceedings Supplements* **63** (1998) 694 – 696.

[30] K. G. Wilson and J. B. Kogut, *The Renormalization group and the epsilon expansion*, *Phys. Rept.* **12** (1974) 75–199.

[31] K. G. Wilson, *The Renormalization Group: Critical Phenomena and the Kondo Problem*, *Rev. Mod. Phys.* **47** (1975) 773.

[32] K. G. Wilson, *The renormalization group and critical phenomena*, *Rev. Mod. Phys.* **55** (1983) 583–600.

[33] K. G. Wilson, *Renormalization group and critical phenomena. 2. Phase space cell analysis of critical behavior*, *Phys. Rev.* **B4** (1971) 3184–3205.

[34] K. G. Wilson, *Renormalization group and critical phenomena. 1. Renormalization group and the Kadanoff scaling picture*, *Phys. Rev.* **B4** (1971) 3174–3183.

[35] D. V. S. Michael E. Peskin, *Introduction to Quantum Field Theory*, ch. 12, pp. 394–406. Addison-Wesley Publishing Company, 1995.

[36] J. Ellis, *TikZ-Feynman: Feynman diagrams with TikZ*, *Comput. Phys. Commun.* **210** (2017) 103–123, [1601.05437].

[37] Supernova Search Team collaboration, P. M. Garnavich et al., *Constraints on cosmological models from Hubble Space Telescope observations of high z supernovae*, *Astrophys. J.* **493** (1998) L53–57, [astro-ph/9710123].

[38] Supernova Search Team collaboration, B. P. Schmidt et al., *The High Z supernova search: Measuring cosmic deceleration and global curvature of the universe using type Ia supernovae*, *Astrophys. J.* **507** (1998) 46–63, [astro-ph/9805200].

[39] Supernova Search Team collaboration, P. M. Garnavich et al., *Supernova limits on the cosmic equation of state*, *Astrophys. J.* **509** (1998) 74–79, [astro-ph/9806396].

[40] Supernova Cosmology Project collaboration, S. Perlmutter et al., *Measurements of the cosmological parameters Omega and Lambda from the first 7 supernovae at z¿=0.35*, *Astrophys. J.* **483** (1997) 565, [astro-ph/9608192].

[41] Supernova Cosmology Project collaboration, S. Perlmutter et al., *Discovery of a supernova explosion at half the age of the Universe and its cosmological implications*, *Nature* **391** (1998) 51–54, [astro-ph/9712212].

[42] S. Weinberg, *Gauge and global symmetries at high temperature*, *Phys. Rev. D* **9** (Jun, 1974) 3357–3378.

[43] L. Dolan and R. Jackiw, *Symmetry behavior at finite temperature*, *Phys. Rev. D* **9** (Jun, 1974) 3320–3341.

[44] L. Randall and G. Servant, *Gravitational waves from warped spacetime*, *JHEP* **05** (2007) 054, [hep-ph/0607158].

[45] B. Bellazzini, C. Csaki, J. Hubisz, J. Serra and J. Terning, *Cosmological and Astrophysical Probes of Vacuum Energy*, *JHEP* **06** (2016) 104, [1502.04702].

[46] S. Coleman and J. Mandula, *All possible symmetries of the s matrix*, *Phys. Rev.* **159** (Jul, 1967) 1251–1256.

[47] R. Haag, J. T. opuszaski and M. Sohniusx, *All possible generators of supersymmetries of the s-matrix*, *Nuclear Physics B* **88** (1975) 257 – 274.

[48] S. P. Martin, *A Supersymmetry primer*, hep-ph/9709356.

[49] P. Fayet, *Supersymmetry and weak, electromagnetic and strong interactions*, *Physics Letters B* **64** (1976) 159 – 162.

[50] P. Fayet, *Spontaneously broken supersymmetric theories of weak, electromagnetic and strong interactions*, *Physics Letters B* **69** (1977) 489 – 494.

[51] P. Fayet, *Relations between the masses of the superpartners of leptons and quarks, the goldstino coupling and the neutral currents*, *Physics Letters B* **84** (1979) 416 – 420.

[52] G. R. Farrar and P. Fayet, *Phenomenology of the production, decay, and detection of new hadronic states associated with supersymmetry*, *Physics Letters B* **76** (1978) 575 – 579.

[53] N. Craig, *The State of Supersymmetry after Run I of the LHC*, in *Beyond the Standard Model after the first run of the LHC Arcetri, Florence, Italy, May 20-July 12, 2013*, 2013, 1309.0528.

[54] D. B. Kaplan and H. Georgi, *SU(2) x U(1) Breaking by Vacuum Misalignment*, *Phys. Lett.* **136B** (1984) 183–186.

[55] S. Weinberg, *Implications of dynamical symmetry breaking*, *Phys. Rev. D* **13** (Feb, 1976) 974–996.

[56] S. Weinberg, *Implications of dynamical symmetry breaking: An addendum*, *Phys. Rev. D* **19** (Feb, 1979) 1277–1280.

[57] C. T. Hill and E. H. Simmons, *Strong dynamics and electroweak symmetry breaking*, *Phys. Rept.* **381** (2003) 235–402, [hep-ph/0203079].

[58] J. Goldstone, *Field Theories with Superconductor Solutions*, *Nuovo Cim.* **19** (1961) 154–164.

[59] K. Agashe, R. Contino and A. Pomarol, *The Minimal composite Higgs model*, *Nucl. Phys.* **B719** (2005) 165–187, [hep-ph/0412089].

[60] R. Contino, L. Da Rold and A. Pomarol, *Light custodians in natural composite Higgs models*, *Phys. Rev.* **D75** (2007) 055014, [hep-ph/0612048].

[61] O. KLEIN, *The atomicity of electricity as a quantum theory law*, *Nature* **118** (Oct, 1926) 516 EP –.

[62] O. Klein, *Quantentheorie und fünfdimensionale relativitätstheorie*, *Zeitschrift für Physik* **37** (Dec, 1926) 895–906.

[63] T. Kaluza, *Zum Unitätsproblem der Physik*, *Sitzungsberichte der Königlich Preußischen Akademie der Wissenschaften (Berlin), Seite p. 966-972* (1921) 966–972.

[64] C. Csáki, S. Lombardo and O. Telem, *TASI Lectures on Non-supersymmetric BSM Models*, in *Proceedings, Theoretical Advanced Study Institute in Elementary Particle Physics : Anticipating the Next Discoveries in Particle Physics (TASI 2016): Boulder, CO, USA, June 6-July 1, 2016*, pp. 501–570, WSP, WSP, 2018, 1811.04279, DOI.

[65] C. Csaki, *TASI lectures on extra dimensions and branes*, in *From fields to strings: Circumnavigating theoretical physics. Ian Kogan memorial collection (3 volume set)*, pp. 605–698, 2004, hep-ph/0404096.

[66] N. Arkani-Hamed, S. Dimopoulos and G. R. Dvali, *The Hierarchy problem and new dimensions at a millimeter*, *Phys. Lett.* **B429** (1998) 263–272, [hep-ph/9803315].

[67] E. G. Adelberger, J. H. Gundlach, B. R. Heckel, S. Hoedl and S. Schlamminger, *Torsion balance experiments: A low-energy frontier of particle physics*, *Prog. Part. Nucl. Phys.* **62** (2009) 102–134.

[68] J. Murata and S. Tanaka, *A review of short-range gravity experiments in the LHC era*, *Classical and Quantum Gravity* **32** (jan, 2015) 033001.

[69] L. J. Hall and D. Tucker-Smith, *Cosmological constraints on theories with large extra dimensions*, *Phys. Rev.* **D60** (1999) 085008, [hep-ph/9904267].

[70] S. Hannestad and G. G. Raffelt, *Stringent neutron star limits on large extra dimensions*, *Phys. Rev. Lett.* **88** (2002) 071301, [hep-ph/0110067].

[71] C. Hanhart, J. A. Pons, D. R. Phillips and S. Reddy, *The Likelihood of GODs' existence: Improving the SN1987a constraint on the size of large compact dimensions*, *Phys. Lett.* **B509** (2001) 1–9, [astro-ph/0102063].

[72] L. Randall and R. Sundrum, *A Large mass hierarchy from a small extra dimension*, *Phys. Rev. Lett.* **83** (1999) 3370–3373, [hep-ph/9905221].

[73] W. D. Goldberger and M. B. Wise, *Modulus stabilization with bulk fields*, *Phys. Rev. Lett.* **83** (1999) 4922–4925, [hep-ph/9907447].

[74] O. DeWolfe, D. Z. Freedman, S. S. Gubser and A. Karch, *Modeling the fifth-dimension with scalars and gravity*, *Phys. Rev.* **D62** (2000) 046008, [hep-th/9909134].

[75] B. Bellazzini, C. Csaki, J. Hubisz, J. Serra and J. Terning, *A Naturally Light Dilaton and a Small Cosmological Constant*, *Eur. Phys. J.* **C74** (2014) 2790, [1305.3919].

[76] C. Eröncel, J. Hubisz and G. Rigo, *Radion activated higgs mechanism*, (Work in progress) .

[77] O. DeWolfe, *TASI Lectures on Applications of Gauge/Gravity Duality*, *PoS* **TASI2017** (2018) 014, [1802.08267].

[78] J. M. Maldacena, *The Large N limit of superconformal field theories and supergravity*, *Int. J. Theor. Phys.* **38** (1999) 1113–1133, [hep-th/9711200].

[79] P. Breitenlohner and D. Z. Freedman, *Positive Energy in anti-De Sitter Backgrounds and Gauged Extended Supergravity*, *Phys. Lett.* **115B** (1982) 197–201.

[80] P. Breitenlohner and D. Z. Freedman, *Stability in Gauged Extended Supergravity*, *Annals Phys.* **144** (1982) 249.

[81] I. R. Klebanov and E. Witten, *AdS / CFT correspondence and symmetry breaking*, *Nucl. Phys.* **B556** (1999) 89–114, [hep-th/9905104].

[82] N. Arkani-Hamed, M. Porrati and L. Randall, *Holography and phenomenology*, *JHEP* **08** (2001) 017, [hep-th/0012148].

[83] G. F. Giudice, *Naturally Speaking: The Naturalness Criterion and Physics at the LHC*, 0801.2562.

[84] P. Bak, C. Tang and K. Wiesenfeld, *Self-organized criticality*, *Phys. Rev. A* **38** (Jul, 1988) 364–374.

[85] P. Bak, C. Tang and K. Wiesenfeld, *Self-organized criticality: An explanation of the 1/f noise*, *Phys. Rev. Lett.* **59** (Jul, 1987) 381–384.

[86] N. W. Watkins, G. Pruessner, S. C. Chapman, N. B. Crosby and H. J. Jensen, *25 years of self-organized criticality: Concepts and controversies*, *Space Science Reviews* **198** (Jan, 2016) 3–44.

[87] M. J. Aschwanden et al., *25 Years of Self-Organized Criticality: Solar and Astrophysics*, *Space Sci. Rev.* **198** (2016) 47–166, [1403.6528].

[88] D. Sornette, *Discrete scale invariance and complex dimensions*, *Phys. Rept.* **297** (1998) 239–270, [cond-mat/9707012].

[89] D. B. Kaplan, J.-W. Lee, D. T. Son and M. A. Stephanov, *Conformality Lost*, *Phys. Rev.* **D80** (2009) 125005, [0905.4752].

[90] S. R. Coleman and E. J. Weinberg, *Radiative Corrections as the Origin of Spontaneous Symmetry Breaking*, *Phys. Rev.* **D7** (1973) 1888–1910.

[91] L. E. Ibanez and G. G. Ross, *SU(2)-L x U(1) Symmetry Breaking as a Radiative Effect of Supersymmetry Breaking in Guts*, *Phys. Lett.* **110B** (1982) 215–220.

[92] J. R. Ellis, J. S. Hagelin, D. V. Nanopoulos and K. Tamvakis, *Weak Symmetry Breaking by Radiative Corrections in Broken Supergravity*, *Phys. Lett.* **125B** (1983) 275.

[93] L. Alvarez-Gaume, J. Polchinski and M. B. Wise, *Minimal Low-Energy Supergravity*, *Nucl. Phys.* **B221** (1983) 495.

[94] P. W. Graham, D. E. Kaplan and S. Rajendran, *Cosmological Relaxation of the Electroweak Scale*, *Phys. Rev. Lett.* **115** (2015) 221801, [1504.07551].

[95] H. Georgi, *Physics Fun with Discrete Scale Invariance*, 1606.03405.

[96] N. Arkani-Hamed, S. Dubovsky, A. Nicolis and G. Villadoro, *Quantum Horizons of the Standard Model Landscape*, *JHEP* **06** (2007) 078, [hep-th/0703067].

[97] R. Rattazzi and A. Zaffaroni, *Comments on the holographic picture of the Randall-Sundrum model*, *JHEP* **04** (2001) 021, [hep-th/0012248].

[98] M. A. Luty, J. Polchinski and R. Rattazzi, *The a-theorem and the Asymptotics of 4D Quantum Field Theory*, *JHEP* **01** (2013) 152, [1204.5221].

[99] V. Emery and S. Kivelson, *Frustrated electronic phase separation and high-temperature superconductors*, *Physica C: Superconductivity* **209** (1993) 597 – 621.

[100] A. Shapere and F. Wilczek, *Classical Time Crystals*, *Phys. Rev. Lett.* **109** (2012) 160402, [1202.2537].

[101] F. Wilczek, *Quantum Time Crystals*, *Phys. Rev. Lett.* **109** (2012) 160401, [1202.2539].

[102] S. A. Hartnoll, A. Lucas and S. Sachdev, *Holographic quantum matter*, 1612.07324.

[103] J. S. Bains, M. P. Hertzberg and F. Wilczek, *Oscillatory Attractors: A New Cosmological Phase*, *JCAP* **1705** (2017) 011, [1512.02304].

[104] D. A. Easson and T. Manton, *Stable Cosmic Time Crystals*, *Phys. Rev.* **D99** (2019) 043507, [1802.03693].

[105] D. Bunk, J. Hubisz and B. Jain, *A Perturbative RS I Cosmological Phase Transition*, *Eur. Phys. J.* **C78** (2018) 78, [1705.00001].

[106] L. Vecchi, *A Natural Hierarchy and a low New Physics scale from a Bulk Higgs*, *JHEP* **11** (2011) 102, [1012.3742].

[107] M. Geller, S. Bar-Shalom and A. Soni, *Higgs-radion unification: Radius stabilization by an SU(2) bulk doublet and the 126 GeV scalar*, *Phys. Rev.* **D89** (2014) 095015, [1312.3331].

[108] A. Pomarol, *Light scalars: From the lattice to the LHC via holography*, *PoS* **CORFU2017** (2018) 061.

[109] S. S. Gubser and I. R. Klebanov, *A Universal result on central charges in the presence of double trace deformations*, *Nucl. Phys.* **B656** (2003) 23–36, [hep-th/0212138].

[110] C. Csaki, M. Graesser, L. Randall and J. Terning, *Cosmology of brane models with radion stabilization*, *Phys. Rev.* **D62** (2000) 045015, [hep-ph/9911406].

[111] C. Csaki, M. L. Graesser and G. D. Kribs, *Radion dynamics and electroweak physics*, *Phys. Rev.* **D63** (2001) 065002, [hep-th/0008151].

[112] C. Eröncel, J. Hubisz and G. Rigo, *Self-Organized Higgs Criticality*, *JHEP* **03** (2019) 046, [1804.00004].

[113] V. L. Berezinsky, *Destruction of long range order in one-dimensional and two-dimensional systems having a continuous symmetry group. I. Classical systems*, *Sov. Phys. JETP* **32** (1971) 493–500.

[114] J. M. Kosterlitz and D. J. Thouless, *Ordering, metastability and phase transitions in two-dimensional systems*, *J. Phys.* **C6** (1973) 1181–1203.

[115] M. A. Amin, J. Fan, K. D. Lozanov and M. Reece, *Cosmological dynamics of Higgs potential fine tuning*, *Phys. Rev.* **D99** (2019) 035008, [1802.00444].

[116] L. Kofman, A. D. Linde, X. Liu, A. Maloney, L. McAllister and E. Silverstein, *Beauty is attractive: Moduli trapping at enhanced symmetry points*, *JHEP* **05** (2004) 030, [hep-th/0403001].

[117] LIGO Scientific, Virgo collaboration, B. Abbott et al., *GW170817: Observation of Gravitational Waves from a Binary Neutron Star Inspiral*, *Phys. Rev. Lett.* **119** (2017) 161101, [1710.05832].

[118] M. Baryakhtar, J. Bramante, S. W. Li, T. Linden and N. Raj, *Dark Kinetic Heating of Neutron Stars and An Infrared Window On WIMPs, SIMPs, and Pure Higgsinos*, *Phys. Rev. Lett.* **119** (2017) 131801, [1704.01577].

[119] D. Croon, A. E. Nelson, C. Sun, D. G. E. Walker and Z.-Z. Xianyu, *Hidden-Sector Spectroscopy with Gravitational Waves from Binary Neutron Stars*, *Astrophys. J.* **858** (2018) L2, [1711.02096].

[120] J. Ellis, A. Hektor, G. Hütsi, K. Kannike, L. Marzola, M. Raidal et al., *Search for Dark Matter Effects on Gravitational Signals from Neutron Star Mergers*, *Phys. Lett.* **B781** (2018) 607–610, [1710.05540].

[121] D. D. Ivanenko and D. F. Kurdgelaidze, *Hypothesis concerning quark stars*, *Astrophysics* **1** (1965) 251–252.

[122] J. R. Ellis, J. I. Kapusta and K. A. Olive, *Phase transition in dense nuclear matter with quark and gluon condensates*, *Phys. Lett.* **B273** (1991) 123–127.

[123] S. Bogdanov, Z. Arzoumanian, D. Chakrabarty, S. Guillot, A. Kust Harding, W. C. G. Ho et al., *Neutron Star Dense Matter Equation of State Constraints with NICER*, in *AAS/High Energy Astrophysics Division #16*, vol. 16 of *AAS/High Energy Astrophysics Division*, p. 104.04, Aug., 2017.

[124] E. E. Flanagan and T. Hinderer, *Constraining neutron star tidal Love numbers with gravitational wave detectors*, *Phys. Rev.* **D77** (2008) 021502, [0709.1915].

[125] T. Hinderer, *Tidal Love numbers of neutron stars*, *Astrophys. J.* **677** (2008) 1216–1220, [0711.2420].

[126] T. Hinderer, B. D. Lackey, R. N. Lang and J. S. Read, *Tidal deformability of neutron stars with realistic equations of state and their gravitational wave signatures in binary inspiral*, *Phys. Rev.* **D81** (2010) 123016, [0911.3535].

[127] S. Postnikov, M. Prakash and J. M. Lattimer, *Tidal Love Numbers of Neutron and Self-Bound Quark Stars*, *Phys. Rev.* **D82** (2010) 024016, [1004.5098].

[128] B. D. Lackey and L. Wade, *Reconstructing the neutron-star equation of state with gravitational-wave detectors from a realistic population of inspiralling binary neutron stars*, *Phys. Rev.* **D91** (2015) 043002, [1410.8866].

[129] B. Margalit and B. D. Metzger, *Constraining the Maximum Mass of Neutron Stars From Multi-Messenger Observations of GW170817*, *Astrophys. J.* **850** (2017) L19, [1710.05938].

[130] A. Bauswein, O. Just, H.-T. Janka and N. Stergioulas, *Neutron-star radius constraints from GW170817 and future detections*, *Astrophys. J.* **850** (2017) L34, [1710.06843].

[131] E. Zhou, A. Tsokaros, L. Rezzolla, R. Xu and K. Ury, *Uniformly rotating, axisymmetric and triaxial quark stars in general relativity*, *Phys. Rev.* **D97** (2018) 023013, [1711.00198].

[132] L. Rezzolla, E. R. Most and L. R. Weih, *Using gravitational-wave observations and quasi-universal relations to constrain the maximum mass of neutron stars*, *Astrophys. J.* **852** (2018) L25, [1711.00314].

[133] E. Annala, T. Gorda, A. Kurkela and A. Vuorinen, *Gravitational-wave constraints on the neutron-star-matter Equation of State*, *Phys. Rev. Lett.* **120** (2018) 172703, [1711.02644].

[134] J. M. Lattimer and M. Prakash, *Neutron star structure and the equation of state*, *Astrophys. J.* **550** (2001) 426, [astro-ph/0002232].

[135] F. Douchin and P. Haensel, *A unified equation of state of dense matter and neutron star structure*, *Astron. Astrophys.* **380** (2001) 151, [astro-ph/0111092].

[136] J. S. Read, B. D. Lackey, B. J. Owen and J. L. Friedman, *Constraints on a phenomenologically parameterized neutron-star equation of state*, *Phys. Rev.* **D79** (2009) 124032, [0812.2163].

[137] K. Hebeler, J. M. Lattimer, C. J. Pethick and A. Schwenk, *Equation of state and neutron star properties constrained by nuclear physics and observation*, *Astrophys. J.* **773** (2013) 11, [1303.4662].

[138] H. Mueller and B. D. Serot, *Relativistic mean field theory and the high density nuclear equation of state*, *Nucl. Phys.* **A606** (1996) 508–537, [nucl-th/9603037].

[139] M. G. Alford, A. Schmitt, K. Rajagopal and T. Schäfer, *Color superconductivity in dense quark matter*, *Rev. Mod. Phys.* **80** (2008) 1455–1515, [0709.4635].

[140] B. K. Agrawal, *Equations of state and stability of color-superconducting quark matter cores in hybrid stars*, *Phys. Rev.* **D81** (2010) 023009, [1001.1584].

[141] M. Bejger, D. Blaschke, P. Haensel, J. L. Zdunik and M. Fortin, *Consequences of a strong phase transition in the dense matter equation of state for the rotational evolution of neutron stars*, *Astron. Astrophys.* **600** (2017) A39, [1608.07049].

[142] D. E. Alvarez-Castillo and D. B. Blaschke, *High-mass twin stars with a multipolytrope equation of state*, *Phys. Rev.* **C96** (2017) 045809, [1703.02681].

[143] M. G. Alford and A. Sedrakian, *Compact stars with sequential QCD phase transitions*, *Phys. Rev. Lett.* **119** (2017) 161104, [1706.01592].

[144] M. G. Alford, S. Han and M. Prakash, *Generic conditions for stable hybrid stars*, *Phys. Rev.* **D88** (2013) 083013, [1302.4732].

[145] Z. F. Seidov, *The Stability of a Star with a Phase Change in General Relativity Theory*, *Sovast* **15** (Oct., 1971) 347.

[146] R. Schaeffer, L. Zdunik and P. Haensel, *Phase transitions in stellar cores. I - Equilibrium configurations*, *AAP* **126** (Sept., 1983) 121–145.

[147] W. Israel, *Singular hypersurfaces and thin shells in general relativity*, *Il Nuovo Cimento B (1965-1970)* **44** (Jul, 1966) 1–14.

[148] W. Israel, *Singular hypersurfaces and thin shells in general relativity*, *Il Nuovo Cimento B (1965-1970)* **48** (Apr, 1967) 463–463.

[149] J. R. Oppenheimer and G. M. Volkoff, *On Massive neutron cores*, *Phys. Rev.* **55** (1939) 374–381.

[150] A. E. H. Love, *Some Problems of Geodynamics*. Cambridge University Press, Cambridge, 1911.

[151] T. Damour and A. Nagar, *Relativistic tidal properties of neutron stars*, *Phys. Rev.* **D80** (2009) 084035, [0906.0096].

[152] A. Akmal, V. R. Pandharipande and D. G. Ravenhall, *The Equation of state of nucleon matter and neutron star structure*, *Phys. Rev.* **C58** (1998) 1804–1828, [nucl-th/9804027].

[153] G. Baym, C. Pethick and P. Sutherland, *The Ground state of matter at high densities: Equation of state and stellar models*, *Astrophys. J.* **170** (1971) 299–317.

[154] J. M. Bardeen, K. S. Thorne and D. W. Meltzer, *A Catalogue of Methods for Studying the Normal Modes of Radial Pulsation of General-Relativistic Stellar Models*, *ApJ* **145** (Aug., 1966) 505.

[155] Alford, Mark G. and Han, Sophia, *Generic conditions for stable hybrid stars*, *EPJ Web of Conferences* **80** (2014) 00038.

[156] N. K. Glendenning and C. Kettner, *Nonidentical neutron star twins*, *Astron. Astrophys.* **353** (2000) L9, [astro-ph/9807155].

[157] K. Schertler, C. Greiner, J. Schaffner-Bielich and M. H. Thoma, *Quark phases in neutron stars and a 'third family' of compact stars as a signature for phase transitions*, *Nucl. Phys.* **A677** (2000) 463–490, [astro-ph/0001467].

[158] P. Haensel, *Equation of state of dense matter and maximum mass of neutron stars*, *EAS Publ. Ser.* **7** (2003) 249, [astro-ph/0301073].

[159] P. Demorest, T. Pennucci, S. Ransom, M. Roberts and J. Hessels, *Shapiro Delay Measurement of A Two Solar Mass Neutron Star*, *Nature* **467** (2010) 1081–1083, [1010.5788].

[160] H. Heiselberg and M. Hjorth-Jensen, *Phase transitions in neutron stars and maximum masses*, *Astrophys. J.* **525** (1999) L45–L48, [astro-ph/9904214].

[161] C. Cutler and E. E. Flanagan, *Gravitational waves from merging compact binaries: How accurately can one extract the binary's parameters from the inspiral wave form?*, *Phys. Rev.* **D49** (1994) 2658–2697, [gr-qc/9402014].

[162] T. Dietrich, S. Bernuzzi and W. Tichy, *Closed-form tidal approximants for binary neutron star gravitational waveforms constructed from high-resolution numerical relativity simulations*, *Phys. Rev.* **D96** (2017) 121501, [1706.02969].

[163] P. Kumar, M. Pürrer and H. P. Pfeiffer, *Measuring neutron star tidal deformability with Advanced LIGO: a Bayesian analysis of neutron star - black hole binary observations*, *Phys. Rev.* **D95** (2017) 044039, [1610.06155].

[164] L. Rezzolla and K. Takami, *Gravitational-wave signal from binary neutron stars: a systematic analysis of the spectral properties*, *Phys. Rev.* **D93** (2016) 124051, [1604.00246].

Cem Eröncel, Ph.D. Candidate

The Physics Department at Syracuse University, Physics Building, Syracuse, NY 13244
+1 (315) 491 52 56 • ceroncel@syr.edu • SkypeID: cemeroncel555
Born in March 26, 1986 • Citizen of Republic of Turkey

Education

- **Ph.D. in Physics** 2014 – current
  Syracuse University, Syracuse, NY, USA
  Thesis Advisor: Prof. Jay Hubisz
  Expected Defense Date: May 2019

- **Master of Science in Physics** 2010 – 2013
  Boğaziçi University, İstanbul, Turkey
  Thesis Title: Exact Renormalization Group on Point Interactions
  Thesis Advisor: Prof. Osman Teoman Turgut

- **Bachelor of Science in Electrical Engineering** 2005 – 2010
  İstanbul Technical University, İstanbul, Turkey
  Thesis Title: Corona Losses
  Thesis Advisor: Prof. Aydoğan Özdemir

Research Experience

- **Visiting Scientist** 2016 – present
  Cornell University, Ithaca, NY, USA
  Working with Prof. Csaba Csáki on the phenomenological implications of gravitational wave observables.

- **Research Assistant** 2016 – present
  Syracuse University, Syracuse, NY, USA
  Working with Prof. Jay Hubisz on the extensions of the Standard Model.

Publications

- **C. Eröncel**, J. Hubisz and G. Rigo, *Self-Organized Higgs Criticality*, *JHEP* **03** (2019) 046 [1804.00004]

- C. Csáki, **C. Eröncel**, J. Hubisz, G. Rigo and J. Terning, *Neutron Star Mergers Chirp about Vacuum Energy*, *JHEP* **09** (2018) 087 [1802.04813]

- O. T. Turgut, **C. Eröncel**, *Exact Renormalization Group for Point Interactions*, *Acta Polytech.* **54** (2014) 156–172, [1412.8623]

Conference Proceedings

- **C. Eröncel**, S. İlhan, A. Özdemir, A. Kaypmaz, *Corona Onset Voltage and Corona Power Losses in an Indoor Corona Cage*, in Proceedings of the Fourteenth International Middle East Power Systems Conference (MEPCON '10), 2010

Talks

- **Self-Organized Higgs Criticality** July 2018
  Institut d'Etudes Scientifiques de Cargese, Cargese, France
  Student presentation in *Mass: From Higgs to Cosmology* summer school
- **Self-Organized Higgs Criticality** May 2018
  University of Pittsburgh, Pittsburgh, PA, USA
  Parallel talk in *Phenomenology 2018 Symposium*
- **Exact Renormalization Group on Point Interactions** August 2013
  Institute of Theoretical and Applied Physics, Marmaris, Turkey
  Student presentation in *International School on Exact and Numerical Methods of Low Dimensional Quantum Structures* summer school
- **Exact Renormalization Group on Point Interactions** June 2013
  Gazi University, İzmir, Turkey
  Presentation in *Conference of Young Physicist*

Interdisciplinary Talks

- **Runaway Ramps of Theoretical High Energy Physics** September 2017
  Remote presentation at an event organized by graduate students at Physics Department of Istanbul Technical University
- **Ph.D. Application Process to US Universities** January 2015
  Remote presentation at an event organized by graduate students at Physics Department of Istanbul Technical University
- **Physics of Rainbows** August 2012
  Remote presentation at an event organized by graduate students at Physics Department of Istanbul Technical University
- **Transposition in Music via Linear Algebra** August 2011
  Joint presentation with my collegues Tuna Pesen and Gizem Şengör in *XXVI. International Conferencen of Physics Students (ICPS '11), 2011*

Organization of Scientific Meetings

- Participated in the organization of the *Feza Gürsey Quantum Field Theory Winter School*, which was a one-week long program aimed at graduate students held in February, 2014 at the Feza Gürsey Institute. Around 60 students participated in the program. I helped with grant writing, communication with lecturers and designed the website.

Teaching Activities

- **Thermodynamics & Statistical Mechanics (undergraduate)** Fall 2017
  Graded and wrote the solution manuals for the homeworks
- **Quantum Mechanics I (graduate)** Fall 2017
  Graded the homeworks, attendad a couple of recitation sessions
- **Major Concepts of Physics II (undergraduate)** Spring 2017 & 2016
  Designed and instructed the lab sections, graded lab reports, homeworks, and exams.
- **Our Corner of the Universe (undergraduate)** Fall 2015
  Instructed the lab sections, graded the lab reports, and exams
- **Quantum Mechanics I (graduate)** Fall 2015
  Graded the homeworks
- **Major Concepts of Physics II (undergraduate)** Spring 2015
  Instructed the lab sections, graded the lab reports, homeworks, and exams
- **General Physics II (undergraduate)** Fall 2014
  Instructed the recitation sections, graded the exams

Schools Attended

- **Higgs: From Mass to Cosmology** July, 2018
  Institut d'Etudes Scientifiques de Cargese, Cargese, France
- **GGI Lectures on the Theory of Fundamental Interactions** January 2018
  Galileo Galilei Institute for Theoretical Physics, Firenze, Italy
- **Prospects in Theoretical Physics: Particle Physics at the LHC and Beyond** July 2017
  Institute of Advanced Study, Princeton, NJ, USA
- **Feza Gürsey Summer School on Group Theory** September 2013
  Feza Gürsey Institute, İstanbul, Turkey
- **International School of Exact and Numerical Models of Low Dimensional Quantum Structures** August 2013
  Institute of Theoretical and Applied Physics (ITAP), Marmaris, Turkey
- **International School on Strings and Fundamental Physics (SFP'12)** July 2012
  DESY, Hamburg, Germany
- **I. Uludağ High Energy Physics Winter School** February 2012
  Uludağ University, Bursa, Turkey
- **International School of Theory & Analysis in Particle Physics** February 2011
  Doğuş University, İstanbul, Turkey

Membership of Scientific Societies

- Associate Member of Institute of Physics 2015 – present
- Member of American Physical Society 2014 – present
- Student member of Institute of Physics 2011 – 2015

Languages

- Turkish: Mother tongue
- English: Fluent in writing and speaking
- German: Fluent in writing and speaking

Computer Skills

- Operating Systems: Linux, Windows
- Programming: Python, C, PHP, SQL, HTML
- Scientific: Mathematica, SAGE, Matlab

Certificates

- **Certificate of Information Technologies** July 2009
  Middle East Technical University, Ankara, Turkey
  This certificate program was offered by Computer Engineering Department and based on asynchronous eduacation on Internet consisting of the courses listed below:
  - Computer Systems and Structures
  - Introduction to Computer Programming with C
  - Data Structures and Algorithms with C
  - Operating Systems with UNIX
  - Software Engineering
  - Database Management Systems
  - Web Programming
  - Software Development Project